Numerical Investigation of Single and Double Differential Cross-Section for the Ionization of Metastable 2S State Hydrogen Atom by Electron Impact

By

Md. Thowhidul Hoque Chowdhury

ID No. 14MMATH003P

A thesis submitted in partial fulfilment of the requirements for the degree of

MASTER of PHILOSOPHY in MATHEMATICS

Department of Mathematics

CHITTAGONG UNIVERSITY OF ENGINEERING AND TECHNOLOGY

NOVEMBER 2023

CERTIFICATION

The thesis titled **"Numerical Investigation of Single and Double Differential Cross-Section for the Ionization of Metastable 2S State Hydrogen Atom by Electron Impact"** submitted by Md. Thowhidul Hoque Chowdhury, Roll No. 14MMATH003P, Session2014-2015 has been accepted as satisfactory in partial fulfilment of the requirement for the degree of Master of Philosophy on Mathematics.

BOARD OF EXAMINERS

1. Supervisor
   Dr. Sunil Dhar
   Professor, Department of Mathematics
   Chittagong University of Engineering and Technology
   Chittagong-4349, Bangladesh. — Chairman

2. Dr. Ashutose Saha
   Professor, Department of Mathematics
   Chittagong University of Engineering and Technology
   Chittagong-4349, Bangladesh. — Member

3. Dr. Md. Golam Hafez
   Professor, Department of Mathematics
   Chittagong University of Engineering and Technology
   Chittagong-4349, Bangladesh. — Member

4. Head
   Dr. Musammet Tahmina Akter
   Professor, Department of Mathematics
   Chittagong University of Engineering and Technology
   Chittagong-4349, Bangladesh. — Member (Ex-Officio)

5. Dr. Anjan Kumar Chowdhury
   Professor and Director, Jamal Nazrul Islam Research Centre for Mathematical and Physical Sciences — Member (External)

List of Publications

Journal Article

- M. Chowdhury, S. Dhar, "Double Differential Cross-Section for the Ionization of Hydrogenic 2S Metastable State", *Open Journal of Microphysics*, vol. 13, no. 1, pp. 1-13, 2023

Conference

- Md. Thowhidul Hoque Chowdhury[1,*], Sunil Dhar[2], "Double Differential Cross-Section (DDCS) of Ionizing Hydrogenic 2S Metastable State considering Exchange Effects" 5th International Conference on Physics for Sustainable Development & Technology, 07-08 September, 2023, Chittagong University of Engineering and Technology, Chittagong, Bangladesh.
- Md. Thowhidul Hoque Chowdhury[1,*], Sunil Dhar[2], "DIFFERENTIAL CROSS SECTION FOR HYDROGENIC METASTABLE STATE BY ELECTRON IMPACT" The 7th International Conference on Mechanical Engineering and Renewable Energy, 16-17 November, 2023, Chittagong University of Engineering and Technology, Chittagong, Bangladesh.

Acknowledgement

At the outset, I express my deepest gratitude to Allah, the almighty and the most beneficent, for granting me the strength and resources to successfully complete the thesis work.

I am deeply grateful to my supervisor, Professor Dr. Sunil Dhar, Department of Mathematics, Chittagong University of Engineering and Technology (CUET), for his unwavering support and guidance throughout my thesis work. His extensive knowledge and expertise in ionization greatly enhanced my understanding of both methodological and theoretical aspects of my research.

I sincerely thank Professor Dr. Musammet Tahmina Akter, the Head, Department of Mathematics, CUET, for her support, resources, and leadership, which were instrumental in my effective research completion.

I would like to thank all faculty members of the Department of Mathematics, CUET, for their support during my M. Phil. studies. I am especially grateful to Professor Dr. Ashutose Saha and Professor Dr. Md. Golam Hafez for their guidance and encouragement from the start of my program.

I am grateful to the authority of CUET for crucial support and resources during my thesis work which greatly contributed to my success.

I am deeply grateful to my parents for their support and belief in my pursuit of knowledge and success, which has been a constant source of inspiration and motivation. I am sincerely grateful to my wife Marzia Akther and son Ihtisham Miraj Chowdhury for their unwavering support and encouragement throughout my journey. Their love and support have been invaluable, and I could not have come this far without them.

I would also like to extend my gratitude to all my relatives, friends, and well-wishers for their warm support and encouragement throughout this journey.

Abstract

This thesis focuses on the ionization of hydrogen atoms by electrons in an asymmetric coplanar geometry, which plays a crucial role in atomic ionization problems. The Double Differential Cross Sections (DDCS) from the ionization of hydrogen atoms with different kinematic conditions offer valuable insights into various fields, including Applied Mathematics, Applied Physics, Atomic Physics, Astrophysics, Plasma Physics, and Fusion Technology.

The present study uses a multiple scattering theory to examine the ionization of metastable 2S-state hydrogen atoms by non-relativistic intermediate and high-energy electrons. This theory has already proven to be successful in previous studies of DDCS results in the ground state and Triple Differential Cross Sections (TDCS) results for metastable 2S, 2P, 3P, 3S and 3D states of hydrogen atoms by electrons.

We start our work by discussing the multiple scattering theory and other relevant theories related to the ionization of hydrogen atoms by electrons. The first Born DDCS for H(2S) ionization at incident energies of 150eV and 250eV are also investigated and the results show significant curve structures. The DDCS for the ionization of metastable 2S state hydrogen atoms by electrons, taking into account the direct T-matrix element and its exchange effects in coplanar asymmetric geometry, produces intriguing curve structures.

The results of the simulation show good qualitative accord with theoretical and experimental data for the hydrogenic ground state. The physical origins of the curve shapes in the cross section results are explained clearly in the study. Further calculations using other familiar methods would also be of interest.

বিমূর্ত

এই থিসিসটি একটি অপ্রতিসম সমতলীয় জ্যামিতিতে ইলেকট্রন দ্বারা হাইড্রোজেন পরমাণুর আয়নকরনের উপর মনোনিবেশ করে, যা পারমানবিক আয়নকরন সমস্যায় গুরুত্বপূর্ণ ভূমিকা পালন করে। বিভিন্ন গতিশীল অবস্থার সাথে হাইড্রোজেন পরমাণুর আয়নকরন থেকে ডাবল ডিফারেনশিয়াল ক্রস সেকশন (DDCS) ফলিত গনিত, ফলিত পদার্থবিদ্যা, পারমানবিক পদার্থবিদ্যা, জ্যোতির্পদার্থবিদ্যা, প্লাজমা পদার্থবিদ্যা এবং ফিউশন প্রযুক্তি সহ বিভিন্ন ক্ষেত্রে মূল্যবান ব্যাখ্যা প্রদান করে।

বর্তমান অধ্যয়ন অ-আপেক্ষিক মধ্যবর্তী এবং উচ্চ শক্তি ইলেকট্রন দ্বারা মেটাস্টেবল 2S স্টেট হাইড্রোজেন পরমাণুর আয়নকরণ পরীক্ষা করার জন্য একটি মাল্টিপল স্ক্যাটারিং তত্ত্ব ব্যবহার করে। এই তত্ত্বটি ইতিমধ্যেই ইলেকট্রন দ্বারা হাইড্রোজেন পরমাণুর গ্রাউন্ড স্টেটে DDCS ফলাফল এবং মেটাস্টেবল 2S, 2P, 3S এবং 3D অবস্থার জন্য ট্রিপল ডিফারেনশিয়াল ক্রস সেকশন (TDCS) ফলাফলের পূর্ববর্তী গবেষণায় সফল বলে প্রমানিত হয়েছে।

আমাদের কাজ মাল্টিপল স্ক্যাটারিং তত্ত্ব এবং ইলেকট্রন দ্বারা হাইড্রোজেন পরমাণুর আয়োনাইজেশন সম্পর্কিত অন্যান্য প্রাসঙ্গিক তত্ত্ব আলোচনা করে শুরু করি। 150eV এবং 250eV আপতিত শক্তিতে H(2S) আয়োনাইজেশনের জন্য ফার্স্ট বর্ন DDCS এর ফলাফল বিশ্লেষণ করা হয় এবং ফলাফলগুলি গুরুত্বপূর্ণ বক্রগুচ্ছ দেখায়। ইলেকট্রন দ্বারা মেটাস্টেবল 2S স্টেট হাইড্রোজেন পরমাণুর আয়োনাইজেশনের জন্য DDCS অপ্রতিসম সমতলীয় জ্যামিতিতে সরাসরি T-ম্যাট্রিক্স উপাদান এবং এর এক্সচেঞ্জ প্রভাবগুলি নেওয়া হয়,আগ্রহজনক বক্রগুচ্ছ তৈরি করে।

সিমুলেশনের ফলাফল হাইড্রোজেনিক গ্রাউন্ড স্টেটের জন্য তাত্ত্বিক এবং পরীক্ষামূলক তথ্যের সাথে ভাল গুণগত চুক্তি দেখায়। ক্রস বিভাগের ফলাফলে ভৌত উৎপত্তি গবেষণায় স্পষ্টভাবে ব্যাখ্যা করা হয়েছে। অন্যান্য পরিচিত পদ্ধতি ব্যবহার করে আরও গবেষণা করা আগ্রহের বিষয় হবে।

Table of Contents

List of Figures

List of Tables

Table No. **Table Caption** **Page No.**

Nomenclature

H	Hydrogen
N	Normalization d constant
DCS	Differential cross Section
TDCS	Triple differential cross Section
DDCS	Double differential cross Section
SDCS	Single differential cross Section
$\bar{\gamma}_1$	Position vector of the atomic electron
$\bar{\gamma}_2$	Position vector of the projectile electron
$\psi_F^{(-)}$	Final state scattering wave function
Φ_I	Initial channel unperturbed wave function
V_I	Perturbation potential in the initial channel
f	Direct scattering amplitude
g	Exchange scattering amplitude
$\bar{p}_1$	Momentum for the ejected electron
$\bar{p}_2$	Momentum for the scattered electron
$\bar{p}_I$	Momentum for the incident electron
E_1 `	Ejected energy of electron
E_2	Scattered energy of electron
E_I	Incident energy of electron
$d\mu$	Solid angle
T_{FI}	Transition matrix
θ_1	Ejected angle
θ_2	Scattered angle
μ_1	Solid angle of ejected electron
μ_2	Solid angle of scattered electron
Ze	Nuclear charge of hydrogenic atom

Chapter 1: INTRODUCTION

1.1 BACKGROUND AND MOTIVATION

The atomic ionization by charged particles is a fundamental area of study in atomic physics. Ionization refers to the process in which a charged particle interacts with an atom, resulting in the removal of one or more electrons from the atom, thereby creating ions.

The study of ionization processes is crucial for understanding various phenomena and applications in physics as well as in applied mathematics. It elucidates the charged particles' behaviour, the properties of atoms, and the interactions between them. This knowledge plays significant role in plasma physics, radiation physics, accelerator science, astrophysics, fusion technology and materials science.

The atomic ionization by charged particles can occur through different mechanisms, depending on the nature of the incident particle and the target atom. For example, ionization can result from the interaction between electron and atom, the impact of an energetic ion on an atom, or the absorption of a photon by an atom.

One of the primary goals in investigating ionization is to determine the cross-sections associated with these processes. Cross-section quantify the probability of a specific interaction occurring between the incident charged particle and the target atom. They represent an effective area that characterizes the likelihood of an interaction-taking place.

1.2 CONTEXT

Cross-sections can be measured experimentally or calculated theoretically. Experimental measurements involve studying the interaction between charged

particles and target atoms under controlled conditions. Sophisticated experimental techniques, such as electron spectrometers, time-of-flight detectors, or ionization chambers, are used to measure the resulting ionization signals.

Theoretical calculations of cross-sections rely on quantum mechanical models and computational methods. Quantum mechanics provides the theoretical framework for understanding the behaviour of charged particles and atoms at the atomic and subatomic levels. Theoretical models often involve solving complex equations derived from quantum mechanics, considering factors such as electron wave functions, potential energy surfaces, and scattering theories.

Accurately determining cross-section results for ionization processes poses significant mathematical challenges. The complexity arises from the quantum nature of both the charged particles and the target atoms, as well as the intricacies of their interactions. Mathematical techniques, numerical methods, and computational simulations are employed to tackle these challenges and obtain accurate cross-section results.

Investigations into the ionization of atoms by charged particles have led to a deeper understanding of atomic and subatomic phenomena. The knowledge gained from these studies has applications in diverse areas, ranging from the development of energy sources like nuclear fusion to the design of particle accelerators and the interpretation of astronomical observations.

Overall, investigating the atomic ionization by charged particles is a multidisciplinary endeavour that combines experimental measurements, theoretical modelling, and mathematical analysis.

1.3 AIMS AND OBJECTIVES

The process of ionizing electrons from hydrogenic metastable 2S-state is an important area of research with various aims and objectives. This particular process involves the removal of an electron from an excited hydrogen atom that is in a long-lived 2S state.

Here are some aims and objectives of studying the process of ionizing electrons from hydrogenic metastable 2S-state atoms:

1.3.1 Understanding Excited-State Dynamics

Ionization process provides insights into the dynamics of excited hydrogen atoms. By studying the process of ionizing electrons from hydrogenic metastable 2S-state atoms, researchers can gain a deeper understanding of the behaviour of atoms in highly excited states, including the mechanisms that lead to the ionization of electrons.

1.3.2 Exploring Electron Correlation Effects

Ionization from metastable 2S-state hydrogen atoms involves complex electron-electron interactions. Studying this process helps in exploring electron correlation effects, which play a significant role in atoms and molecules. Understanding these effects is crucial for developing accurate theoretical models and computational methods in quantum chemistry.

1.3.3 Probing Quantum Electrodynamics (QED)

The process of ionizing electrons from hydrogenic metastable 2S-state can provide opportunities to test and probe the predictions of quantum electrodynamics (QED), which is the theory that describes the interactions between charged particles and electromagnetic fields. Precise experimental measurements of ionization rates and cross-sections may be compared with theoretical calculations, allowing for tests of QED and assessments of its accuracy.

1.3.4 Applications in Plasma Physics

The process of ionizing electrons from hydrogenic metastable 2S-state has implications for plasma physics. Understanding the ionization processes in plasmas is crucial for applications such as plasma diagnostics, fusion research, and the development of plasma-based technologies.

1.3.5 Astrophysical Relevance

The study of the process of ionizing electrons from hydrogenic metastable 2S-state has implications for astrophysics. Excited hydrogen atoms can be found in various astrophysical environments, such as stellar atmospheres, interstellar medium and cosmological plasmas. Understanding the ionization processes from these states helps in interpreting observational data and modeling astrophysical phenomena accurately.

1.3.6 Laser-Atom Interactions

Ionization from hydrogenic metastable 2S-state is of interest in laser-atom interactions. Excited-state hydrogen atoms can be used as targets for laser-induced ionization experiments, which allow for investigations of strong-field physics and the control of atomic and molecular processes using laser fields. Understanding the ionization dynamics from metastable states contributes to the development of advanced laser techniques and applications.

1.4 SIGNIFICANCE, SCOPE AND DEFINITIONS

In our current research, we are utilizing a wave function developed by Das [1], Das and Seal [2]-[4], which characterizes a multiple scattering state. This approach has allowed us to make significant advancements in our understanding of ionization research. By using this wave function, we are able to conduct more detailed and nuanced analyses, which has the potential to improve our comprehension of the mechanisms underlying ionization. Overall, this research has the potential to contribute to new knowledge in the field of

ionization research, and has the potential to have practical applications in various fields of applied mathematics.

1.4.1 Units

To conduct our non-relativistic scattering analysis, we utilized atomic units (au) with values of h=1, e=1, and m_e=1. In terms of energy measurement, we choose to use the electron Volt (eV) as our unit of measurement for all incident, scattered, and ejected energies. Additionally, we measured all angles in degrees. This system of measurement is commonly used in atomic and nuclear physics, and using eV as our energy unit allowed us to effectively compare our estimations with both experimental outcomes and other previous theoretical studies.

1.4.2 Range of energy

Our study focused on hydrogen atoms within an energy range of 100eV to 250eV.

1.4.3 Differential Cross-Section (DCS)

The DCS is a fundamental concept in the realm of particle physics and quantum mechanics. It serves as a mathematical tool to describe and predict how particles behave when they collide. Specifically, it helps us understand the likelihood of particles scattering at various angles or acquiring specific momenta during such collisions. In essence, it offers crucial insights into how particles change their paths or trajectories when they come into contact with one another during experimental collisions. This information is vital for scientists as it aids in unravelling the intricate interactions and characteristics of particles at the quantum level.

1.4.4 Single Differential Cross-Section (SDCS)

The single differential cross-section (SDCS) represents the ionization probability of a hydrogen atom into a specific final state per unit energy

transfer. It is denoted by $\frac{d\sigma}{dE}$ where $d\sigma$ is the differential cross-section (DCS) and dE is the energy transfer from the incident particle to the ionized electron. The single differential cross-section (SDCS) provides information about the energy distribution of the ionized electrons.

1.4.5 Double Differential Cross Section (DDCS)

The double differential cross section (DDCS) denoted by $\frac{d^2\sigma}{dEd\mu_1}$ represents the ionization probability per unit solid angle and per unit energy transfer. Here, dE is the energy transfer from the incident particle to the ionized electron, and $d\mu_1$ is the solid angle element. The double differential cross section (DDCS) gives more elaborated information about the process of ionization by taking into account both the angular distribution and the energy transfer of the ionized electrons.

1.4.6 Triple Differential Cross Section (TDCS)

TDCS denoted as $\frac{d^3\sigma}{dEd\mu_1 d\mu_2}$ is a concept in particle physics and quantum mechanics that extends the notion of the differential cross section (DCS). It quantifies the probability of a scattering event in which three specific variables are simultaneously measured after a collision or interaction between particles.

The triple differential cross section provides a detailed description of how particles scatter or interact, considering the directions in which they are interacted ($d\mu_1$ and $d\mu_1$) as well as the energy distribution of one of the particles (dE) as they emerge from the collision process. It is a valuable tool in experiments and theoretical calculations for understanding complex particle interactions and their outcomes.

1.4.7 Ionization Cross Sections for Low-Energy Collisions: A Brief Overview

Bathe [1] was the first to approach the theoretical study of atomic ionization by fast particles using quantum mechanics. Early research on

ionization primarily focused on the first Born approximation, while experimental research centred on total cross sections. Because actual findings were available, particularly for double differential cross sections [5]–[11] and single differential cross sections [3], [6], [12], and [13], hydrogen atom ionization by electrons provided an excellent platform for testing perturbation theory. The use of (e, 2e) coincidence experiments to analyse DDCS has yielded vast amounts of information about single ionization. These types of experiments were first performed by Ehrhadt et al. [14], Amaldi et al. [15] and many more have been carried out by various researchers [16]-[23].

Ehrhardt et al. [21] conducted a review of these experiments. Over the last fifty years, the study of DDCS in ionizing a hydrogen atom using electron collisions has become increasingly compelling. This approach has allowed researchers to investigate ionization processes in both the ground state [24]-[33] and [34]-[48] metastable states of hydrogen atoms in-depth, as demonstrated by numerous studies conducted by various researchers.

The DDCS is the theory's most sensitive tool for studying single ionization, because in the (e, 2e) reaction, all kinematic parameters are completely specified, which avoids any loss of information through averaging over unobserved variables. By integrating the triple differential cross section across different angular directions, we can derive numerous double and single differential cross sections. The total ionization cross section depends only on the incident electron energy and may be found by integrating across all emitted electrons, scattering angles and energies, $d\mu_1$, $d\mu_2$ or dE.

When dealing with asymmetric geometries, the momentum distribution among outgoing electrons is not uniform. Specifically, the Ehrhardt type of asymmetric geometry [14], [21] features a small and fixed scattering angle of the fast electron, which results in a small magnitude of the momentum transfer

$|\bar{t}| = |\overline{p_1} - \overline{p_2}|$. Meanwhile, the angle, θ_1 of the slow electron is changed, leading to variations in the momenta of the outgoing electron.

Hafid et al. [39] have provided evidence that utilizing Brauner et al. [49] corrected double continuum wave function [49], on hydrogen atoms, produces results that are similar to second Born approximations. The BBK (Brauner, Briggs, and Klar) theory [49] centres on improving the final state wave function by factoring in all long-range Coulomb interactions, such as electron-electron repulsion, to guarantee the appropriate boundary condition is satisfied as the particle separations reach infinity.

The initial theoretical investigation on double differential cross-sections (DDCS) was executed at very high energies, utilizing the plane-wave Born approximation by Massey & Mohr [50] and Mc Carrol [51]**.** After a considerable amount of time, experimental measurements of DDCS in angle and energy were carried out by Shyn [52]-[57] and other research groups [58]-[68] at even higher energies. As a result, Shyn [6] conducted experiments to measure the Double Differential Cross Section (DDCS) of secondary electrons emitted from atomic hydrogen when exposed to electrons. These measurements were taken over an angular range from 12° to 156° and at intermediate incident energy levels. The theoretical studies on double differential cross-sections (DDCS) based on Born approximation were conducted by Das [68], Das and Seal [2]-[3] at intermediate energies for ionization of hydrogen atoms by electron.

Experiments conducted by Shyn [6] have revealed several important features, including absolute DDCS measurements. These measurements were then successfully reproduced in a theoretical treatment using a second Born calculation performed by Byron et al. [24] for the (e, 2e) reaction in atomic hydrogen. The Eikonal Born Series (EBS) theory has also been shown to provide a good representation of measurements, with results that are very close to the second Born values [75] [76] further refined EBS results with UEBS calculations.

Other significant findings have been obtained by Balyan and Srivastava [77] using EBS, Curran and Walters [8] using a coupled pseudo-state calculation, and Brauner et al. [49] using the asymptotic three body Coulomb conditions and the final state wave function.

1.4.8 Theoretical Studies on Atomic Ionization: Insights and Applications

Born Series

The Born Series is a mathematical method used to evaluate the scattering amplitude in atomic ionization problems. It involves expanding the final channel scattering state wave function [78] in a series and truncating it to different terms to obtain different Born approximations. The direct scattering amplitude in the Born series can be expressed as:

$$f = \sum_{n=1}^{\infty} \bar{f}_{Bn} \qquad (1.1)$$

where the nth Born term, $\bar{f}_{Bn}$ is composed of n instances of the direct interaction potential, V_d and (n-1) instances of the direct Green's operator, G_d^+ represented by $(E - H_d + i\varepsilon), \varepsilon \to 0^+$. The Hamiltonian, H_d is a combination of the kinetic energy operator of the projectile and the target. On the other hand, the interaction potential is given by, $V_d = Z/\gamma_2 - Z/\gamma_{12}$.

Here, Z is +1 for incident electrons and -1 for incident positrons and $\gamma_{12} = |\overline{\gamma_2} - \overline{\gamma_1}|$, where $\overline{\gamma_2}$ is the position vector of the projectile and $\overline{\gamma_1}$ is that of the target electron.

1.4.9 The first Born approximation

The first Born amplitude is a simplified version of the Born series for the first Born term. For the electron impact ionization of ground-state atomic hydrogen, we can simplify the first Born amplitude by using the initial scattering wave function $\Psi_I^+(\bar{\gamma}_2, \bar{\gamma}_1)$ to replace the full scattering wave function in the direct scattering amplitude $f(\bar{p}_1, \bar{p}_2)$. This estimation takes the form:

$$\Psi_I^+(\bar{\gamma}_2, \bar{\gamma}_1) = (2\pi)^{-\frac{3}{2}} exp(i\bar{p}_1, \bar{p}_2)\varphi_{1S}(\bar{\gamma}_1)$$

Here, $\varphi_{1S}(\bar{\gamma}_1)$ represents the ground state wave function of the hydrogen atom. The direct scattering amplitude in this case is given by:

$$f(\bar{p}_1, \bar{p}_2) = -(2\pi)^2 \left\langle exp(i\bar{p}_2, \bar{\gamma}_2)\Psi_c^{(-)}{}_{,\bar{p}_1}(\bar{\gamma}_1) \middle| 1/\gamma_{21} - 1/\gamma_2 \middle| \Psi_I^+(\bar{\gamma}_2, \bar{\gamma}_1) \right\rangle \qquad (1.2)$$

Where $\Psi_c^{(-)}$ represents the complex conjugate of the outgoing wave function.

The first Born term, denoted as $\bar{f}_{B1}$, can be expressed as:

$$\bar{f}_{B1}(\bar{p}_1, \bar{p}_2) = -(2\pi)^{-1}\left\langle exp(i\bar{p}_1, \bar{\gamma}_2)\Psi_c^{(-)}{}_{,\bar{p}_1}(\bar{\gamma}_1)\middle|1/\gamma_{21}\middle|exp(i\bar{p}_I, \bar{p}_2)\varphi_{1S}(\bar{\gamma}_1)\right\rangle \quad (1.3)$$

Here, the term $(-1/\gamma_2)$ is eliminated due to the orthogonality of the initial and final target states.

When we integrate with respect to $\bar{\gamma}_1$, we get the expression for the matrix element $M(\bar{t},\ \bar{p}_1)$:

$$M(\bar{t}, \bar{p}_1) = \left\langle \Psi_c^{(-)}{}_{,\bar{p}_1}(\bar{\gamma}_1)\middle|exp(i\bar{t}, \bar{\gamma}_1)\middle|\varphi_{1S}(\bar{\gamma}_1)\right\rangle$$

This matrix element can be written as:

$$M(\bar{t},\ \bar{p}_1) = \frac{4\sqrt{2}\exp(\pi\alpha_1/2)\Gamma(1-i\alpha_1)(t^2-\bar{p}_1.\bar{t}-i\alpha_1\bar{p}_1.\bar{t})\exp(i\alpha_1 ln\nu)}{\pi t^2\{t^2-(i+p_1)^2\}\{1+(\bar{t}-\bar{p}_1)^2\}^2}$$

(1.4)

Here, ν is defined as $\nu = \frac{1+(\bar{t}-\bar{p}_1)^2}{t^2-(i+p_1)^2}$ and α_1 is equal to $1/p_1$ and $\Psi_c^{(-)}{}_{,\bar{p}_1}(\bar{\gamma}_1)$ is the Coulomb wave function for momentum $\bar{p}_1$, satisfying incoming wave boundary condition.

One interesting observation about the first Born amplitude, f_{B1} is that it displays distinct characteristics when it comes to its response to small and large momentum transfers. For small momentum transfers, f_{B1} varies like t^{-1} because the ionization is mainly into the continuum P state. This can be attributed to the fact that $M(\bar{t},\ \bar{p}_1)$ is proportional to the dot product of $\bar{t}$ and $\bar{p}_1$ in this region.

On the other hand, for large momentum transfers, $M(\bar{t},\ \bar{p}_1)$ is proportional to t^{-4}, which causes f_{B1} to fall off like t^{-6}, a characteristic of ionization into the S-state. This means that as the momentum transfer increases beyond a certain point, the ionization process becomes more likely to produce the S-state.

1.4.10 The second Born approximation

The direct second Born scattering amplitude for an atom with Z electrons, denoted as $\bar{f}_{B2}(\bar{p}_1, \bar{p}_2)$, can be expressed [81] as

$\bar{f}_{B2}(\bar{p}_1, \bar{p}_2)=$

$$(8\pi^4)^{-1} \sum_n \int d\bar{q}\{1/q^2 - {p_n}^2 - i\varepsilon\} \left\langle exp(i\bar{p}_1, \bar{\gamma}_2)\Psi_c^{(-)}{}_{,\bar{p}_1}(\bar{\gamma}_1)\middle|V\middle|exp(i\bar{q}.\bar{\gamma}_2)\varphi_n(\bar{\gamma}_1)\right\rangle$$

$$\langle exp(i\bar{q}.\bar{\gamma}_2)\varphi_n(\bar{\gamma}_1)|V|exp(i\bar{p}_i, \bar{\gamma}_2)\varphi_{1S}(\bar{\gamma}_1)\rangle, where\ \varepsilon \to 0^+ \quad (1.5)$$

Here, $V_d = 1/\gamma_{12} - 1/\gamma_2$, and ${p_n}^2 = {p_I}^2 - (w_n - w_{1s})$

This expression can be understood as depicting two distinct events involving an incoming electron and its interaction with the potential V. In the first event, the electron interacts with the target, causing it to transition to an intermediate state with energy w_n, which could be either a bound state or a continuum state. During this interaction, the electron imparts a momentum change of $\bar{p}_I - \bar{q}$ to the system. In the second event, the target, now in the intermediate state, undergoes ionization, leading to the creation of a continuum state with momentum $\bar{p}_I$. This ionization process results in a different momentum transfer, specifically $\bar{p}_I - \bar{q}$.

The direct second Born scattering amplitude (1.5) for an atom with Z electrons can be simplified using the Bethe [68] integral as shown in the following equation

$\bar{f}_{B2}(\bar{p}_1, \bar{p}_2)=$

$$(2/\pi^2) \sum_n \int d\bar{q}\{1/(q^2 - {p_n}^2 - i\varepsilon)\Delta_i^2\Delta_f^2\} \sum_n \left\langle \Psi_c^{(-)}{}_{,\bar{p}_1}(\bar{\gamma}_1)\middle|(exp(i\Delta_f, \bar{\gamma}_1) - 1)\middle|\varphi_n(\bar{\gamma}_1)\right\rangle$$

$$\left\langle \varphi_n(\bar{\gamma}_1)\middle|(exp(-i\Delta_f, \bar{\gamma}_1) - 1)\middle|\varphi_{1S}(\bar{\gamma}_1)\right\rangle \quad (1.6)$$

Where $\Delta_I = \bar{q} - \bar{p}_I$ and $\Delta_f = \bar{q} - \bar{p}_2$

The result of simplified second Born term can be expressed as:

$\bar{f}_{B2}(\bar{p}_1, \bar{p}_2)=$

$$(2/\pi^2) \int d\bar{q}\{1/(q^2 - {p_n}^2 - i\varepsilon)\Delta_I^2\Delta_f^2\} \left\langle \Psi_c^{(-)}{}_{,\bar{p}_1}(\bar{\gamma}_1)\middle|(exp(i\Delta_f, \bar{\gamma}_1) - 1)(exp(-i\Delta_f, \bar{\gamma}_1) - 1)\middle|\varphi_{1s}(\bar{\gamma}_1)\right\rangle$$

(1.7)

Here $p^2 = p_i^2 - 2\bar{w}$

The triple Differential cross sections (TDCS) can be given by

$$\frac{d^3\sigma}{d\mu_1 d\mu_2 dE_1} = \frac{p_1 p_2}{p_i}\left|\bar{f}_{B1} + \bar{f}_{SB2}\right|^2 \tag{1.8}$$

The second Born double differential cross section (DDCS) results can be obtained by integrating the triple differential cross section (TDCS) results over μ_2 as given by

$$\frac{d^2\sigma}{d\mu_1 dE_1} = \int \frac{d^3\sigma}{d\mu_1 d\mu_2 dE_1} d\mu_2 \tag{1.9}$$

1.4.11 BBK model (Theory of Brauner, Briggs, Klar)

Brauner et al. [49] have improved the wave function used to describe the interaction between electrons and ions in hydrogen atoms by including both electron-ion interactions and electron-electron repulsion. The wave function conforms to the appropriate boundary condition as the separation between particles approaches infinity. The wave function has the following structure:

$$\Psi^{(-)}_{fBBK}(\bar{\gamma}_1,\ \bar{\gamma}_2) = (2\pi)^{-3/2} exp(i\bar{p}_1,\bar{\gamma}_1) C(-\alpha_1,\bar{p}_1,\bar{\gamma}_1)(2\pi)^{-3/2} exp(i\bar{p}_2,\bar{\gamma}_2)$$
$$C(-\alpha_2,\bar{p}_2,\bar{\gamma}_2) C(-\alpha_{12},\bar{p}_{12},\bar{\gamma}_{12}) \qquad (1.10)$$

where the Coulomb factor C is given by:

$$C(\alpha,\ \bar{p},\bar{\gamma}) = \exp(-\pi\alpha/2)\Gamma(1-i\alpha)_1F_1(-i\alpha,1,-i(pr+\bar{p}.\bar{\gamma}))$$

Here, $\alpha_1 = \frac{1}{p_1}, \alpha_2 = \frac{1}{p_2}$ and $\alpha_1 = \frac{1}{2p_{12}}$ where $\bar{p}_{12} = \frac{\bar{p}_1 - \bar{p}_2}{2}$ and $\bar{\gamma}_{12} = \frac{\bar{\gamma}_1 - \bar{\gamma}_2}{2}$

Brauner et al. [49] derived an expression for the correct asymptotic type of the three-body Coulomb wave function and showed that the wave function (1.10) satisfies this asymptotic condition exactly.

In BBK calculation, one has the Perturbation Potential as

$$V_I(\bar{\gamma}_1,\bar{\gamma}_2) = \text{-}1/\gamma_2 + 1/\gamma_{12}$$

For Ground State

$$\emptyset_I(\bar{\gamma}_1,\bar{\gamma}_2) = (2\pi)^{-3/2} exp(i\bar{p}_2.\bar{\gamma}_2)\varphi_{1S}(\bar{\gamma}_1)$$
$$= (2\pi)^{-3/2} exp(i\bar{p}_2,.\bar{\gamma}_2)\frac{1}{\sqrt{\pi}} e^{-\gamma_1}$$

For metastable 2S State

$$\emptyset_I(\bar{\gamma}_1,\bar{\gamma}_2) = (2\pi)^{-3/2} exp(i\bar{p}_2.\bar{\gamma}_2)\varphi_{2S}(\bar{\gamma}_1)$$
$$= (2\pi)^{-3/2} exp(i\bar{p}_2.\bar{\gamma}_2)\frac{1}{4\sqrt{2\pi}}(2-\gamma_1)e^{\frac{-\gamma_1}{2}}$$

For metastable 2P State

$$\emptyset_I(\bar{\gamma}_1,\bar{\gamma}_2) = (2\pi)^{-3/2} exp(i\bar{p}_2.\bar{\gamma}_2)\varphi_{2P}(\bar{\gamma}_1)$$
$$= (2\pi)^{-3/2} exp(i\bar{p}_2.\bar{\gamma}_2)\frac{1}{4\sqrt{2\pi}}\gamma_1 e^{\frac{-\gamma_1}{2}} cos\theta$$

For metastable 3S State

$$\emptyset_I(\bar{\gamma}_1,\bar{\gamma}_2) = (2\pi)^{-3/2} exp(i\bar{p}_2.\bar{\gamma}_2)\varphi_{3S}(\bar{\gamma}_1)$$

$$= (2\pi)^{-3/2} exp(i\bar{p}_2.\bar{\gamma}_2) \frac{1}{81\sqrt{3\pi}} (27 - 18\gamma_1 + 2{\gamma_1}^2) e^{\frac{-\gamma_1}{3}}$$

For metastable 3P State

$$\emptyset_I(\bar{\gamma}_1, \bar{\gamma}_2) = (2\pi)^{-3/2} exp(i\bar{p}_2.\bar{\gamma}_2) \varphi_{3P}(\bar{\gamma}_1)$$

$$= (2\pi)^{-3/2} exp(i\bar{p}_2.\bar{\gamma}_2) \frac{\sqrt{2}}{81\sqrt{\pi}} (6 - \gamma_1)\gamma_1 e^{\frac{-\gamma_1}{3}} cos\theta$$

Hence

$$T_{BBK}(\bar{p}_1, \bar{p}_2) = \int d^3\gamma_1 d^3\gamma_2 \Psi^{(-)}_{BBK}(\bar{\gamma}_1, \bar{\gamma}_2)\, V_I(\bar{\gamma}_1, \bar{\gamma}_2) \emptyset_I(\bar{\gamma}_1, \bar{\gamma}_2) \quad (1.11)$$

The application of a certain theory yielded TDCS and DDCS results that were consistent with experimental and theoretical findings in certain scenarios, such as the highly asymptotic Ehrhardt type geometry [14]. However, for ionization from ground state hydrogen atoms with increasing momentum transfer, significant deviations were observed from experimental results [6]. To address this, theoretical calculations were developed by Hafid et al. [39] and Hanssen et al. [83] based on the BBK theorem for small momentum transfer asymmetric scattering from metastable hydrogen states, specifically the 2S and 2P states, with electron impact. On the other hand theoretical assessment were calculated by Das and Seal [3] and Konovalov et al. [84] based on SDCS. The calculated results were compared to experimental Shyn [6] and theoretical results [3], [84] respectively and found to be qualitatively in excellent agreement.

1.4.12 The multiple scattering theory of atomic ionization of hydrogen by electrons

The multiple scattering theory [2] uses a three-particle wave function of Das [1] to correct for the first-order interaction potentials. Further normalization is needed to make it more accurate in the asymptotic domain. It is important to note that the main contribution to the T-matrix elements comes from the finite domain in the coordinate space where the wave function needs to be accurate. The accuracy in the asymptotic domain is mainly necessary for determining the particle-flux. We have discussed this theory in detail in our thesis work.

1.4.13 The T-matrix and approximations to the final state wave function

The T-matrix element governing the atomic ionization of hydrogen by electrons [54] can be expressed as

$$T_{FI} = \left\langle \psi_F^{(-)}(\bar{\gamma}_1, \bar{\gamma}_2) \middle| V_I(\bar{\gamma}_1, \bar{\gamma}_2) \middle| \Phi_{\mathrm{i}}(\bar{\gamma}_1, \bar{\gamma}_2) \right\rangle \tag{1.12}$$

Here, $\Phi_{\mathrm{I}}(\bar{\gamma}_1, \bar{\gamma}_2) = \frac{1}{2\sqrt{2}\pi^2} \exp(\mathrm{i}\bar{\mathrm{p}}_2.\bar{\gamma}_2)\exp(-\bar{\gamma}_1)$, [Wave Function of Hydrogen's Ground State]

$V_I = 1/\gamma_{12} - 1/\gamma_2$

In addition, final state wave function $\Psi_F^{(-)}(\bar{\gamma}_1, \bar{\gamma}_2)$ satisfies the equation

$$[\tfrac{\Delta_1^2}{2} - \tfrac{\Delta_2^2}{2} + \tfrac{1}{\gamma_{12}} - \tfrac{1}{\gamma_1} - \tfrac{1}{\gamma_2} - E]\, \Psi_F^{(-)}(\bar{\gamma}_1, \bar{\gamma}_2) = 0 \tag{1.13}$$

Due to the complexity of the equation, an exact solution cannot be obtained, therefore an approximate solution must be used.

This solution matches the first-order Faddeev [85] wave function. The approximate solution, subject to incoming boundary conditions, is given by equation

$$\Phi_{p_1,p_2}^{(-)}(\bar{\gamma}_1, \bar{\gamma}_2) = \Big[\phi_{\bar{p}_1}^{(-)}(\bar{\gamma}_1) e^{i\bar{p}_2.\bar{\gamma}_2} + \phi_{\bar{p}_2}^{(-)}(\bar{\gamma}_2) e^{i\bar{p}_1.\bar{\gamma}_1} + \phi_{\bar{p}}^{(-)}(\bar{\gamma}) e^{i\bar{P}.\bar{R}} - 2e^{i\bar{p}_1.\bar{\gamma}_1 + i\bar{p}_2.\bar{\gamma}_2}\Big](2\pi)^3 \tag{1.14}$$

Where $\bar{\gamma} = \frac{\bar{\gamma}_1 - \bar{\gamma}_2}{2}$, $\bar{\Omega} = \frac{\bar{\gamma}_1 + \bar{\gamma}_2}{2}, \bar{p} = \bar{p}_1 - \bar{p}_2, \bar{P} = \bar{p}_1 + \bar{p}_2$

And $\phi_{\bar{q}}^{(-)}(\bar{\gamma}) = e^{\frac{\pi\alpha}{2}}\Gamma(1 + i\alpha)e^{i\bar{q}.\bar{\gamma}}F_1(-i\alpha, -i[qr + \bar{q}.\bar{\gamma}])$

Also, $\alpha_1 = \frac{1}{p_1}$ for $\bar{q} = \bar{p}_1$

$\alpha_2 = \frac{1}{p_2}$ for $\bar{q} = \bar{p}_2$

$\alpha = -\frac{1}{p}$ for $\bar{q} = \bar{p}$

The wave function (1.14) is not exact in the asymptotic region due to the long range of the potentials, $\frac{1}{\gamma_1}$, $\frac{1}{\gamma_2}$ and $\frac{1}{\gamma_{12}}$. However, the wave function can be made more accurate by normalizing it with a multiplicative constant $\mathrm{N}(\bar{p}_1, \bar{p}_2)$ that depends on the momenta $\bar{p}_1$ and $\bar{p}_2$.

To obtain the normalized wave function, we multiply the wave function $\Phi^{(-)}_{p_1,p_2}$ (given by equation (1.14)) by the normalization constant $\mathrm{N}(\bar{p}_1, \bar{p}_2)$, as follows:

$$\Psi^{(-)}_{p_1,p_2} = \mathrm{N}(\bar{p}_1, \bar{p}_2)\Phi^{(-)}_{p_1,p_2}$$

Here, $\Psi^{(-)}_{p_1,p_2}$ is the normalized wave function and $\mathrm{N}(\bar{p}_1, \bar{p}_2)$ is the normalization constant.

1.4.14 Normalization of the wave function

We have an exact wave function given by $\Psi_F^{(-)} = \Psi^{(-)}_{\bar{p}_1,\bar{p}_2}$ that satisfies the normalization condition approximately, which can be written as:

$$\left\langle \Psi^{(-)}_{\bar{p}_1,\bar{p}_2} \middle| \Psi^{(-)}_{\bar{q}_1,\bar{q}_2} \right\rangle \approx \delta(\bar{q}_1 - \bar{p}_1)\delta(\bar{q}_1 - \bar{p}_1) \tag{1.16}$$

Here, δ represents the Dirac delta function.

We now want to determine the normalization constant $N = N(\bar{p}_1, \bar{p}_2)$ for the approximate wave function given by $\Psi_F^{0(-)} = \Psi^{0(-)}_{p_1,p_2}$. To do this, we require that the approximate wave function satisfies the normalization condition approximately as well, which can be written as:

$$\left\langle \Psi^{0(-)}_{\bar{p}_1,\bar{p}_2} \middle| \Psi^{0(-)}_{\bar{q}_1,\bar{q}_2} \right\rangle \approx \delta(\bar{q}_1 - \bar{p}_1)\delta(\bar{q}_1 - \bar{p}_1) \tag{1.17}$$

By integrating over, the momenta of the two emitted particles, $\bar{q}_1$ and $\bar{q}_2$ gives

$$\int \left\langle \Psi^{0(-)}_{\bar{p}_1,\bar{p}_2} \middle| \Psi^{0(-)}_{\bar{q}_1,\bar{q}_2} \right\rangle d^3\bar{q}_1 d^3\bar{q}_2 \approx 1 \tag{1.18}$$

This allows us to write

$$|N(\bar{p}_1,\bar{p}_2)|^{-2} \approx \int \left\langle \Phi^{0(-)}_{\bar{p}_1,\bar{p}_2} \middle| \Phi^{0(-)}_{\bar{q}_1,\bar{q}_2} \right\rangle d^3\bar{q}_1 d^3\bar{q}_2 \tag{1.19}$$

In equation (1.19), there are a total of (1.16) integrals on the right-hand side. Among these, seven integrals can be accurately calculated.

The remaining four integrals in equation (1.19) involve the expression

$$\int \tilde{\varphi}^{(-)*}_{\bar{q}_1}(\bar{q}_1')\tilde{\varphi}^{(-)}_{\bar{p}_1}(\bar{p}_2 - \bar{q}_1')d^3\bar{q}_1 d^3\bar{q}_1'$$

which is difficult to evaluate numerically. However, a relatively accurate computation of these integrals can be achieved by using the normalization condition

$$\int \tilde{\varphi}^{(-)*}_{\bar{p}_1}(\bar{t})\tilde{\varphi}^{(-)}_{\bar{q}_1}(\bar{t})d^3t = \delta(\bar{q}_1 - \bar{p}_1) \tag{1.20}$$

Where $\tilde{\varphi}^{(-)}_{\bar{q}_1}(\bar{t})$ is highly peaked at $\bar{t} = \bar{p}_1$, similar to a Dirac delta function.

$$\int \tilde{\varphi}^{(-)*}_{\bar{p}_1}(\bar{t})\tilde{\varphi}^{(-)}_{\bar{q}_1}(\bar{t})d^3t d^3\bar{q}_1 = 1 \tag{1.21}$$

Equation (1.21) is obtained from the integral of $\int \tilde{\varphi}^{(-)*}_{\bar{q}_1}(\bar{q}_1')\tilde{\varphi}^{(-)}_{\bar{p}_1}(\bar{p}_2 - \bar{q}_1')d^3\bar{q}_1 d^3\bar{q}_1'$ where one of the functions is highly peaked at $\bar{t} = \bar{p}_1$.

$$\left|\int \tilde{\varphi}^{(-)*}_{\bar{p}_1}(\bar{t})d^3t\right| \int \tilde{\varphi}^{(-)}_{\bar{p}_1}(\bar{p}_1)d^3\bar{q}_1\Big| \approx 1 \tag{1.22}$$

Equation (1.22) expresses the result of equation (1.21) approximately as the product of the integral of $\tilde{\varphi}^{(-)*}_{\bar{p}_1}(\bar{t})$ and the integral of $\tilde{\varphi}^{(-)}_{\bar{p}_1}(\bar{p}_1)$ over all momenta.

This can be written as:

$$\int \tilde{\varphi}^{(-)*}_{\bar{p}_1}(\bar{t})d^3t = \tilde{\varphi}^{(-)*}_{\bar{p}_1}(0) = \exp(\pi\alpha_1/2)\Gamma(1 - i\alpha_1) \tag{2.23}$$

Here, $\alpha_1 = 1/p_1$, and the integral of the Fourier transform of the wave function with respect to the momentum variable can be approximated as the reciprocal of the value of the first integral evaluated at time equal to zero:

$$\int \tilde{\varphi}^{(-)*}_{\bar{q}_1}(\bar{p}_1)d^3t \approx 1/\tilde{\varphi}^{(-)*}_{\bar{p}_1}(0)$$

The integral of the product of the Fourier transforms of the wave functions φ with respect to the momentum variables p_1 and p_2, integrated over all momenta, can be obtained in the same way. The final expression for the normalization constant is then given by:

$$\mathrm{N}(\bar{p}_1, \bar{p}_2)^{-2} = \left|7 - 2[\lambda_1 + \lambda_2 + \lambda_3] - \left[\frac{2}{\lambda_1} + \frac{2}{\lambda_2} + \frac{2}{\lambda_3}\right] + \left[\frac{\lambda_1}{\lambda_2} + \frac{\lambda_1}{\lambda_3} + \frac{\lambda_2}{\lambda_1} + \frac{\lambda_2}{\lambda_3} + \frac{\lambda_3}{\lambda_1} + \frac{\lambda_3}{\lambda_2}\right]\right|$$

$$= M \exp(i\varepsilon) \qquad (1.24)$$

Here, $\lambda_1 = e^{\pi\alpha_1/2}\Gamma(1 - i\alpha_1)$ where $\alpha_1 = 1/p_1$, $\lambda_2 = e^{\pi\alpha_2/2}\Gamma(1 - i\alpha_2)$, where $\alpha_1 = 1/p_2$, and $\lambda_3 = e^{\pi\alpha_3/2}\Gamma(1 - i\alpha)$ where $\alpha = -1/p$. The phase factor ε in the expression (1.24) arises from non-neighboring elements, due to the approximation made in equation (1.17). Numerical results show that this phase ε is very small in all cases, which partly justifies the approximations used. In this calculation, ε is neglected, and the absolute value of the right-hand side of equation (1.24) is taken as an estimation of $|\mathrm{N}(\bar{p}_1, \bar{p}_2)^{-2}|$.

1.4.15 Precision of the wave function

The wave function $\Psi_f^{0(-)}$ satisfies the wave equation (1.13) as:

$$(H-E)\Psi_f^{0(-)}(\bar{\gamma}_1,\bar{\gamma}_2) = [-\Delta_1^2/2 - \Delta_2^2/2 + 1/\gamma_{12} - 1/\gamma_1 - 1/\gamma_2 - E]\Psi_f^{0(-)}(\bar{\gamma}_1,\bar{\gamma}_2)$$
$$= N\{(1/\gamma_{12} - 1/\gamma_2)\exp(i\bar{p}_2.\bar{\gamma}_2)[\phi_{p_1}^{(-)}(\bar{\gamma}_1) - \exp(i\bar{p}_1.\bar{\gamma}_1)] + (1/\gamma_{12} - 1/\gamma_2)\exp(i\bar{p}_1.\bar{\gamma}_1)$$
$$[\phi_{p_2}^{(-)}(\bar{\gamma}_2) - \exp(i\bar{p}_2.\bar{\gamma}_2)] - (-1/\gamma_1 - 1/\gamma_2)\exp(i\bar{P}.\bar{R})[\phi_p^{(-)}(\bar{\gamma}) - \exp(i\bar{p}.\bar{\gamma})]\}/(2\pi)^3 \quad (1.25)$$

However, when the momenta $\bar{p}_1$, $\bar{p}_2$ and $|\bar{p}| = |\bar{p}_1 - \bar{p}_2|$ become large, the Coulomb waves in equation (1.25) approach plane waves, and the right-hand side of equation (1.25) becomes small. Specifically, for large momenta, we have:

$\phi_p^{(-)}(\bar{\gamma}) \to \exp(i\bar{p}.\bar{\gamma})$, (keeping $\bar{\gamma}$ fixed, $p \to \infty$)

$\phi_p^{(-)}(\bar{\gamma}) \to \exp(i\bar{p}.\bar{\gamma})$, (keeping $\bar{p}$ fixed, $\bar{\gamma} \to \infty$)

Thus, in the limit of very large momenta, the wave equation (1.25) is exactly satisfied.

Furthermore, for finite momenta, the wave function $\Psi_f^{0(-)}$ may not be accurate in certain domains. When one momentum (e.g., $\bar{p}_2$) is large, and the other is not, we can approximate equation (1.25) as:

$$(H-E)\Psi_f^{0(-)}(\bar{\gamma}_1,\bar{\gamma}_2) \cong N(1/\gamma_{12} - 1/\gamma_2)\exp(i\bar{p}_2.\bar{\gamma}_2)[\phi_{p_1}^{(-)}(\bar{\gamma}_1) - \exp(i\bar{p}_1.\bar{\gamma}_1)]/(2\pi)^3 \quad (1.26)$$

We can compare this result with the first Born approximation, which yields:

$$(H-E)[\phi_{p_1}^{(-)}(\bar{\gamma}_1) - \exp(i\bar{p}_2.\bar{\gamma}_2)]/(2\pi)^3 = (1/\gamma_{12} - 1/\gamma_2)\exp(i\bar{p}_2.\bar{\gamma}_2)\phi_{p_1}^{(-)}(\bar{\gamma}_1)/(2\pi)^3 \quad (1.27)$$

We observe that the right-hand side of equation (1.26) is smaller than that of equation (1.27). Therefore, in general, the multiple scattering results (given by equation (1.26)) are expected to be more precise than the first Born results (given by equation (1.27)).

1.4.16 Lifetime of Hydrogen atom

The hydrogen atom's metastable 2S state is like a temporary energy trap, existing longer than most excited states but not as long as the ground state. Its lifetime is quantified using parameters like half-life, decay constant, or the Einstein coefficient. In this case, the lifetime, t_I is calculated using the inverse of the Einstein coefficient, A_{ij} as shown [86], [87] in the following equation

$$t_I = \sum(A_{ij})^{-1} \tag{1.28}$$

Here, A_{ij} denote Einstein coefficient.

1.5 RESEARCH METHODOLOGY

The ionization rate per unit time and unit target, compared to the incident electron flux ionization cross-sections, can be used to check the accuracy of perturbation theory. The ionization of atomic hydrogen by electrons is a good example for this purpose, as experimental results such as TDCS and DDCS exist. In these calculations, the ejected electron has been detected simultaneously with the scattered electron, in what is known as an (e, 2e) coincidence experiment. This theory is well-established and widely used in this field.

1.5.1 Scattering Mechanism

One type of electron-induced ionization process in atomic hydrogen involves the creation of a singly ionized state, and can be represented as

$$e^- + H(2S) \rightarrow H^+ + 2e^- \tag{1.29}$$

In the context of atomic hydrogen, the symbol 2S represents a metastable state that has been studied using TDCS (Triple Differential Cross Section) measurements obtained from (e, 2e) coincidence experiments.

In the study of ionization of hydrogen atoms by electrons in metastable 2S-state, the TDCS (two-dimensional differential cross section) is commonly

used, which is represented by $\frac{d^3\sigma}{d\mu_1 d\mu_2 dE_1}$. This function depends on various variables such as E_i, E_1, or E_2, θ_1, θ_2 and $\phi = \phi_1 - \phi_2$, assuming unpolarized incident electrons and targets.

By integrating TDCS over $d\mu_2$ and $d\mu_1$, we can obtain the DDCS (double differential cross section) and SDCS (single differential cross section) respectively. These cross sections are essential in analysing the ionization of hydrogen atoms by electrons in the 2S-state.

In this study, our primary goal is to calculate the total ionization cross section for the interaction between electrons and metastable 2S-state hydrogen atoms. To achieve this, we integrate the Double Differential Cross Section (DDCS) and Single Differential Cross Section (SDCS) over all possible outgoing scattering angles and energies. Importantly, these cross sections are solely dependent on the incident energy E_I.

In (e, 2e) coincidence experiments, distinguishing between coplanar and non-coplanar geometries is vital for precise theoretical analysis of the collision dynamics.

To better understand, the kinematics of an (e, 2e) reaction, Fig. 2.1 illustrates the different components involved in the collision. It is essential to consider these various arrangements when analysing the results of (e, 2e) coincidence experiments.

1.5.2 T-Matrix Element

The direct Transition matrix element for ionization of hydrogen atoms by electron [33], may be written as,

$$T_{FI} = \left\langle \psi_F^{(-)}(\bar{\gamma}_1, \bar{\gamma}_2) \middle| V_I(\bar{\gamma}_1, \bar{\gamma}_2) \middle| \Phi_i(\bar{\gamma}_1, \bar{\gamma}_2) \right\rangle \tag{1.30}$$

Where the perturbation potential $V_I(\bar{\gamma}_1, \bar{\gamma}_2)$ is given by

$$V_I(\bar{\gamma}_1, \bar{\gamma}_2) = \frac{1}{\gamma_{12}} - \frac{1}{\gamma_2} \tag{1.31}$$

For hydrogen atoms nuclear charge is Ze=1, γ_1 and γ_2 are the distances of the two electrons from the nucleus and γ_{12} is the distance between the two electrons.

The initial channel unperturbed wave function is given by

$$\Phi_i(\bar{\gamma}_1, \bar{\gamma}_2) = \frac{e^{i\bar{p}_i \cdot \bar{\gamma}_2}}{(2\pi)^{\frac{3}{2}}} \phi_{2S}(\bar{\gamma}_1) \tag{1.32}$$

Where $\phi_{2S}(\bar{\gamma}_1) = \frac{1}{4\sqrt{2\pi}}(2 - \gamma_1)e^{-\lambda_1 \gamma_1}$

Here $\lambda_1 = \frac{1}{2}$ and $\phi_{2S}(\bar{\gamma}_1)$ is the hydrogen 2S state wave function and $\psi_F^{(-)}(\bar{\gamma}_1, \bar{\gamma}_2)$ is the final three particle scattering state wave function [7] and co-ordinate of the two electrons are $\bar{\gamma}_1$ and $\bar{\gamma}_2$ respectively.

Here the approximate wave function $\psi_F^{(-)}$ the is given by

$$\psi_F^{(-)}(\bar{\gamma}_1, \bar{\gamma}_2) = N(\bar{p}_1, \bar{p}_2)\Big[\phi_{\bar{p}_1}^{(-)}(\bar{\gamma}_1)e^{i\bar{p}_2 \cdot \bar{\gamma}_2} + \phi_{\bar{p}_2}^{(-)}(\bar{\gamma}_2)e^{i\bar{p}_1 \cdot \bar{\gamma}_1} + \phi_{\bar{p}}^{(-)}(\bar{\gamma})e^{i\bar{P} \cdot \bar{R}} - 2e^{i\bar{p}_1 \cdot \bar{\gamma}_1 + i\bar{p}_2 \cdot \bar{\gamma}_2}\Big]/(2\pi)^3 \tag{1.33}$$

Here, $N(\bar{p}_1, \bar{p}_2)$ is normalization constant, $\bar{\gamma} = \frac{\bar{\gamma}_1 - \bar{\gamma}_2}{2}$, $\bar{R} = \frac{\bar{\gamma}_1 + \bar{\gamma}_2}{2}$, $\bar{p} = \bar{p}_2 - \bar{p}_1$, $\bar{P} = \bar{p}_2 + \bar{p}_1$, and $\phi_q^{(-)}(\bar{\gamma})$ is Coulomb wave function.

Applying equations (1.31), (1.32) and (1.33) in equation (1.30), we get

$$T_{FI} = T_b + T_b' + T_I - 2T_{PB} \tag{1.34}$$

For first Born estimation equation may be written as

$$T_b = \frac{1}{16\pi^2}\left\langle \phi_{\bar{p}_1}^{(-)}(\bar{\gamma}_1)e^{i\bar{p}_2.\bar{\gamma}_2}\left|\frac{1}{\gamma_{12}} - \frac{1}{\gamma_2}\right|e^{i\bar{p}_i.\bar{\gamma}_2}(2-\gamma_1)e^{-\lambda_1\gamma_1}\right\rangle$$

$$= \frac{1}{16\pi^2}\int\left[\phi_{\bar{p}_1}^{(-)*}(\bar{\gamma}_1)e^{-i\bar{p}_2.\bar{\gamma}_2}\left(\frac{1}{\gamma_{12}} - \frac{1}{\gamma_2}\right)e^{i\bar{p}_i.\bar{\gamma}_2}(2-\gamma_1)e^{-\lambda_1\gamma_1}\right]d^3\gamma_1 d^3\gamma_2$$

$$= \frac{1}{16\pi^2}\int\phi_{\bar{p}_1}^{(-)*}(\bar{\gamma}_1)e^{-i\bar{p}_2.\bar{\gamma}_2}\frac{1}{\gamma_{12}}2e^{i\bar{p}_i.\bar{\gamma}_2}e^{-\lambda_1\gamma_1}d^3\gamma_1 d^3\gamma_2$$

$$- \frac{1}{16\pi^2}\int\phi_{\bar{p}_1}^{(-)*}(\bar{\gamma}_1)e^{-i\bar{p}_2.\bar{\gamma}_2}\frac{1}{\gamma_2}2e^{i\bar{p}_i.\bar{\gamma}_2}e^{-\lambda_1\gamma_1}d^3\gamma_1 d^3\gamma_2$$

$$- \frac{1}{16\pi^2}\int\phi_{\bar{p}_1}^{(-)*}(\bar{\gamma}_1)e^{-i\bar{p}_2.\bar{\gamma}_2}\frac{1}{\gamma_{12}}\gamma_1 e^{i\bar{p}_i.\bar{\gamma}_2}e^{-\lambda_1\gamma_1}d^3\gamma_1 d^3\gamma_2$$

$$+ \frac{1}{16\pi^2}\int\phi_{\bar{p}_1}^{(-)*}(\bar{\gamma}_1)e^{-i\bar{p}_2.\bar{\gamma}_2}\frac{1}{\gamma_2}\gamma_1 e^{i\bar{p}_i.\bar{\gamma}_2}e^{-\lambda_1\gamma_1}d^3\gamma_1 d^3\gamma_2$$

$$= Tb_1 + Tb_2 + Tb_3 + Tb_4 \tag{1.35}$$

Here

$$Tb_1 = \frac{1}{16\pi^2}\int\phi_{\bar{p}_1}^{(-)*}(\bar{\gamma}_1)e^{-i\bar{p}_2.\bar{\gamma}_2}\frac{1}{\gamma_{12}}2e^{i\bar{p}_i.\bar{\gamma}_2}e^{-\lambda_1\gamma_1}d^3\gamma_1 d^3\gamma_2$$

$$Tb_2 = -\frac{1}{16\pi^2}\int\phi_{\bar{p}_1}^{(-)*}(\bar{\gamma}_1)e^{-i\bar{p}_2.\bar{\gamma}_2}\frac{1}{\gamma_2}2e^{i\bar{p}_i.\bar{\gamma}_2}e^{-\lambda_1\gamma_1}d^3\gamma_1 d^3\gamma_2$$

$$Tb_3 = -\frac{1}{16\pi^2}\int\phi_{\bar{p}_1}^{(-)*}(\bar{\gamma}_1)e^{-i\bar{p}_2.\bar{\gamma}_2}\frac{1}{\gamma_{12}}\gamma_1 e^{i\bar{p}_i.\bar{\gamma}_2}e^{-\lambda_1\gamma_1}d^3\gamma_1 d^3\gamma_2$$

$$Tb_4 = \frac{1}{16\pi^2}\int\phi_{\bar{p}_1}^{(-)*}(\bar{\gamma}_1)e^{-i\bar{p}_2.\bar{\gamma}_2}\frac{1}{\gamma_2}\gamma_1 e^{i\bar{p}_i.\bar{\gamma}_2}e^{-\lambda_1\gamma_1}d^3\gamma_1 d^3\gamma_2 = \frac{1}{2}\frac{\partial}{\partial\lambda_1}(tb_2)$$

In our study [41], we computed the first Born term T_b for the Triple Differential Cross-Section (TDCS) and determined additional terms T_b', T_I, T_{PB}. We then mathematically calculated these terms in equation (1.35) using the Lewis integral [88]. These calculations led to the specification of the triple differential cross-section for the T-Matrix element as described in the following equation (1.36).

$$\frac{d^3\sigma}{d\mu_1 d\mu_2 dE_1} = \frac{p_1 p_2}{p_i}|T_{FI}|^2. \tag{1.36}$$

For first Born approximation, our consideration is $T_{FI} = T_b$

By integrating the TDCS result [41] based on equation (1.36), we can obtain the DDCS result using the following equation

$$\frac{d^2\sigma}{dE_1 d\mu_1} = \int\frac{d^3\sigma}{dE_1 d\mu_1 d\mu_2}d\mu_2 \tag{1.37}$$

Hence, the double differential cross sections (DDCS) were computed using the MATLAB programming language, as described by equation (1.37).

Finally, by integrating the Double Differential Cross-Section (DDCS) result from equation (1.37), we can obtain the Single Differential Cross-Section (SDCS) using the following equation.

$$\frac{d\sigma}{dE_1} = \int \frac{d^2\sigma}{dE d\mu_1} d\mu_1 \tag{1.38}$$

Therefore, the single differential cross sections (SDCS) were calculated using the MATLAB programming language based on equation (1.38).

The second Born terms of the equation (1.34) can be presented as follows:

$$T_b' = \left\langle \phi_{\bar{p}_2}^{(-)}(\bar{\gamma}_2) e^{i\bar{p}_1.\bar{\gamma}_1} \middle| V_I \middle| \Phi_i(\bar{\gamma}_1, \bar{\gamma}_2) \right\rangle \tag{1.39}$$

$$T_b' = \frac{1}{16\pi^2} \int \left[\phi_{\bar{p}_2}^{(-)*}(\bar{\gamma}_2) e^{-i\bar{p}_1.\bar{\gamma}_1} \left(\frac{1}{\gamma_{12}} - \frac{1}{\gamma_2} \right) e^{i\bar{p}_i.\bar{\gamma}_2} (2 - \gamma_1) e^{-\lambda_1\gamma_1} \right] d^3\gamma_1 d^3\gamma_2$$

$$= \frac{1}{8\pi^2} \int \phi_{\bar{p}_2}^{(-)*}(\bar{\gamma}_2) e^{-i\bar{p}_1.\bar{\gamma}_1} \frac{1}{\gamma_{12}} e^{i\bar{p}_i.\bar{\gamma}_2} e^{-\lambda_1\gamma_1} d^3\gamma_1 d^3\gamma_2$$

$$- \frac{1}{8\pi^2} \int \phi_{\bar{p}_2}^{(-)*}(\bar{\gamma}_2) e^{-i\bar{p}_1.\bar{\gamma}_1} \frac{1}{\gamma_2} e^{i\bar{p}_i.\bar{\gamma}_2} e^{-\lambda_1\gamma_1} d^3\gamma_1 d^3\gamma_2$$

$$- \frac{1}{16\pi^2} \int \phi_{\bar{p}_2}^{(-)*}(\bar{\gamma}_2) e^{-i\bar{p}_1.\bar{\gamma}_1} \frac{1}{\gamma_{12}} \gamma_1 e^{i\bar{p}_i.\bar{\gamma}_2} e^{-\lambda_1\gamma_1} d^3\gamma_1 d^3\gamma_2$$

$$+ \frac{1}{16\pi^2} \int \phi_{\bar{p}_2}^{(-)*}(\bar{\gamma}_2) e^{-i\bar{p}_1.\bar{\gamma}_1} \frac{1}{\gamma_2} \gamma_1 e^{i\bar{p}_i.\bar{\gamma}_2} e^{-\lambda_1\gamma_1} d^3\gamma_1 d^3\gamma_2$$

$$= t_{BP1} + t_{BP2} + t_{BP3} + t_{BP4} \tag{1.40}$$

Where

$$t_{BP1} = \frac{1}{8\pi^2} \int \phi_{\bar{p}_2}^{(-)*}(\bar{\gamma}_2) e^{-i\bar{p}_1.\bar{\gamma}_1} \frac{1}{\gamma_{12}} e^{i\bar{p}_i.\bar{\gamma}_2} e^{-\lambda_1\gamma_1} d^3\gamma_1 d^3\gamma_2$$

$$t_{BP2} = -\frac{1}{8\pi^2} \int \phi_{\bar{p}_2}^{(-)*}(\bar{\gamma}_2) e^{-i\bar{p}_1.\bar{\gamma}_1} \frac{1}{\gamma_2} e^{i\bar{p}_i.\bar{\gamma}_2} e^{-\lambda_1\gamma_1} d^3\gamma_1 d^3\gamma_2$$

$$t_{BP3} = -\frac{1}{16\pi^2} \int \phi_{\bar{p}_2}^{(-)*}(\bar{\gamma}_2) e^{-i\bar{p}_1.\bar{\gamma}_1} \frac{1}{\gamma_{12}} \gamma_1 e^{i\bar{p}_i.\bar{\gamma}_2} e^{-\lambda_1\gamma_1} d^3\gamma_1 d^3\gamma_2$$

$$t_{BP4} = \frac{1}{16\pi^2} \int \phi_{\bar{p}_2}^{(-)*}(\bar{\gamma}_2) e^{-i\bar{p}_1.\bar{\gamma}_1} \frac{1}{\gamma_2} \gamma_1 e^{i\bar{p}_i.\bar{\gamma}_2} e^{-\lambda_1\gamma_1} d^3\gamma_1 d^3\gamma_2$$

Here

$$t_{BP3} = \frac{1}{2} \frac{\partial}{\partial \gamma_1} (t_{BP1})$$

$$t_{BP4} = \frac{1}{2} \frac{\partial}{\partial \gamma_1} (t_{BP2})$$

Again, $T_I = \frac{1}{16\pi^2} \int \left[\phi_{\bar{p}}^{(-)*}(\bar{\gamma}) e^{-i\bar{P}.\bar{R}} \left(\frac{1}{\gamma_{12}} - \frac{1}{\gamma_2} \right) e^{i\bar{p}_i.\bar{\gamma}_2} (2 - \gamma_1) e^{-\lambda_1\gamma_1} \right] d^3\gamma_1 d^3\gamma_2$

$$= \frac{1}{8\pi^2} \int \phi_{\bar{p}}^{(-)*}(\bar{\gamma}) e^{-i\bar{P}.\bar{R}} \frac{1}{\gamma_{12}} e^{i\bar{p}_i.\bar{\gamma}_2} e^{-\lambda_1\gamma_1} d^3\gamma_1 d^3\gamma_2$$

$$- \frac{1}{8\pi^2} \int \phi_{\bar{p}}^{(-)*}(\bar{\gamma}) e^{-i\bar{P}.\bar{R}} \frac{1}{\gamma_2} e^{i\bar{p}_i.\bar{\gamma}_2} e^{-\lambda_1\gamma_1} d^3\gamma_1 d^3\gamma_2$$

$$- \frac{1}{16\pi^2}\int \phi_{\bar{p}}^{(-)*}(\bar{\gamma})e^{-i\bar{P}.\bar{R}}\frac{1}{\gamma_{12}}\gamma_1 e^{i\bar{p}_i.\bar{\gamma}_2}e^{-\lambda_1\gamma_1}d^3\gamma_1 d^3\gamma_2$$

$$+ \frac{1}{16\pi^2}\int \phi_{\bar{p}}^{(-)*}(\bar{\gamma})e^{-i\bar{P}.\bar{R}}\frac{1}{\gamma_2}\gamma_1 e^{i\bar{p}_i.\bar{\gamma}_2}e^{-\lambda_1\gamma_1}d^3\gamma_1 d^3\gamma_2$$

$$= t_{I1} + t_{I2} + t_{I3} + t_{I4} \quad (1.41)$$

Where

$$t_{I1} = \frac{1}{8\pi^2}\int \phi_{\bar{p}}^{(-)*}(\bar{\gamma})e^{-i\bar{P}.\bar{R}}\frac{1}{\gamma_{12}}e^{i\bar{p}_i.\bar{\gamma}_2}e^{-\lambda_1\gamma_1}d^3\gamma_1 d^3\gamma_2$$

$$t_{I2} = -\frac{1}{8\pi^2}\int \phi_{\bar{p}}^{(-)*}(\bar{\gamma})e^{-i\bar{P}.\bar{R}}\frac{1}{\gamma_2}e^{i\bar{p}_i.\bar{\gamma}_2}e^{-\lambda_1\gamma_1}d^3\gamma_1 d^3\gamma_2$$

$$t_{I3} = -\frac{1}{16\pi^2}\int \phi_{\bar{p}}^{(-)*}(\bar{\gamma})e^{-i\bar{P}.\bar{R}}\frac{1}{\gamma_{12}}\gamma_1 e^{i\bar{p}_i.\bar{\gamma}_2}e^{-\lambda_1\gamma_1}d^3\gamma_1 d^3\gamma_2$$

$$t_{I4} = \frac{1}{16\pi^2}\int \phi_{\bar{p}}^{(-)*}(\bar{\gamma})e^{-i\bar{P}.\bar{R}}\frac{1}{\gamma_2}\gamma_1 e^{i\bar{p}_i.\bar{\gamma}_2}e^{-\lambda_1\gamma_1}d^3\gamma_1 d^3\gamma_2$$

Here

$$t_{I3} = \frac{1}{2}\frac{\partial}{\partial\gamma_1}(t_{I1})$$

$$t_{I4} = \frac{1}{2}\frac{\partial}{\partial\gamma_1}(t_{I2})$$

Again,

$$T_{pb} = \frac{1}{16\pi^2}\int\left[e^{-i\bar{p}_1.\bar{\gamma}_1}e^{-i\bar{p}_2.\bar{\gamma}_2}\left(\frac{1}{\gamma_{12}}-\frac{1}{\gamma_2}\right)e^{i\bar{p}_i.\bar{\gamma}_2}(2-\gamma_1)e^{-\lambda_1\gamma_1}\right]d^3\gamma_1 d^3\gamma_2$$

$$= \frac{1}{8\pi^2}\int e^{-i\bar{p}_1.\bar{\gamma}_1}e^{-i\bar{p}_2.\bar{\gamma}_2}\frac{1}{\gamma_{12}}e^{i\bar{p}_i.\bar{\gamma}_2}e^{-\lambda_1\gamma_1}d^3\gamma_1 d^3\gamma_2$$

$$- \frac{1}{8\pi^2}\int e^{-i\bar{p}_1.\bar{\gamma}_1}e^{-i\bar{p}_2.\bar{\gamma}_2}\frac{1}{\gamma_2}e^{i\bar{p}_i.\bar{\gamma}_2}e^{-\lambda_1\gamma_1}d^3\gamma_1 d^3\gamma_2$$

$$- \frac{1}{16\pi^2}\int e^{-i\bar{p}_1.\bar{\gamma}_1}e^{-i\bar{p}_2.\bar{\gamma}_2}\frac{1}{\gamma_{12}}\gamma_1 e^{i\bar{p}_i.\bar{\gamma}_2}e^{-\lambda_1\gamma_1}d^3\gamma_1 d^3\gamma_2$$

$$+ \frac{1}{16\pi^2}\int e^{-i\bar{p}_1.\bar{\gamma}_1}e^{-i\bar{p}_2.\bar{\gamma}_2}\frac{1}{\gamma_2}\gamma_1 e^{i\bar{p}_i.\bar{\gamma}_2}e^{-\lambda_1\gamma_1}d^3\gamma_1 d^3\gamma_2$$

$$= t_{pb1} + t_{pb2} + t_{pb3} + t_{pb4} \quad (1.42)$$

Where

$$t_{pb1} = \frac{1}{8\pi^2}\int e^{-i\bar{p}_1.\bar{\gamma}_1}e^{-i\bar{p}_2.\bar{\gamma}_2}\frac{1}{\gamma_{12}}e^{i\bar{p}_i.\bar{\gamma}_2}e^{-\lambda_1\gamma_1}d^3\gamma_1 d^3\gamma_2$$

$$t_{pb2} = -\frac{1}{8\pi^2}\int e^{-i\bar{p}_1.\bar{\gamma}_1}e^{-i\bar{p}_2.\bar{\gamma}_2}\frac{1}{\gamma_2}e^{i\bar{p}_i.\bar{\gamma}_2}e^{-\lambda_1\gamma_1}d^3\gamma_1 d^3\gamma_2$$

$$t_{pb3} = -\frac{1}{16\pi^2}\int e^{-i\bar{p}_1.\bar{\gamma}_1}e^{-i\bar{p}_2.\bar{\gamma}_2}\frac{1}{\gamma_{12}}\gamma_1 e^{i\bar{p}_i.\bar{\gamma}_2}e^{-\lambda_1\gamma_1}d^3\gamma_1 d^3\gamma_2$$

$$t_{pb4} = \frac{1}{16\pi^2}\int e^{-i\bar{p}_1.\bar{\gamma}_1}e^{-i\bar{p}_2.\bar{\gamma}_2}\frac{1}{\gamma_2}\gamma_1 e^{i\bar{p}_i.\bar{\gamma}_2}e^{-\lambda_1\gamma_1}d^3\gamma_1 d^3\gamma_2$$

Here

$$t_{pb3} = \frac{1}{2}\frac{\partial}{\partial\gamma_1}(t_{pb1})$$

$$t_{pb4} = \frac{1}{2}\frac{\partial}{\partial \gamma_1}(t_{pb2})$$

The exchange effect amplitude is approximated using the following approximation:

$$g(\overline{p_1}, \overline{p_2}) = f(\overline{p_2}, \overline{p_1}) \tag{1.43}$$

After, obtaining the analytical expressions for T_b, T_b', T_I and T_{PB} numerical calculations were performed using the Lewis integral [88] and Gaussian quadrature formula. The triple differential cross section (TDCS) was obtained from the following numerical results

$$\frac{d^3\sigma}{d\mu_1 d\mu_2 dE_1} = \frac{p_1 p_2}{p_i}\left[\frac{3}{4}|f-g|^2 + \frac{1}{4}|f+g|^2\right] \tag{1.44}$$

By integrating the Triple Double Differential Cross Section (TDCS) derived from Equation (1.44), we can obtain the Double Differential Cross Section (DDCS) using the following equation

$$\frac{d^2\sigma}{dE_1 d\mu_1} = \int \frac{d^3\sigma}{dE_1 d\mu_1 d\mu_2} d\mu_2 \tag{1.45}$$

Hence, we calculated the Double Differential Cross Section (DDCS) using MATLAB programming, based on equation (1.45)

By integrating DDCS result from equation (1.45), we can obtain the Single Differential Cross Section (SDCS) result using the following equation

$$\frac{d\sigma}{dE_1} = \int \frac{d^2\sigma}{dE_1 d\mu_1} d\mu_1 \tag{1.46}$$

Hence, SDCS were computed using the MATLAB programming language based on equation (1.46).

1.6 THESIS OUTLINE

In this thesis, we provide a theoretical exploration of atomic ionization problems.

Chapter 1 provides an overview of the theoretical background, presents a comprehensive summary of the literature review and methodology relevant to our work.

Chapter 2 explains our approach to compute the first Born double differential cross sections (DDCS) for ionizing metastable 2S state hydrogen atoms with electrons at intermediate and high energies.

Chapter 3 applies our method to calculate the second Born double differential cross section for ionization of metastable 2S state hydrogen atoms by electrons, both in theoretical analysis and numerical computations.

Chapter 4 deals with calculating the Single Differential Cross Section (SDCS) for ionizing metastable 2S state hydrogen atoms using electron impact.

Chapter 5 further expands our analysis by calculating the DDCS and SDCS for electron impact ionization of metastable 2S state hydrogen atoms with exchange effects.

Chapter 6 finally, we offer concluding remarks and discuss possible directions for future research.

Chapter 2: DOUBLE DIFFERENTIAL CROSS-SECTION OF FIRST BORN

2.1 INTRODUCTION

An important reaction in atomic collisions is ionization and has far-reaching implications in multiple scientific fields. For example, in atomic physics, it has the power to alter energy levels and spectral properties of atoms. Astrophysics sees ionization shaping the birth and progression of stars, planets, and interstellar clouds. Plasma physics relies on ionization to generate and maintain plasmas, where a majority of particles exist in an ionized state. In the realm of fusion technology, ionization becomes crucial in facilitating nuclear fusion reactions by surmounting the electrostatic repulsion among nuclei. Important insights into ionization dynamics have been gained through the analysis of double differential cross sections (DDCS), which provide information about the energy and angle distributions of emitted electrons. The quantum mechanical formulation of ionization by fast particles was pioneered by Bethe [68]. Advancements in multi-parameter detection techniques and computational procedures have enabled comprehensive experiments to determine the kinematic parameters (such as momentum and energies) of all particles involved. These experiments have been successfully employed to explore intricate aspects of the ionization process in both ground [24]-[32] and metastable states [41]-[51]. Atomic ionization collisions provide valuable insights into the angular and energy distribution of secondary electrons, as captured by the double differential cross section (DDCS) [3]. In order to comprehend the process of ionization of atomic systems caused by electron impact energy, scientists frequently use atomic hydrogen as target [75].

In these (e, 2e) experiments, the scattered electrons and the emitted electron are detected simultaneously, allowing for a comprehensive exploration of the ionization dynamics.

Electron influence plays a significant role in the ionization of atomic hydrogen, and data on ground state ionization of rare gas atoms are often considered as benchmark information. Though atomic hydrogen was the most simple and ideal system for theoretical study, there was a dearth of data available for the system itself. Numerous group of researchers have produced DDCS measurements for ionization, which offer important insights into the internal structure of atomic or molecular systems as well as collision dynamics [2], [6], [19]-[21], [30], [51]-[60], and [63]-[65].

Here, we have calculated the DDCS for the ionization of hydrogenic metastable 2S states using incident energies of 150eV and 250eV. We have utilized a wave function approach [3], [32], [41] and integrate the DDCS over the scattering angle. One intriguing aspect is the use of the wave function of hydrogenic metastable 2S state to calculate the DDCS. To the best of our knowledge, no previous experimental or theoretical investigations have focused on the DDCS of hydrogen atoms in the metastable 2S state at high and medium energies. Therefore, our findings on the ionization of metastable 2S-state hydrogen atoms by electron impact will therefore be extremely beneficial and make a substantial contribution to this important area of study.

2.2 THEORY

The purpose of developing a theory is to provide an explanation, prediction, or understanding of a particular phenomenon. The theory must be formulated within a specific framework, which serves as a structure to support the research study's theoretical perspective. This framework sets the boundaries and assumptions that define the scope of the theory and guides its development. The theoretical framework is essential in enabling the theory to

be challenged and extended, contributing to the advancement of existing knowledge.

Relevant theories of our research work are interpreted here:

2.2.1 Scattering Mechanism

The ionization rate per unit time and unit target, compared to the incident electron flux ionization cross sections, can be used to check the accuracy of perturbation theory. The ionization of atomic hydrogen by electrons is a good example for this purpose, as experimental results such as TDCS and DDCS exist. In these calculations, the ejected electron has been detected simultaneously with the scattered electron, in what is known as an (e, 2e) coincidence experiment, as described in chapter 1. This theory is well-established and widely used in the field.

One type of electron-induced ionization process in atomic hydrogen involves the creation of a singly ionized state, and can be represented as

$$e^- + H(2S) \rightarrow H^+ + 2e^- \qquad (2.1)$$

When discussing atomic hydrogen, the symbol 2S denotes a metastable state that has been investigated in coplanar geometry by analysing TDCS readings from (e, 2e) coincidence studies. The term "triple differential cross section," or TDCS, refers to the likelihood that an incident electron with momentum $\bar{p}_i$ and energy E_i will result in two electrons with energies E_1 and E_2 and momenta $\bar{p}_1$ and $\overline{p}_2$, respectively, upon collision with the target. The computation of TDCS also considers the emission angles of these electrons, which are centred around directions (θ_1, ϕ_1) and (θ_2, ϕ_2), respectively.

Studies of hydrogen atom ionization by electrons in metastable 2S-states commonly use the TDCS, which is represented by $\frac{d^3\sigma}{d\mu_1 d\mu_2 dE_1}$. This function depends on various variables such as $\mathrm{E_i}$, $\mathrm{E_1}$, or $\mathrm{E_2}$, θ_1, θ_2 and $\phi = \phi_1 - \phi_2$, assuming unpolarized incident electrons and targets.

By integrating TDCS over $d\mu_1$ and $d\mu_2$, we can obtain the DDCS (double differential cross section) and SDCS (single differential cross section). These cross sections are essential in analysing the ionization of hydrogen atoms in the 2S-state by electrons.

To obtain the total ionization cross section, we integrate DDCS and SDCS with respect to scattering angles and energies, which only depend on the incident energy, E_i. Thus, the focus of this chapter is on obtaining DDCS for ionization of hydrogen atoms by electrons in metastable 2S-state.

Differentiating between distinct kinematical arrangements is crucial for (e, 2e) coincidence investigations since they are important for the theoretical analysis of the collision. It is especially crucial to distinguish between coplanar and non-coplanar geometries.

The momenta $\bar{p}_i, \bar{p}_1$, and $\bar{p}_2$ are all in the same plane in coplanar geometries, while the momentum $\bar{p}_2$ is outside the reference plane $(\bar{p}_i, \bar{p}_1)$ in non-coplanar geometries. These different geometries have significant implications for the analysis of the collision.

2.2.2 T-matrix element

The direct Transition matrix element for ionization of hydrogen atoms by electron [33], may be written as,

$$T_{FI} = \left\langle \psi_F^{(-)}(\bar{\gamma}_1, \bar{\gamma}_2) \middle| V_I(\bar{\gamma}_1, \bar{\gamma}_2) \middle| \Phi_i(\bar{\gamma}_1, \bar{\gamma}_2) \right\rangle \tag{2.2}$$

Where the perturbation potential $V_I(\bar{\gamma}_1, \bar{\gamma}_2)$ is given by

$$V_I(\bar{\gamma}_1, \bar{\gamma}_2) = \frac{1}{\gamma_{12}} - \frac{1}{\gamma_2}$$

The nuclear charge of a hydrogen atom is Ze=1, its two electrons' distances from the nucleus are γ_1 and γ_2, and their distance from one another is γ_{12} (Fig. 2.1).

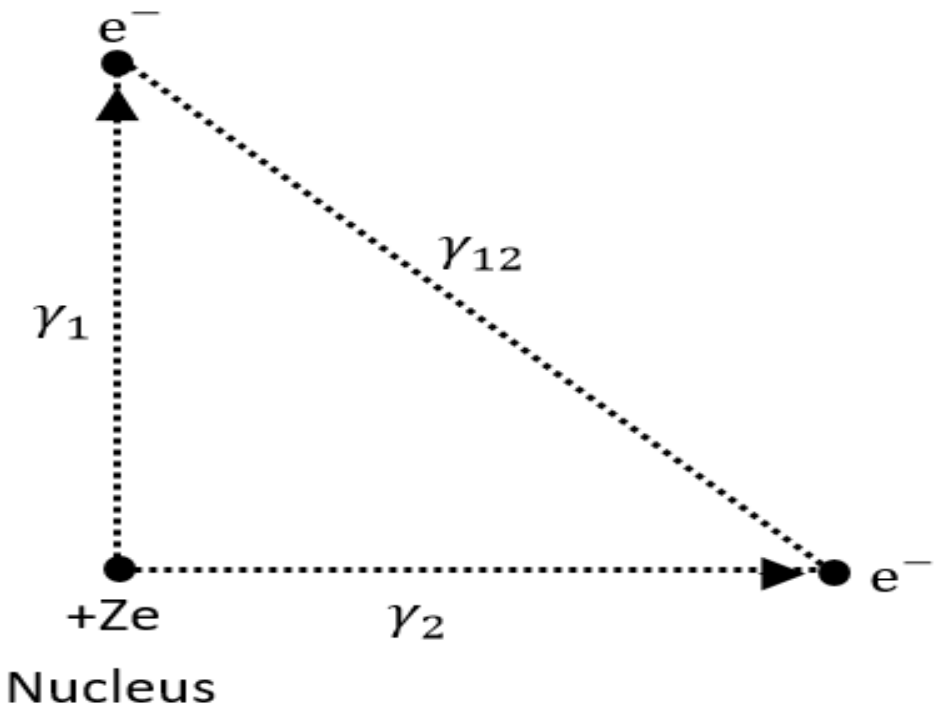

Fig. 2.1 Collision effect between two electrons.

The initial channel unperturbed wave function can be expressed as follows:

$$\Phi_i(\bar{\gamma}_1, \bar{\gamma}_2) = \frac{e^{i\bar{p}_i \cdot \bar{\gamma}_2}}{(2\pi)^{\frac{3}{2}}} \phi_{2S}(\bar{\gamma}_1) \tag{2.3}$$

Where $\phi_{2S}(\bar{\gamma}_1) = \frac{1}{4\sqrt{2\pi}}(2 - \gamma_1)e^{-\lambda_1 \gamma_1}$

Here, the hydrogen 2S state wave function in this case is represented by $\lambda_1 = \frac{1}{2}$ and $\phi_{2S}(\bar{\gamma}_1)$, whereas the final three-particle scattering state wave function is represented by $\psi_F^{(-)}(\bar{\gamma}_1, \bar{\gamma}_2)$, and the coordinates of the two electrons are $\bar{\gamma}_1$ and $\bar{\gamma}_2$, respectively.

In this case, the approximate wave function $\psi_F^{(-)}$ is provided by

$$\psi_F^{(-)}(\bar{\gamma}_1, \bar{\gamma}_2) = N(\bar{p}_1, \bar{p}_2)\Big[\phi_{\bar{p}_1}^{(-)}(\bar{\gamma}_1)e^{i\bar{p}_2 \cdot \bar{\gamma}_2} + \phi_{\bar{p}_2}^{(-)}(\bar{\gamma}_2)e^{i\bar{p}_1 \cdot \bar{\gamma}_1} + \phi_{\bar{p}}^{(-)}(\bar{\gamma})e^{i\bar{P} \cdot \bar{R}} - 2e^{i\bar{p}_1 \cdot \bar{\gamma}_1 + i\bar{p}_2 \cdot \bar{\gamma}_2}\Big]/(2\pi)^3 \tag{2.4}$$

Here, $N(\bar{p}_1, \bar{p}_2)$ is normalization constant, $\bar{\gamma} = \frac{\bar{\gamma}_1 - \bar{\gamma}_2}{2}$, $\bar{R} = \frac{\bar{\gamma}_1 + \bar{\gamma}_2}{2}$, $\bar{p} = \bar{p}_2 - \bar{p}_1$,

$\bar{P} = \bar{p}_2 + \bar{p}_1$, and $\phi_q^{(-)}(\bar{\gamma})$ is Coulomb wave function.

Applying equations (2.3) and (2.4) in equation (2.2), we get

$$T_{FI} = T_b + T_b' + T_I - 2T_{PB} \tag{2.5}$$

Equation (2.5), for the first Born estimation, can be expressed as

$$T_{FI} = T_b \tag{2.6}$$

Here, $T_b = \frac{1}{16\pi^2}\left\langle \phi_{\bar{p}_1}^{(-)}(\bar{\gamma}_1) e^{i\bar{p}_2.\bar{\gamma}_2} \left| \frac{1}{\gamma_{12}} - \frac{1}{\gamma_2} \right| e^{i\bar{p}_i.\bar{\gamma}_2}(2-\gamma_1) e^{-\lambda_1\gamma_1} \right\rangle$

$$= \frac{1}{16\pi^2}\int \left[\phi_{\bar{p}_1}^{(-)*}(\bar{\gamma}_1) e^{-i\bar{p}_2.\bar{\gamma}_2}\left(\frac{1}{\gamma_{12}} - \frac{1}{\gamma_2}\right) e^{i\bar{p}_i.\bar{\gamma}_2}(2-\gamma_1) e^{-\lambda_1\gamma_1}\right] d^3\gamma_1 d^3\gamma_2$$

$$= \frac{1}{16\pi^2}\int \phi_{\bar{p}_1}^{(-)*}(\bar{\gamma}_1) e^{-i\bar{p}_2.\bar{\gamma}_2} \frac{1}{\gamma_{12}} 2e^{i\bar{p}_i.\bar{\gamma}_2} e^{-\lambda_1\gamma_1} d^3\gamma_1 d^3\gamma_2$$

$$- \frac{1}{16\pi^2}\int \phi_{\bar{p}_1}^{(-)*}(\bar{\gamma}_1) e^{-i\bar{p}_2.\bar{\gamma}_2} \frac{1}{\gamma_2} 2e^{i\bar{p}_i.\bar{\gamma}_2} e^{-\lambda_1\gamma_1} d^3\gamma_1 d^3\gamma_2$$

$$- \frac{1}{16\pi^2}\int \phi_{\bar{p}_1}^{(-)*}(\bar{\gamma}_1) e^{-i\bar{p}_2.\bar{\gamma}_2} \frac{1}{\gamma_{12}} \gamma_1 e^{i\bar{p}_i.\bar{\gamma}_2} e^{-\lambda_1\gamma_1} d^3\gamma_1 d^3\gamma_2$$

$$+ \frac{1}{16\pi^2}\int \phi_{\bar{p}_1}^{(-)*}(\bar{\gamma}_1) e^{-i\bar{p}_2.\bar{\gamma}_2} \frac{1}{\gamma_2} \gamma_1 e^{i\bar{p}_i.\bar{\gamma}_2} e^{-\lambda_1\gamma_1} d^3\gamma_1 d^3\gamma_2$$

$$= Tb_1 + Tb_2 + Tb_3 + Tb_4 \tag{2.7}$$

Now,

$$Tb_1 = \frac{1}{16\pi^2}\int \phi_{\bar{p}_1}^{(-)*}(\bar{\gamma}_1) e^{-i\bar{p}_2.\bar{\gamma}_2} \frac{1}{\gamma_{12}} 2e^{i\bar{p}_i.\bar{\gamma}_2} e^{-\lambda_1\gamma_1} d^3\gamma_1 d^3\gamma_2$$

$$Tb_2 = -\frac{1}{16\pi^2}\int \phi_{\bar{p}_1}^{(-)*}(\bar{\gamma}_1) e^{-i\bar{p}_2.\bar{\gamma}_2} \frac{1}{\gamma_2} 2e^{i\bar{p}_i.\bar{\gamma}_2} e^{-\lambda_1\gamma_1} d^3\gamma_1 d^3\gamma_2$$

$$Tb_3 = -\frac{1}{16\pi^2}\int \phi_{\bar{p}_1}^{(-)*}(\bar{\gamma}_1) e^{-i\bar{p}_2.\bar{\gamma}_2} \frac{1}{\gamma_{12}} \gamma_1 e^{i\bar{p}_i.\bar{\gamma}_2} e^{-\lambda_1\gamma_1} d^3\gamma_1 d^3\gamma_2$$

$$Tb_4 = \frac{1}{16\pi^2}\int \phi_{\bar{p}_1}^{(-)*}(\bar{\gamma}_1) e^{-i\bar{p}_2.\bar{\gamma}_2} \frac{1}{\gamma_2} \gamma_1 e^{i\bar{p}_i.\bar{\gamma}_2} e^{-\lambda_1\gamma_1} d^3\gamma_1 d^3\gamma_2 = \frac{1}{2}\frac{\partial}{\partial\lambda_1}(tb_2)$$

The first Born term for TDCS is T_b; other terms, T_b', T_I, and T_{PB}, are computed in our work [41]. The above terms of eq. (2.7) have then been analytically computed using exploratory computation utilizing the Lewis integral [88], and the TDCS for the T-Matrix element are described by

$$\frac{d^3\sigma}{d\mu_1 d\mu_2 dE_1} = \frac{p_1 p_2}{p_i}|T_{FI}|^2. \quad (2.8)$$

After integrating the first Born term of TDCS result [41] of equation (2.8), we can use the following equation to obtain the DDCS result

$$\frac{d^2\sigma}{dE_1 d\mu_1} = \int \frac{d^3\sigma}{dE_1 d\mu_1 d\mu_2} d\mu_2 \quad (2.9)$$

Equation (2.9) represents the DDCS that have been calculated using the MATLAB computer programming language.

2.3 RESULTS AND DISCUSSIONS

The ionization of metastable 2S state hydrogen atoms by electrons at high incidence energy $\boldsymbol{E_I = 250eV}$ results in DDCS being calculated here for the emitted electron energies $\boldsymbol{E_1}$ = 4eV, 10eV, 20eV, 50eV, and 80eV. Once more, for emitted electron energies $\boldsymbol{E_1}$ = 4eV, 10eV, 20eV, 30eV, and 50eV, at intermediate incident energy $\boldsymbol{E_I = 150eV}$. The scattered angle $\boldsymbol{\theta_2}$ varies from 0° to 100°, whereas the emitted angle $\boldsymbol{\theta_1}$ varies from 0° to 180°, which is regarded the horizontal axis and the vertical axis in all figures is DDCS. We provide the ionization of hydrogen atoms by electrons from the ground state, as demonstrated by experimental evidence [6] and computational results [3], [67] for comparison with our present estimation. The continuum state of atomic hydrogen is represented by the final state scattering wave function $\boldsymbol{\psi_F^{(-)}(\overline{\gamma}_1, \overline{\gamma}_2)}$.

In Fig. 2.2(a), for incident energy E_I =250eV and ejection energy E_1=4eV, the current first Born result overlays with those of [3] at about θ_1=10°. At higher ejection angles, θ_1 lies above those of [3], creating an onward peak, and lies closely below the experimental values at lesser θ_1. It also meets with those of [6] at θ_1=5° and θ_1=175°, respectively, and with those of [67] at approximately θ_1= 62°, θ_1= 100°, and θ_1= 173°.

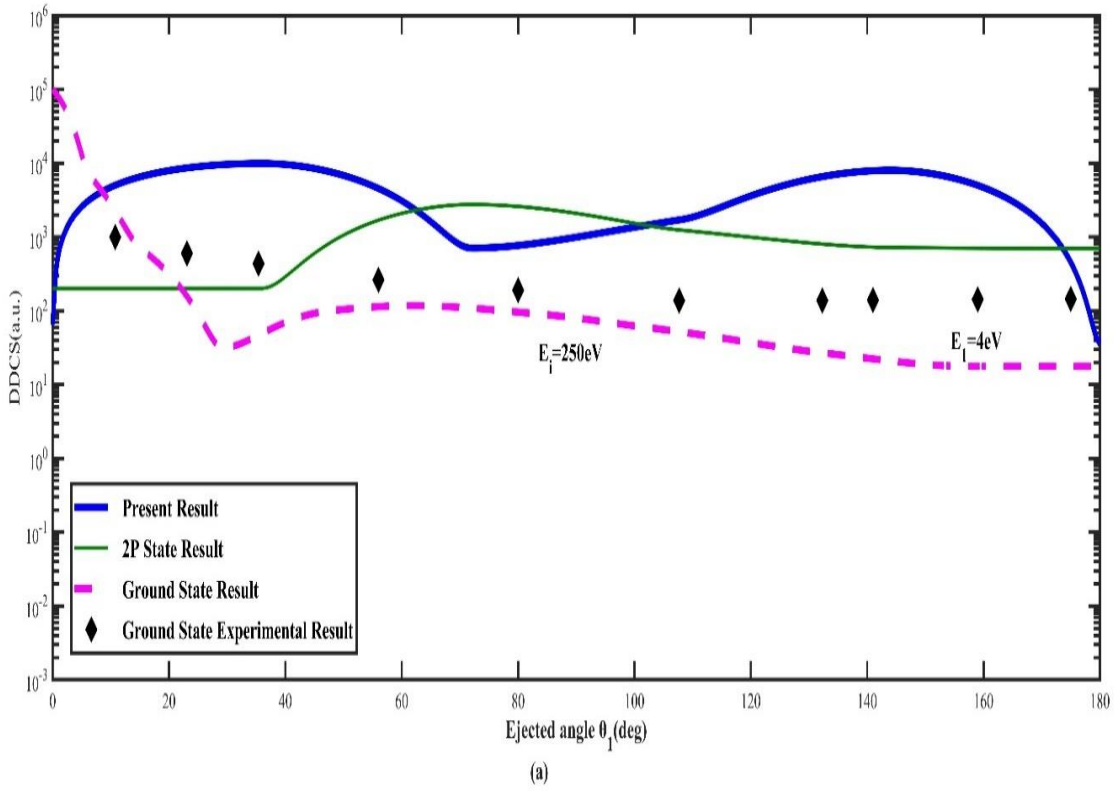

Fig. 2.2 DDCS for the Ionization of atomic hydrogen by incident energy E_I =250 eV and emitted energies are (a) 4eV and (b) 10eV respectively.

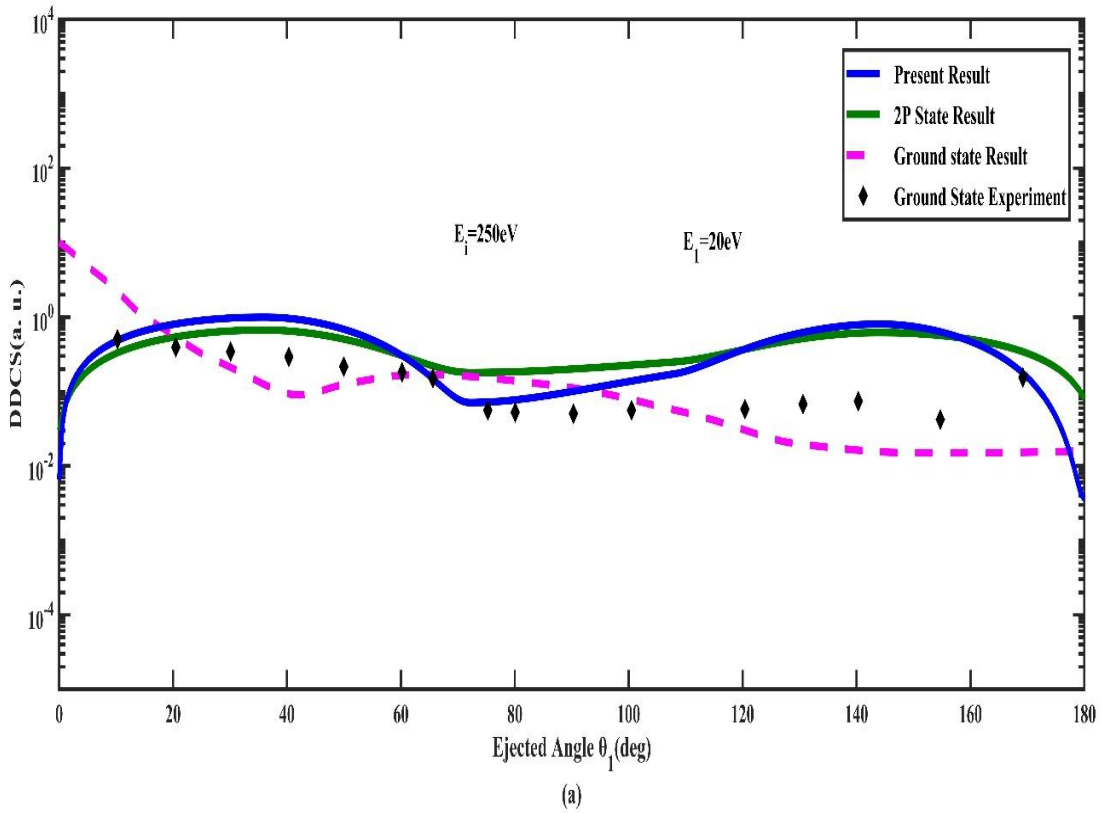

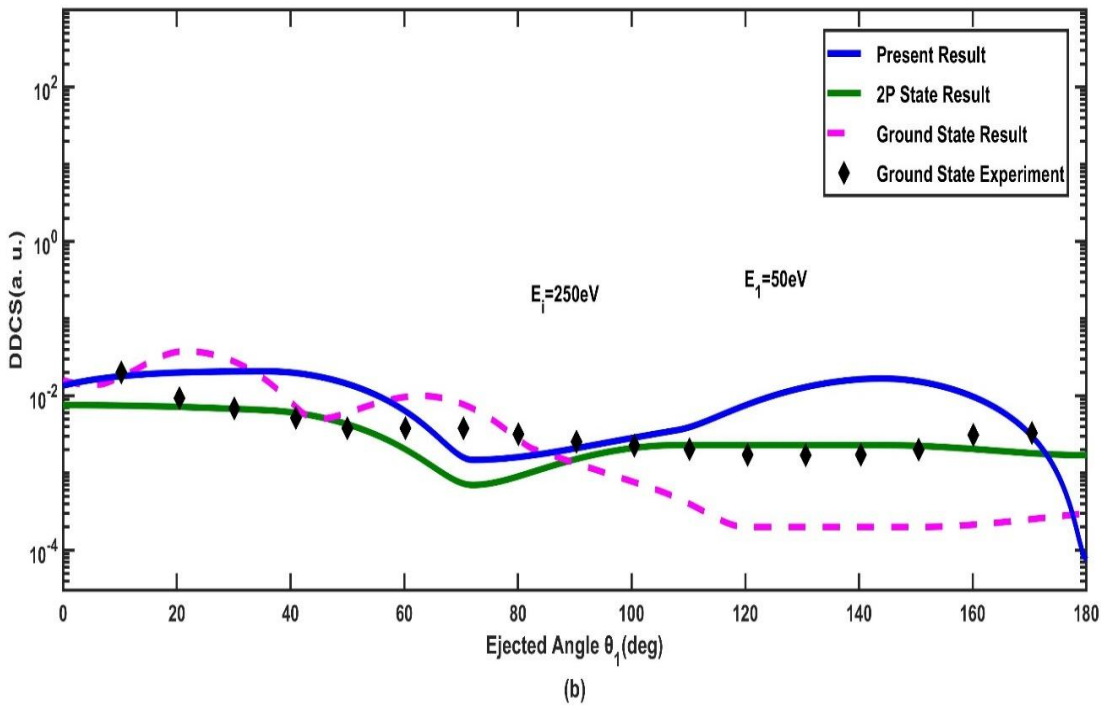

Fig. 2.3 DDCS for the Ionization of atomic hydrogen by incident energy E_I =250 eV and emitted energies are (a) 20eV and (b) 50eV respectively.

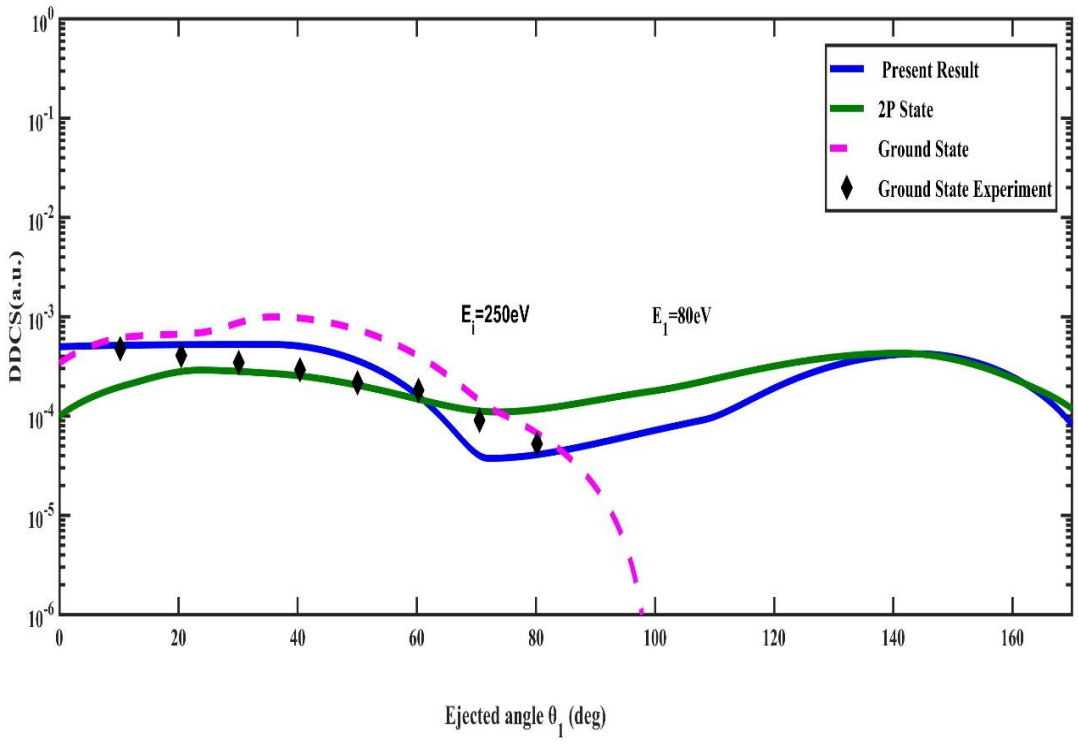

Fig. 2.4 DDCS for the Ionization of atomic hydrogen by incident energy E_I =250 eV and emitted energy is 80eV.

In Fig. 2.2(b), E_1=10eV, our result meets approximately θ_1=20°, θ_1=60°, θ_1=100° and θ_1=177° with those of ground state result [3], and concurs four times at almost θ_1=5°, θ_1=45°, θ_1=138° and θ_1=155° with those of [67]. Additionally, there are multiple intersections between the curve and those of [6], and the peak flattens and eventually vanishes as the energy increases, indicating a good judgment.

The current finding exhibits patterns comparable to the 2P state [67], as well as similar to the hydrogenic ground state experimental results [6] at θ_1=65° and θ_1=170° in Fig. 2.3(a), E_1=20eV, which demonstrates good qualitative assessment.

In Fig. 2.3(b), E_1=50eV, the current result matches with the ground state result [3] five times, at θ_1= 18°, θ_1= 35°, θ_1= 55°, θ_1= 80° and θ_1= 176°. It also coincides four times with the value of the ground state experiment [6].

Furthermore, it forms a large peak at a greater angle, indicating an excellent evaluation.

Finally, in Fig. 2.4, E_1=80eV, at ejection angles up to θ_1= 80°, the current result, the theoretical result, the experimental result, and the 2P state result all show similarities in shape. However, the current result and the 2P state results [67] show a peak with a large size at higher angles, indicating a good evaluation. Our results demonstrate a high level of consistency with both the experimental and theoretical evidence for the hydrogenic ground state.

In Fig. 2.5(a), for incident energy E_i=150eV and ejection energy E_1=4eV, the current result intersects with those of the 2P state outcomes [67] at approximately θ_1=80° , θ_1=110° and θ_1=170°. It also agrees with ground state results [3] at approximately θ_1=10° and θ_1=177°, and is closer to θ_1=70° and intersects at θ_1=172° with those of the ground state experiment results [6].

Our curve lies above the experimental values [6] and intersects with those of the 2P state results [67] many times in Fig. 2.5(b), E_1=10eV. It is comparatively closer to the ground state results [3] at smaller angles. The ground state findings are approximately met at θ_1=10°, current findings reaching a maximum at θ_1=150°. At larger ejection angles, θ_1 the curve also meets with the ground state results [3].

Our current findings in Fig. 2.6(a), E_1=20eV, correlates with those ground state results at different times at θ_1=32°, θ_1=55°, θ_1=100° and θ_1=175° [3], and passes at θ_1=62°, θ_1=100° and θ_1=165° with ground state experiment results [6]. Our outcome produces a peak at θ_1=140° and a passing that is closer to the theoretical and experimental values. It demonstrates an effective qualitative assessment.

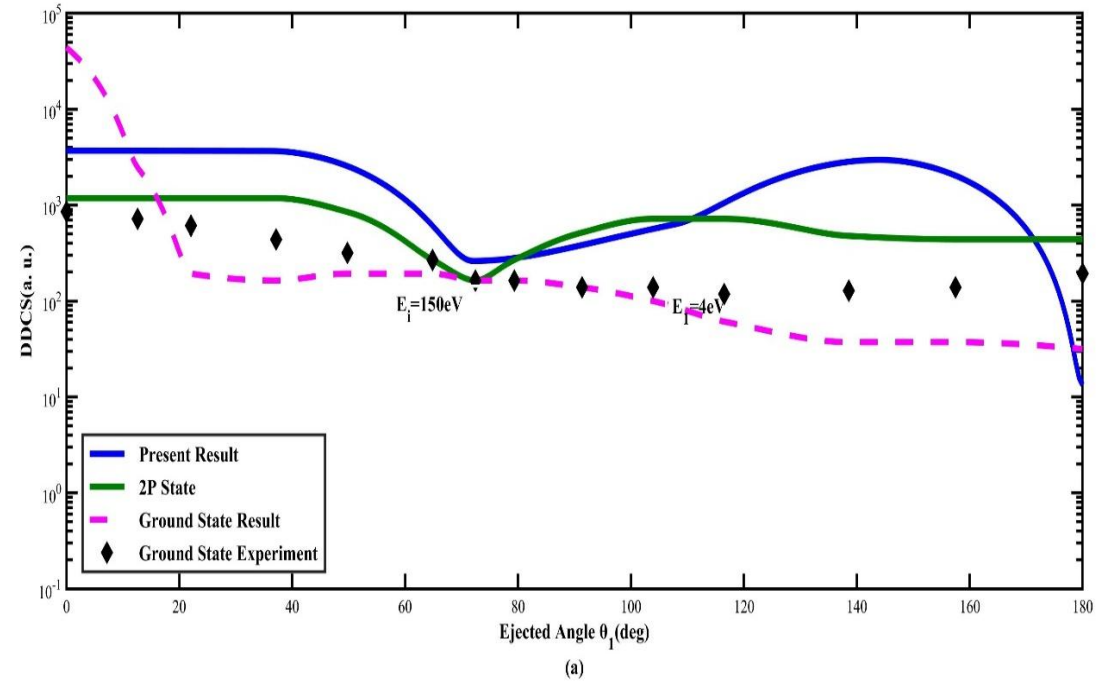

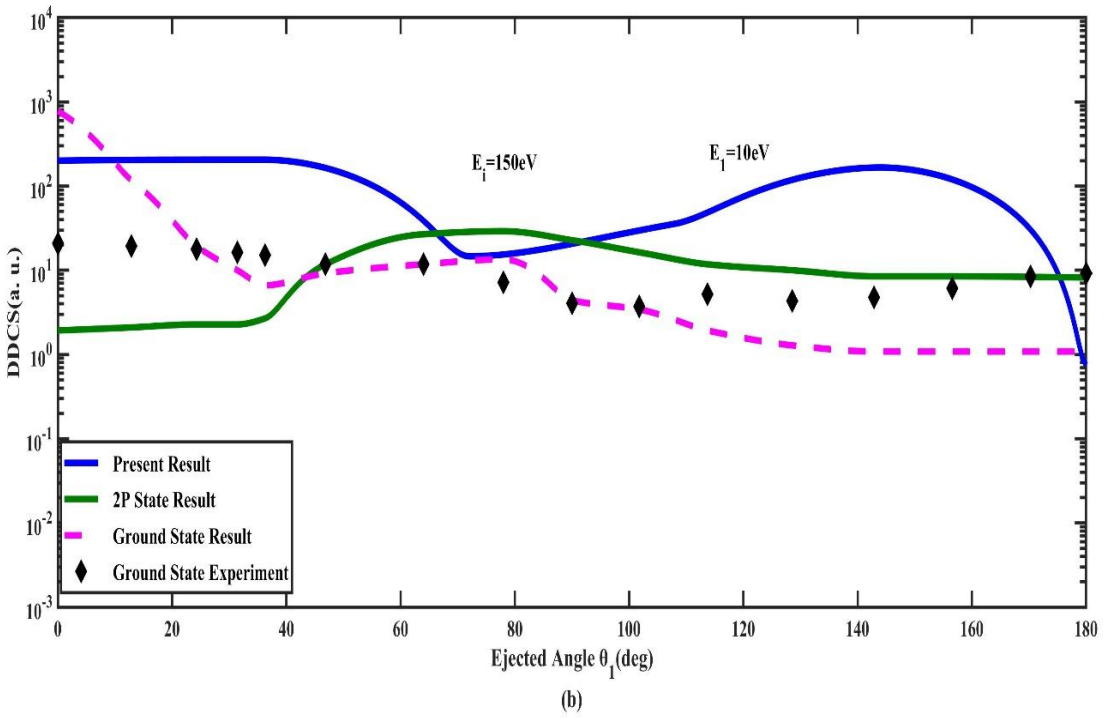

Fig. 2.5 DDCS for the Ionization of atomic hydrogen by incident energy E_I =150 eV and emitted energies are (a) 4eV and (b) 10eV respectively.

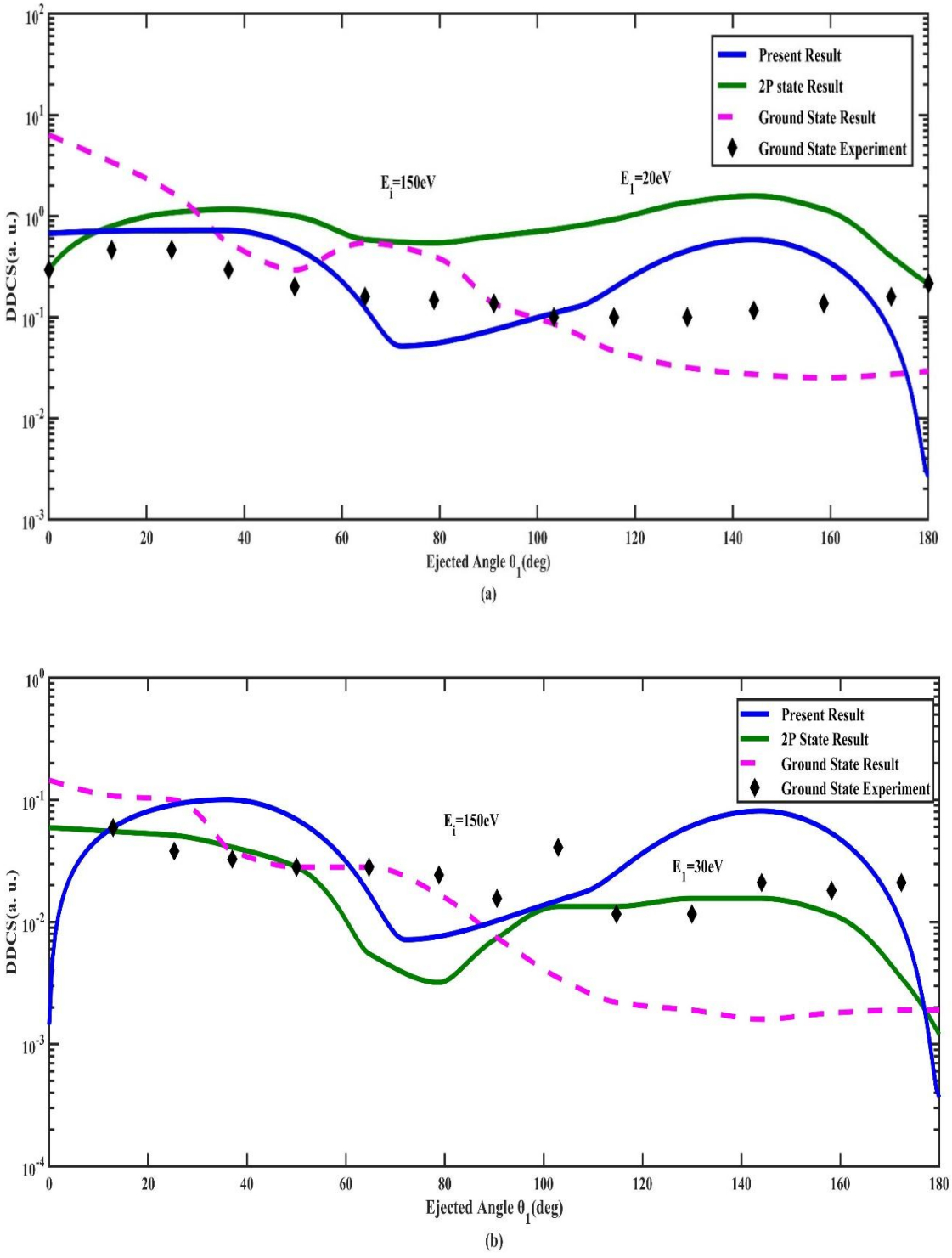

Fig. 2.6 DDCS for the Ionization of atomic hydrogen by incident energy E_I =150 eV and emitted energies are (a) 20eV and (b) 30eV respectively.

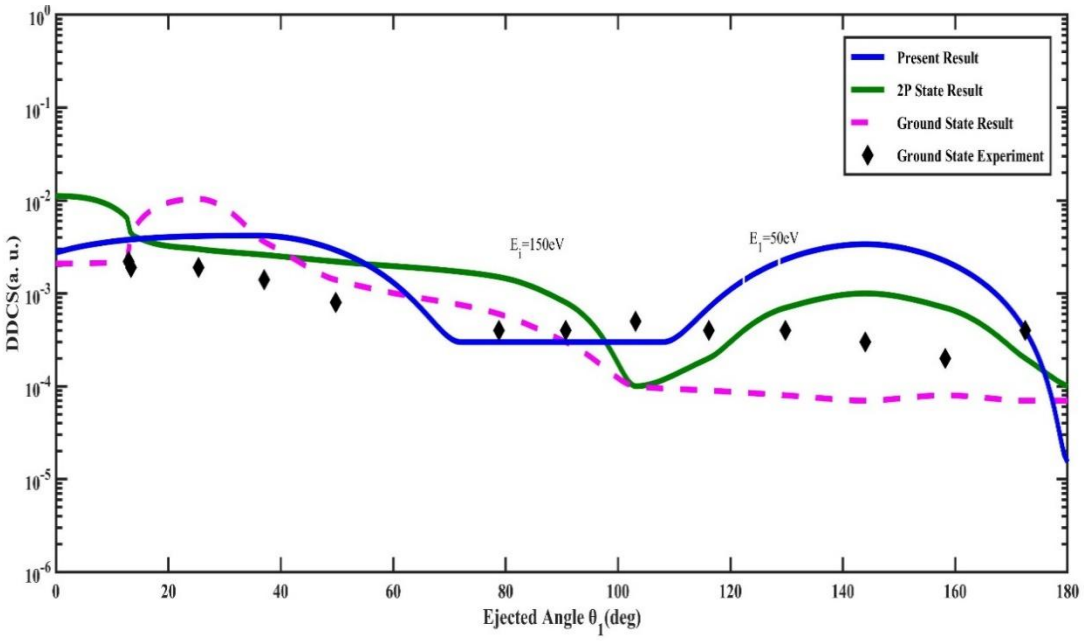

Fig.2.7 DDCS for the Ionization of atomic hydrogen by incident energy E_I =150 eV and emitted energy is 50eV.

Again, E_1=30eV in Fig 2.6(b), the theoretical result forms two peak nearby θ_1=40°, θ_1=145° and lower deep at about θ_1=75°. These current results demonstrate appropriate qualitative exhibition when compared to ground state results [3], 2P state data [67], and ground state experiment findings [6].

In Fig. 2.7, we finally consider release energy as E_1=50eV. At θ_1=14°, θ_1=55°,θ_1=97° and θ_1=177°, our curve overlays four times those of [67]. At higher angles, between 70° and 110°, a smaller deep created when the experimental curve-runs comparatively nearer to the present outcome, indicating a suitable judgment.

It has been noted that the current first Born result only corresponds once, at $\theta_1 = 60°$, with the result, and that it concurs twice, at lower and higher ejection angles θ_1, with the experimental results of Shyn, Roy, Mandal, and Sil [7]. We may also observe that, in the incident energy E_I=250eV, the findings can be carefully examined in table 2.1 on the following page, where values of the

various ejection angles θ_1 are shown for various values of the scattering

Table 2.1. DDCS results for four different values of emitted electron energies (E_1=4eV, E_1=20eV, E_1= 50eV and E_1= 80eV) in the ionization of hydrogen atoms for 250eV electron correspond to varied scattering angles θ_2.

θ_2(deg)	θ_1(deg)	$E_1 = 4eV$	$E_1 = 20eV$	$E_1 = 50eV$	$\mathbf{E_1 = 80eV}$
		DDCS	DDCS	DDCS	DDCS
0	0	64.9	0.00652	0.01359	0.000499
1	36	9926.0	0.99705	0.02075	0.000525
2	72	707.4	0.07106	0.00147	0.000037
4	108	1719.1	0.17268	0.00359	0.000091
10	144	8019.1	0.80550	0.01676	0.000424
20	180	36.1	0.00362	0.00007	0.000001
30	216	11292.4	1.13412	0.02361	0.000598
40	252	179.8	0.01806	0.00037	0.000009
60	288	3244.3	0.32588	0.00010	0.006784
90	324	5887.9	0.59143	0.00019	0.012313
100	360	0	0	0	0

angles θ_2.

2.4 CONCLUSION

The DDCS estimation for the ionization of metastable 2S-state hydrogen atoms by the 150 eV and 250 eV electron effects is presented in this work.

By assisting in the understanding of different configurations of the DDCS, the current computation employing multiple scattering theory [3] significantly advances the field of metastable 2S-state ionization problems. Since the DDCS results of the hydrogenic metastable 2S-state ionization process lack experimental data, a comparison between the present computational conclusions and the experimental findings is not possible. Thus, it will be useful to compare the hydrogenic ground state experimental data with the electron ionization of metastable 2S state hydrogen atoms.

Chapter 3: DEFFERENTIAL CROSS-SECTION FOR DIRECT AMPLITUDE

3.1 INTRODUCTION

The process of ionization in ion-atom collisions has been extensively studied and analysed through various techniques, such as assessing DDCS for emitted energy and emitted angles. Bethe was the first to propose a quantum mechanical model for ionization by fast particles [68].

Advancements in experimental techniques, such as multi-parameter detection, combined with computational procedures, have enabled researchers to conduct comprehensive experiments in which kinematical parameters of all particles involved, such as momentum and energy can be determined. The finer details of ionization processes in both the ground state [24]–[32] and the metastable state [41]–[51] have been effectively studied by these experiments.

The Differential Double Differential Cross Sections (DDCS) of ionization provide valuable information regarding the internal structure of atomic or molecule systems as well as the dynamics of collisions. Experimental evaluations of the DDCS for ionization have been obtained for both angle and energy [27]-[30] by several research groups. Additionally, other groups have also reported their findings on DDCS measurements [31]-[41].

These experimental studies have greatly enhanced our understanding of the ionization process, providing valuable insights into the dynamics of the collision and the structure of the target atom or molecule. The results from these experiments have also been used to validate theoretical models and computational methods, which further enhances our knowledge of the ionization process.

This study focuses on calculating the DDCS for ionization of hydrogenic metastable 2S state by electron impact at incident energies of 150eV and 250eV. The calculation is based on a wave function that has been previously used in related studies [10]-[12]. The DDCS is obtained by integrating over the scattering angle.

This work is important since it is the first theoretical or experimental examination of the DDCS of electron ionization of metastable 2S-state hydrogen atoms at intermediate and high energies. This work opens up a new area of inquiry in this area by using the wave function of the metastable 2S state hydrogen atom by electrons.

The findings of this study can contribute to a better understanding of the ionization mechanism in hydrogenic metastable 2S state by electron impact. Moreover, the results obtained can provide valuable insights for future experimental and theoretical studies in this area.

3.2 THEORY

The direct Transition matrix element for ionization of hydrogen atoms by electron [54] has been written in equation (1.12) of chapter 1 as,

$$T_{FI} = \left\langle \psi_F^{(-)}(\bar{\gamma}_1, \bar{\gamma}_2) \middle| V_I(\bar{\gamma}_1, \bar{\gamma}_2) \middle| \Phi_i(\bar{\gamma}_1, \bar{\gamma}_2) \right\rangle \tag{3.1}$$

Where the perturbation potential $V_I(\bar{\gamma}_1, \bar{\gamma}_2)$ is given by

$$V_I(\bar{\gamma}_1, \bar{\gamma}_2) = \frac{1}{\gamma_{12}} - \frac{1}{\gamma_2} \tag{3.2}$$

The nuclear charge of a hydrogen atom is Ze=1, its two electrons' distances from the nucleus are γ_1 and γ_2, and their distance from one another is γ_{12} (Fig. 2.1). The initial channel unperturbed wave function can be expressed as follows:

$$\Phi_i(\bar{\gamma}_1, \bar{\gamma}_2) = \frac{e^{i\bar{p}_i \cdot \bar{\gamma}_2}}{(2\pi)^{\frac{3}{2}}} \phi_{2S}(\bar{\gamma}_1) \tag{3.3}$$

Where $\phi_{2S}(\bar{\gamma}_1) = \frac{1}{4\sqrt{2\pi}}(2 - \gamma_1)e^{-\lambda_1 \gamma_1}$

Here, the hydrogen 2S state wave function in this case is represented by $\lambda_1 = \frac{1}{2}$ and $\phi_{2S}(\bar{\gamma}_1)$, whereas the final three-particle scattering state wave function is represented by $\psi_F^{(-)}(\bar{\gamma}_1, \bar{\gamma}_2)$, and the coordinates of the two electrons are $\bar{\gamma}_1$ and $\bar{\gamma}_2$, respectively.

In this case, the approximate wave function $\psi_F^{(-)}$ is provided by

$$\psi_F^{(-)}(\bar{\gamma}_1, \bar{\gamma}_2) = N(\bar{p}_1, \bar{p}_2)\Big[\phi_{\bar{p}_1}^{(-)}(\bar{\gamma}_1)e^{i\bar{p}_2 \cdot \bar{\gamma}_2} + \phi_{\bar{p}_2}^{(-)}(\bar{\gamma}_2)e^{i\bar{p}_1 \cdot \bar{\gamma}_1} + \phi_{\bar{p}}^{(-)}(\bar{\gamma})e^{i\bar{P} \cdot \bar{R}} - 2e^{i\bar{p}_1 \cdot \bar{\gamma}_1 + i\bar{p}_2 \cdot \bar{\gamma}_2}\Big]/(2\pi)^3 \tag{3.4}$$

Here

$N(\bar{p}_1, \bar{p}_2)$ is normalization constant, $\bar{\gamma} = \frac{\bar{\gamma}_1 - \bar{\gamma}_2}{2}$, $\bar{R} = \frac{\bar{\gamma}_1 + \bar{\gamma}_2}{2}$, $\bar{p} = \bar{p}_2 - \bar{p}_1$, $\bar{P} = \bar{p}_2 + \bar{p}_1$, and $\phi_q^{(-)}(\bar{\gamma})$ is Coulomb wave function.

Applying equations (3.2), (3.3) and (3.4) in equation (3.1), we get

$$T_{FI} = T_b + T_b' + T_I - 2T_{PB} \tag{3.5}$$

The first Born approximation may be expressed as

$$T_b = \frac{1}{16\pi^2}\left\langle \phi_{\bar{p}_1}^{(-)}(\bar{\gamma}_1)e^{i\bar{p}_2.\bar{\gamma}_2}\left|\frac{1}{\gamma_{12}}-\frac{1}{\gamma_2}\right|e^{i\bar{p}_i.\bar{\gamma}_2}(2-\gamma_1)e^{-\lambda_1\gamma_1}\right\rangle$$

$$= \frac{1}{16\pi^2}\int\left[\phi_{\bar{p}_1}^{(-)*}(\bar{\gamma}_1)e^{-i\bar{p}_2.\bar{\gamma}_2}\left(\frac{1}{\gamma_{12}}-\frac{1}{\gamma_2}\right)e^{i\bar{p}_i.\bar{\gamma}_2}(2-\gamma_1)e^{-\lambda_1\gamma_1}\right]d^3\gamma_1 d^3\gamma_2$$

$$= \frac{1}{16\pi^2}\int\phi_{\bar{p}_1}^{(-)*}(\bar{\gamma}_1)e^{-i\bar{p}_2.\bar{\gamma}_2}\frac{1}{\gamma_{12}}2e^{i\bar{p}_i.\bar{\gamma}_2}e^{-\lambda_1\gamma_1}d^3\gamma_1 d^3\gamma_2$$

$$-\frac{1}{16\pi^2}\int\phi_{\bar{p}_1}^{(-)*}(\bar{\gamma}_1)e^{-i\bar{p}_2.\bar{\gamma}_2}\frac{1}{\gamma_2}2e^{i\bar{p}_i.\bar{\gamma}_2}e^{-\lambda_1\gamma_1}d^3\gamma_1 d^3\gamma_2$$

$$-\frac{1}{16\pi^2}\int\phi_{\bar{p}_1}^{(-)*}(\bar{\gamma}_1)e^{-i\bar{p}_2.\bar{\gamma}_2}\frac{1}{\gamma_{12}}\gamma_1 e^{i\bar{p}_i.\bar{\gamma}_2}e^{-\lambda_1\gamma_1}d^3\gamma_1 d^3\gamma_2$$

$$+\frac{1}{16\pi^2}\int\phi_{\bar{p}_1}^{(-)*}(\bar{\gamma}_1)e^{-i\bar{p}_2.\bar{\gamma}_2}\frac{1}{\gamma_2}\gamma_1 e^{i\bar{p}_i.\bar{\gamma}_2}e^{-\lambda_1\gamma_1}d^3\gamma_1 d^3\gamma_2$$

$$= Tb_1 + Tb_2 + Tb_3 + Tb_4 \tag{3.6}$$

Here

$$Tb_1 = \frac{1}{16\pi^2}\int\phi_{\bar{p}_1}^{(-)*}(\bar{\gamma}_1)e^{-i\bar{p}_2.\bar{\gamma}_2}\frac{1}{\gamma_{12}}2e^{i\bar{p}_i.\bar{\gamma}_2}e^{-\lambda_1\gamma_1}d^3\gamma_1 d^3\gamma_2$$

$$Tb_2 = -\frac{1}{16\pi^2}\int\phi_{\bar{p}_1}^{(-)*}(\bar{\gamma}_1)e^{-i\bar{p}_2.\bar{\gamma}_2}\frac{1}{\gamma_2}2e^{i\bar{p}_i.\bar{\gamma}_2}e^{-\lambda_1\gamma_1}d^3\gamma_1 d^3\gamma_2$$

$$Tb_3 = -\frac{1}{16\pi^2}\int\phi_{\bar{p}_1}^{(-)*}(\bar{\gamma}_1)e^{-i\bar{p}_2.\bar{\gamma}_2}\frac{1}{\gamma_{12}}\gamma_1 e^{i\bar{p}_i.\bar{\gamma}_2}e^{-\lambda_1\gamma_1}d^3\gamma_1 d^3\gamma_2$$

$$Tb_4 = \frac{1}{16\pi^2}\int\phi_{\bar{p}_1}^{(-)*}(\bar{\gamma}_1)e^{-i\bar{p}_2.\bar{\gamma}_2}\frac{1}{\gamma_2}\gamma_1 e^{i\bar{p}_i.\bar{\gamma}_2}e^{-\lambda_1\gamma_1}d^3\gamma_1 d^3\gamma_2 = \frac{1}{2}\frac{\partial}{\partial\lambda_1}(tb_2)$$

T_b, is the first Born term and other terms T_b', T_I, T_{PB} for TDCS are calculated in the our work of [41] and have discussed about them in chapter 1. The above terms of eq. (3.5) have then been analytically computed using exploratory computation utilizing the Lewis integral [88], and the triple differential cross-sections for the T-Matrix element are described by

$$\frac{d^3\sigma}{d\mu_1 d\mu_2 dE_1} = \frac{p_1 p_2}{p_i}|T_{FI}|^2 \tag{3.7}$$

After integrating the TDCS result [41] of equation (3.7), we can use the following equation to obtain the DDCS result

$$\frac{d^2\sigma}{dE_1 d\mu_1} = \int\frac{d^3\sigma}{dE_1 d\mu_1 d\mu_2}d\mu_2 \tag{3.8}$$

Equation (3.8) represents the double differential cross-sections (DDCS) that have been calculated using the computer programming language MATLAB.

3.3 RESULTS AND DISCUSSIONS

For emitted electron energies E_1= 4eV, 10eV, 20eV, 50eV, and 80eV, DDCS are found here for the ionization of the metastable 2S state hydrogen atoms by electrons at high incidence energy E_I=250eV. At intermediate incident energy E_I=150eV for emitted electron energies E_1=4eV, 10eV, 20eV, 30eV and 50eV. With DDCS acting as the vertical axis in all figures, the scattered angle θ_2 changes from 0° to 100°, and the emitted angle θ_1 varies from 0° to 180° as the horizontal axis. We provide here for evaluation the ionization of hydrogen atoms by electrons from the ground state, as demonstrated by experimental evidence [6] and computational results [3], [67].

For incident energy, E_I=250eV in Fig. 3.1(a), emitted energy E_1=4eV the current result coincides around θ_1=20° with those of [3], [6], intersects several times with those of [3], [6], [67] and at higher emitting angle θ_1 lies below closely with the experimental values [6]. Again, our present result and first Born result show similarity in behaviour.

In Fig. 3.1(b), E_1=10eV our result intersects at θ_1=10° and θ_1=170° with those of [6], overlaps two times around θ_1=50°and θ_1=135° with those of [67]. Consequently the curve creates peak flattens at around θ_1=25°, ultimately disappears. which indicates good estimation. Here, our present result and first Born result are almost identical.

In Fig. 3.2(a), E_1=20eV the present outcome intersects three times at θ_1=20°, θ_1=60° and θ_1=180° with those of [3], [6] respectively. Furthermore it overlays around θ_1=60°, θ_1=108° and θ_1=170° with those of [67] which represents good qualitative assessment. Again, the present result closely matches the first Born result.

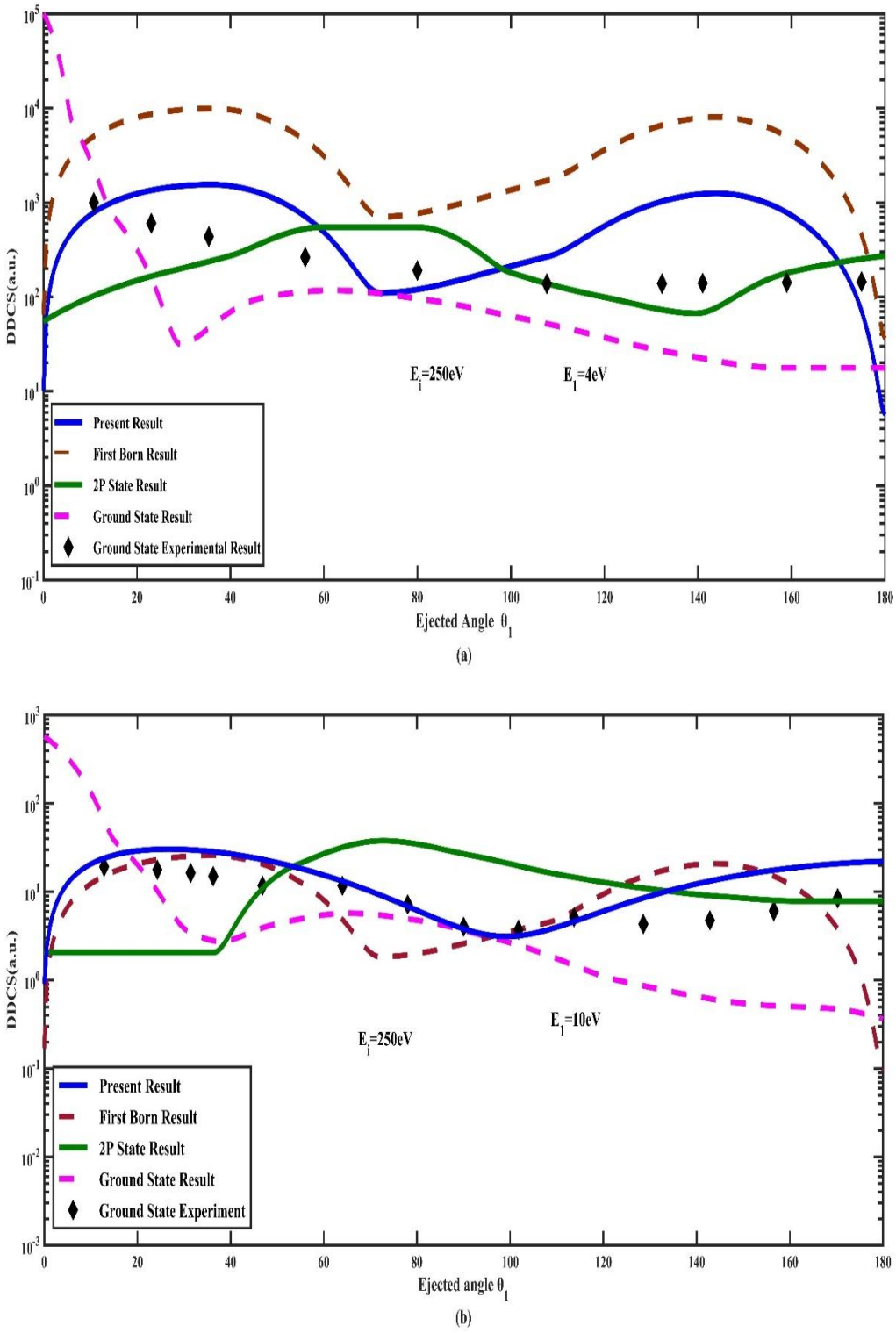

Fig. 3.1 Second Born DDCS for ionized hydrogen atom by incident energy 250 eV and the emitted electron energies are (a) 4eV and (b) 10eV respectively.

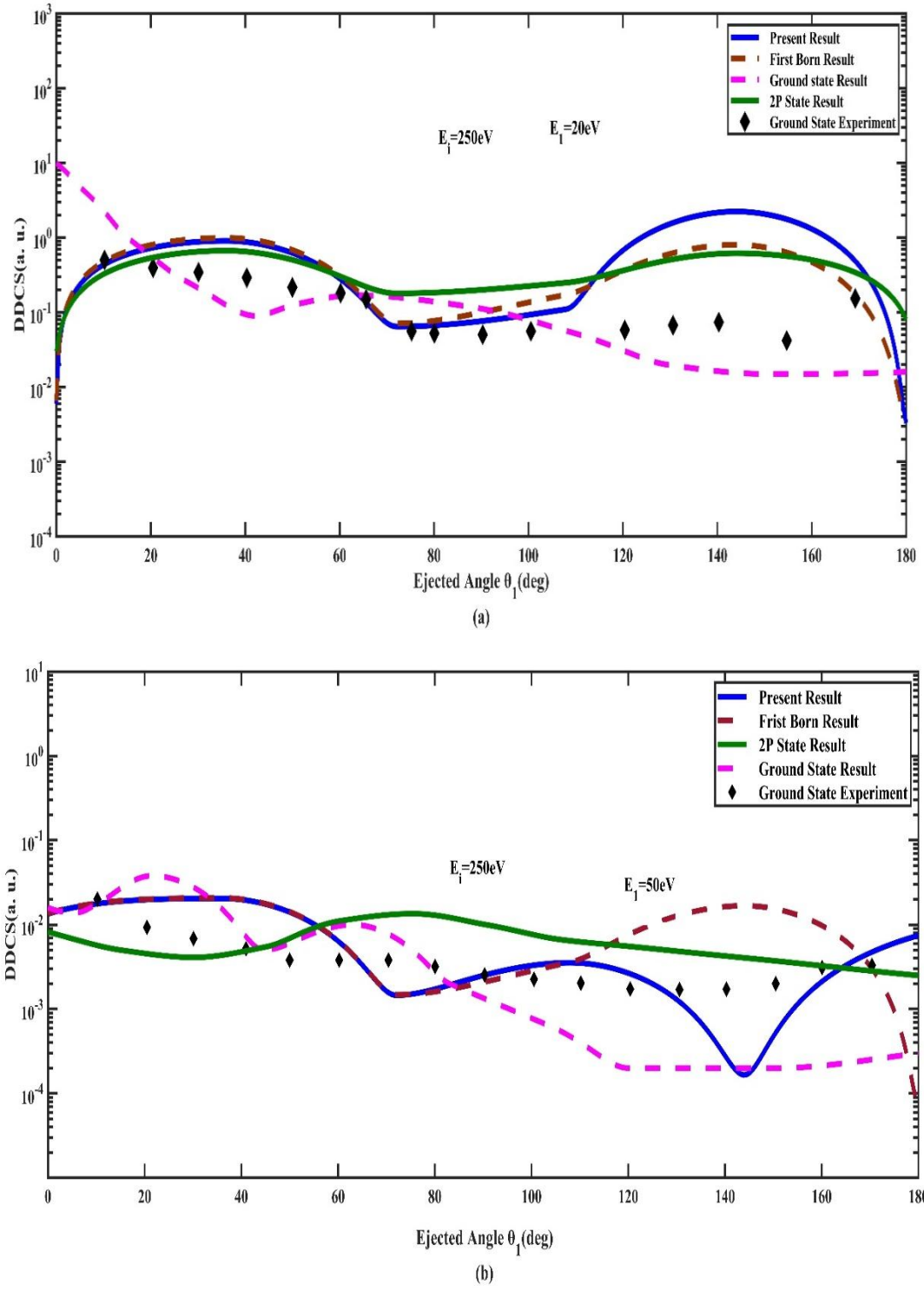

Fig. 3.2 Second Born DDCS for ionized hydrogen atom by incident energy 250 eV and the emitted electron energies are (a) 20eV and (b) 50eV respectively.

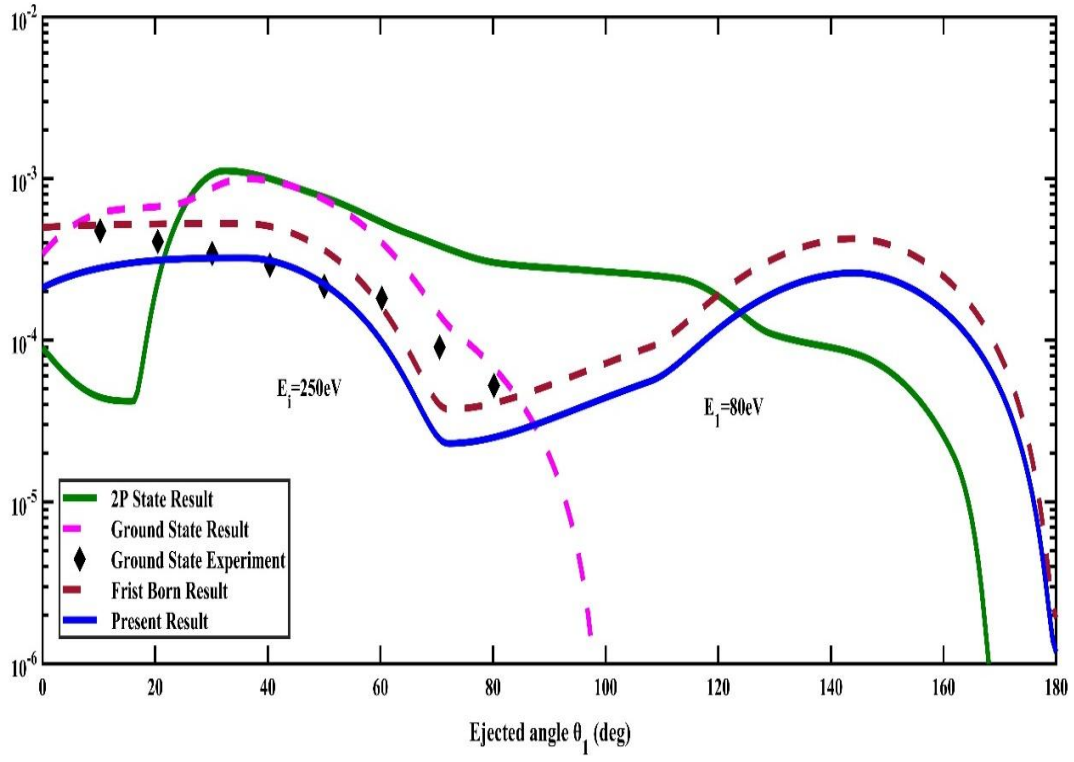

Fig. 3.3 Second Born DDCS for ionized hydrogen atom by incident energy 250 eV and the emitted electron energy is 80eV.

In Fig. 3.2(b), E_1=50eV our outcome concurs several times with those of ground state experiment [6] at θ_1= 8°, θ_1= 60°,θ_1= 90°, θ_1= 125°, θ_1=65 and θ_1= 165°. The present result differs slightly at around θ_1=145° from the first Born result which indicates good assessment.

Lastly, in Fig 3.3, E_1=80eV it is clear that the experimental result, the theoretical result and our obtained result show similar nature in shape at emitted angles up to θ_1=80° and present curve creates a peak alike those of 2P state results[67] at higher angle which refers the good assessment. Also, the present and first Born results are nearly identical. The present DDCS result indicates a good judgement with the theoretical data [3], [67] as well as hydrogenic ground state experimental results [6].

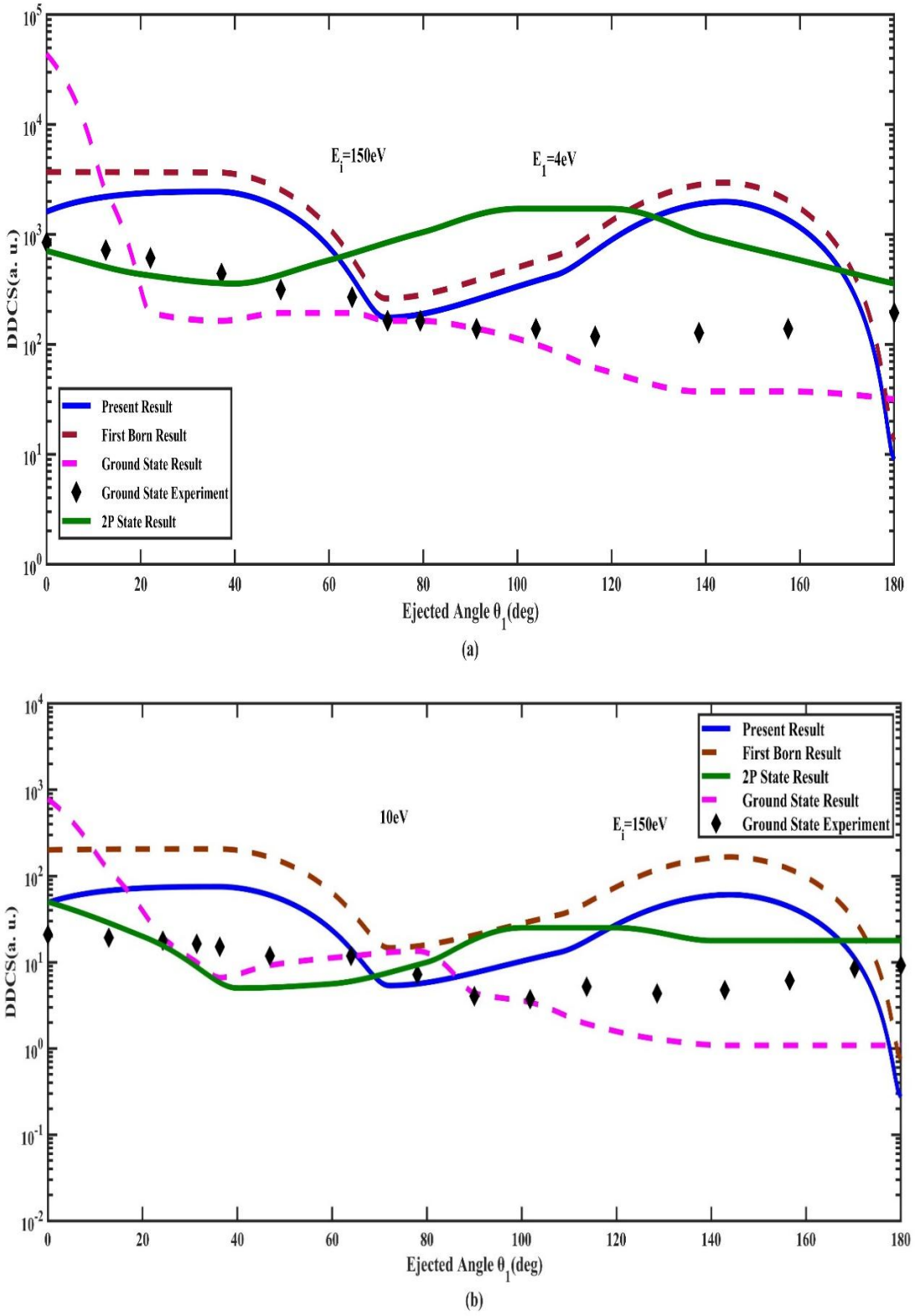

Fig. 3.4 Second Born DDCS for ionized hydrogen atom by incident energy 150 eV and the emitted electron energies are (a) 4eV and (b) 10eV respectively.

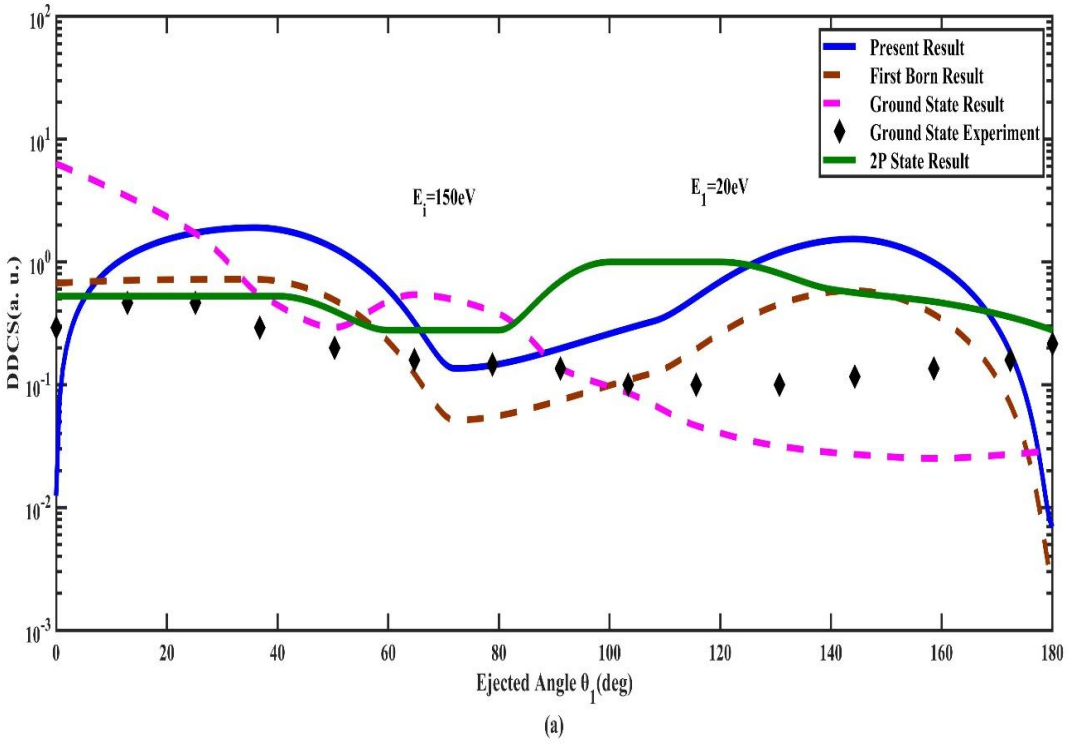

Fig. 3.5 Second Born DDCS for ionized hydrogen atom by incident energy 150 eV and the emitted electron energies are (a) 20eV and (b) 30eV respectively.

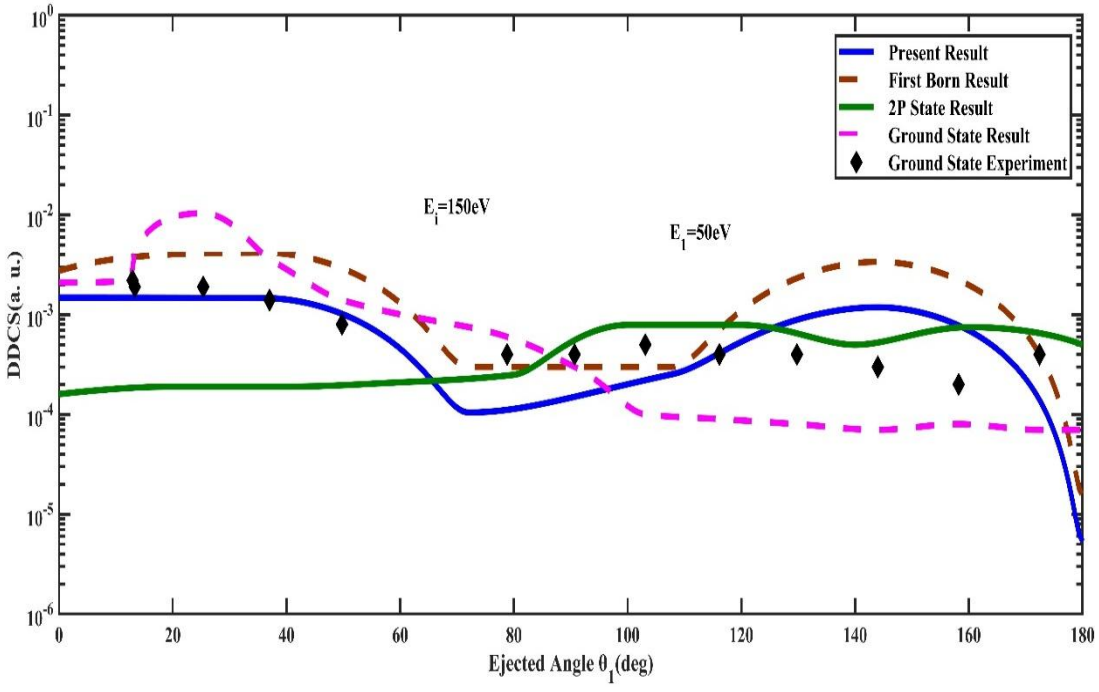

Fig. 3.6 Second Born DDCS for ionized hydrogen atom by incident energy 150 eV and the emitted electron energy is 50eV

For incident energy E_i=150eV, in Fig. 3.4(a), emitted energy E_1=4eV, our outcome intersects at θ_1=70° and θ_1=175° with those of ground state experiment results [6] and overlays three times around θ_1=60°,θ_1=127° and θ_1=170° with those of 2P state outcomes [67], approximately θ_1=17°, θ_1=70° and θ_1=177° overlays ground state results [3]. Here, the present result is very similar to the first Born result.

In Fig. 3.4(b), E_1=10eV, our outcome overlays around θ_1=60°,θ_1=85° and θ_1=170° with those of the ground state experiment results [6] and creates peak far above those of 2P state results [67] , comparatively closer to the ground state results [3] at lesser angles, often goes above to the experimental values. It performs maximum value at θ_1=42° and at θ_1=150° and intersects with those of 2P state results [67], at various emitting angle, θ_1 =70°, θ_1 =122° and θ_1 =170°.

The current outcome closely resembles the initial Born result. Here, the current result closely aligns with the initial Born result [5].

For incident energy E_i=150eV, in Fig. 3.5(a), E_1=20eV our present estimation coincides several times at θ_1=7°,θ_1=70°,θ_1=85° and θ_1=170° with those of ground state experimental results [6], consequently intersects at θ_1=28°, θ_1=60°, θ_1=125° and θ_1=178° with ground state results [3]. Our result overlays with those of 2P state results [67]. In this case, the current outcome closely aligns with the initial Born result [5].

When we increase the ejected electron energy to E_1=50eV while keeping the incident energy at E_I=150eV, an interesting curve structure is observed in Fig. 3.6. The present DDCS result of the metastable 2S-state coincides with the ground state experimental results [6] at the recoil region and creates a peak at higher angles. However, at around θ_1=80°, the present calculation shows a reverse attitude with those of [3] [67]. Despite this, the first Born calculation [5] shows good agreement with the present data.

One can observe that the results are as follows: in the example of E_I=250eV, the values of the various ejection angles θ_1 are shown for various

values of the scattering angles θ_2 for four values of the emitted electron energy E_1.

Table 3.1. DDCS results for the ionization of hydrogen atoms, emitting angles θ_1 corresponding to different scattering angles θ_2, at various kinematic conditions.

θ_2(deg)	θ_1(deg)	$E_1 = 4eV$	$E_1 = 20eV$	$E_1 = 50eV$	$\mathbf{E_1 = 80eV}$
		DDCS	DDCS	DDCS	DDCS
0	0	10.9605	0.00594	0.01341	0.000211
1	36	1673.7067	0.90760	0.02047	0.000322
2	72	119.3104	0.06469	0.00145	0.000023
4	108	289.9023	0.11044	0.00354	0.000055
10	144	1352.1792	2.24380	0.00016	0.000260
20	180	6.0926	0.00330	0.00745	0.000001
30	216	1904.1441	1.03254	0.02329	0.000367
40	252	30.3221	0.01644	0.00037	0.000006
60	288	547.1037	0.05011	0.00669	0.000105
90	324	992.7764	0.53843	0.01214	0.000191
100	360	0	0	0	0

3.4 CONCLUSIONS

Here, DDCS for ionization of metastable 2S-state hydrogen atoms by electron has been estimated at various kinematic situations.

To know details about these systems of the second born DDCS, the up-to-date estimations are obtained by applying the multiple scattering theory [3] which give us a remarkable role in the area of metastable 2S-state ionization problems. Since no previous experimental data has been found for the DDCS results of the ionization of metastable 2S-state hydrogen atom so it is impossible to compare the present computational results with the previous experimental

findings. Therefore, ground state experimental result will be significant for comparison with those of present computational work for the ionization of hydrogenic metastable 2S state by electrons, which gives noteworthy part in the area of ionization problems for future study.

Chapter 4: SINGLE DIFFERENTIAL CROSS-SECTION

4.1 INTRODUCTION

The field of atomic physics involves the study of atomic ionization by charged particles like electrons, photon and positrons, which presents interesting and challenging problems in applied mathematics. Various types of cross-sections, such as single, double, and triple differential, have been determined under different kinematic situations [3]-[10]. The availability of new experimental results over the past 50 years has led to advancements in this research field, with applications in astrophysics, plasma physics, fusion technology etc. This research investigates ionization from metastable 2S-state hydrogen atoms, ionization of medium-heavy atoms and linear superposition of 2S-state hydrogen atoms by charged particles [35], [37], [42], [69]-[74]. Experimental results for metastable 2S-state are also expected to be available in the near future.

The double differential cross-sections (DDCS) provide information about the distribution of secondary electrons in terms of energy and angle, while the single differential cross-sections (SDCS) describe the energy distribution of secondary electrons. These DDCS and SDCS data are useful in studying astrophysical and upper atmospheric phenomena, electron deprivation spectra, and secondary effects produced by slow secondary electrons, among other applications [3]. The current calculations utilize the Lewis integral [88].

Several experimental studies have been conducted to evaluate the double differential cross-sections (DDCS) in angle and energy, primarily for the helium atom due to its simplicity, which allows for minimized experimental

complications. Shyn and other research groups have obtained these evaluations [6], [9], [10], [52]-[55], [57]. On the theoretical side, the best available calculations for DDCS are based on the plane-wave Born approximations [38], [51].

Atomic hydrogen is the simplest and most convenient system for theoretical analysis, but data for DDCS was insufficient until Shyn's work [6]. He provided accurate estimations of DDCS for atomic hydrogen in the incident energy range of 25eV-250eV and over the angular range of 12°-156°. In this study, incident energies of 100eV, 150eV, 200eV, and 250eV were considered for the metastable 2S-state of the hydrogen atom over an angular range of 0°-180°.

The present study used a multiple scattering theory [3] to calculate the double differential cross sections (DDCS) for ionization of metastable 2S-state hydrogen atoms by 150eV and 250eV incident electron energies. The multiple scattering wave function, which includes higher order and correlation effects for two electrons moving in a Coulomb field, was employed in the calculation [2], [4], [42]. This wave function has also been used to obtain attractive outcomes for triple differential cross sections (TDCS) in electron hydrogen ionization collisions at non-relativistic energies [2], [4], [42] and for ionization of medium-heavy atoms by electrons at relativistic energies [4], [42].

The theory of Das and Seal [2] has been found to be suitable for calculating DDCS and SDCS for ionization of metastable 2S-state hydrogen atoms by electrons at intermediate energies. The wave function used in the present study provides a modest and easily applicable approach for calculating DDCS and SDCS for ionization of metastable 2S-state hydrogen atoms by electrons [2]. Qualitatively, the results of BBK theory [49] were found to be better, while the results of Das and Seal [2] were better quantitatively.

The DDCS results were obtained by integrating the TDCS results over the scattered electron directions and compared with the experimental results of Shyn [6] as well as the theoretical results of Das and Seal [3]. The SDCS results

were obtained by an additional integration and compared with the measured results of Shyn [6] and those of Das and Seal [3] and Konovolov & Mc Carthy [84].

4.2 THEORY

Triple differential cross sections (TDCS) in coplanar geometry investigations have provided the most comprehensive information to date on the single ionization process. The TDCS measures the probability that an incident electron with momentum $\bar{p}_i$ and energy E_i will collide with the target and produce two electrons with energies E_1 and E_2 and momenta $\bar{p}_1$ and $\bar{p}_2$ respectively, emitted into solid angles $d\mu_1$ and $d\mu_2$ centered on directions (θ_1, ϕ_1) and (θ_2, ϕ_2). Specifically, the experiments focused on the ionization process of

$$e^- + H(2S) \rightarrow H^+ + 2e^- \tag{4.1}$$

Where, the metastable state of hydrogen atoms is indicated by the symbol 2S.

The study focuses on Single Differential Cross Sections (SDCS) obtained from (e, 2e) coincidence experiments, where the TDCS is integrated over $d\mu_1$, $d\mu_2$ or dE_2 to form various double and single differential cross sections. The kinematic arrangements are distinguished by coplanar and non-coplanar geometries, as well as asymmetric and symmetric geometries, which have implications for the theoretical analysis of the collision. Ehrhardt et al. [21] initially described this distinction for asymmetric geometries in which a fast electron with energy E_I collides with the target atom and a fast ("scattered") and a slow ("ejected") electron are simultaneously detected. Symmetric geometries, where $\theta_1 \cong \theta_2$ and $E_1 \cong E_2$, were first studied by Amaldi et al. [15] and have since been the subject of numerous experiments, as shown in Fig. 2.1 in Chapter 2.

4.2.1 T-matrix element

The direct Transition matrix element for ionization of hydrogen atoms by electron [54] has been written in equation (1.12) of chapter 1 as,

$$T_{FI} = \left\langle \psi_F^{(-)}(\bar{\gamma}_1, \bar{\gamma}_2) \middle| V_I(\bar{\gamma}_1, \bar{\gamma}_2) \middle| \Phi_i(\bar{\gamma}_1, \bar{\gamma}_2) \right\rangle \tag{4.2}$$

Where the perturbation potential $V_I(\bar{\gamma}_1, \bar{\gamma}_2)$ is given by

$$V_I(\bar{\gamma}_1, \bar{\gamma}_2) = \frac{1}{\gamma_{12}} - \frac{1}{\gamma_2} \tag{4.3}$$

The nuclear charge of a hydrogen atom is Ze=1, its two electrons' distances from the nucleus are γ_1 and γ_2, and their distance from one another is γ_{12} (Fig. 2.1). The initial channel unperturbed wave function is given by

$$\Phi_i(\bar{\gamma}_1, \bar{\gamma}_2) = \frac{e^{i\bar{p}_i \cdot \bar{\gamma}_2}}{(2\pi)^{\frac{3}{2}}} \phi_{2S}(\bar{\gamma}_1) \tag{4.4}$$

Where $\phi_{2S}(\bar{\gamma}_1) = \frac{1}{4\sqrt{2\pi}}(2 - \gamma_1)e^{-\lambda_1 \gamma_1}$

Here, the hydrogen 2S state wave function in this case is represented by $\lambda_1 = \frac{1}{2}$ and $\phi_{2S}(\bar{\gamma}_1)$, whereas the final three-particle scattering state wave function is represented by $\psi_F^{(-)}(\bar{\gamma}_1, \bar{\gamma}_2)$, and the coordinates of the two electrons are $\bar{\gamma}_1$ and $\bar{\gamma}_2$, respectively.

Here the approximate wave function $\psi_F^{(-)}$ the is given by

$$\psi_F^{(-)}(\bar{\gamma}_1, \bar{\gamma}_2) = N(\bar{p}_1, \bar{p}_2)\left[\phi_{\bar{p}_1}^{(-)}(\bar{\gamma}_1)e^{i\bar{p}_2 \cdot \bar{\gamma}_2} + \phi_{\bar{p}_2}^{(-)}(\bar{\gamma}_2)e^{i\bar{p}_1 \cdot \bar{\gamma}_1} + \phi_{\bar{p}}^{(-)}(\bar{\gamma})e^{i\bar{P} \cdot \bar{R}} - 2e^{i\bar{p}_1 \cdot \bar{\gamma}_1 + i\bar{p}_2 \cdot \bar{\gamma}_2}\right]/(2\pi)^3 \tag{4.5}$$

Here, $N(\bar{p}_1, \bar{p}_2)$ is normalization constant, $\bar{\gamma} = \frac{\bar{\gamma}_1 - \bar{\gamma}_2}{2}$, $\bar{R} = \frac{\bar{\gamma}_1 + \bar{\gamma}_2}{2}$, $\bar{p} = \bar{p}_2 - \bar{p}_1$, $\bar{P} = \bar{p}_2 + \bar{p}_1$, and $\phi_q^{(-)}(\bar{\gamma})$ is Coulomb wave function.

Applying equations (4.3), (4.4) and (4.5) in equation (4.2), we get

$$T_{FI} = T_b + T_b' + T_I - 2T_{PB} \tag{4.6}$$

Here

$$T_b = \left\langle \phi^{(-)}_{\bar{p}_1}(\bar{\gamma}_1) e^{i\bar{p}_2.\bar{\gamma}_2} \middle| V_I \middle| \Phi_i(\bar{\gamma}_1, \bar{\gamma}_2) \right\rangle \tag{4.7}$$

$$T'_b = \left\langle \phi^{(-)}_{\bar{p}_2}(\bar{\gamma}_2) e^{i\bar{p}_1.\bar{\gamma}_1} \middle| V_I \middle| \Phi_i(\bar{\gamma}_1, \bar{\gamma}_2) \right\rangle \tag{4.8}$$

$$T_I = \left\langle \phi^{(-)}_{\bar{p}}(\bar{\gamma}) e^{i\bar{P}.\bar{R}} \middle| V_I \middle| \Phi_i(\bar{\gamma}_1, \bar{\gamma}_2) \right\rangle \tag{4.9}$$

$$T_{PB} = \left\langle e^{i\bar{p}_1.\bar{\gamma}_1 + i\bar{p}_2.\bar{\gamma}_2} \middle| V_I \middle| \Phi_i(\bar{\gamma}_1, \bar{\gamma}_2) \right\rangle \tag{4.10}$$

The first T_b Born estimated in our work [5].

$$T'_b = \frac{1}{16\pi^2} \int \left[\phi^{(-)*}_{\bar{p}_2}(\bar{\gamma}_2) e^{-i\bar{p}_1.\bar{\gamma}_1} \left(\frac{1}{\gamma_{12}} - \frac{1}{\gamma_2} \right) e^{i\bar{p}_i.\bar{\gamma}_2} (2 - \gamma_1) e^{-\lambda_1\gamma_1} \right] d^3\gamma_1 d^3\gamma_2$$

$$= \frac{1}{8\pi^2} \int \phi^{(-)*}_{\bar{p}_2}(\bar{\gamma}_2) e^{-i\bar{p}_1.\bar{\gamma}_1} \frac{1}{\gamma_{12}} e^{i\bar{p}_i.\bar{\gamma}_2} e^{-\lambda_1\gamma_1} d^3\gamma_1 d^3\gamma_2$$

$$- \frac{1}{8\pi^2} \int \phi^{(-)*}_{\bar{p}_2}(\bar{\gamma}_2) e^{-i\bar{p}_1.\bar{\gamma}_1} \frac{1}{\gamma_2} e^{i\bar{p}_i.\bar{\gamma}_2} e^{-\lambda_1\gamma_1} d^3\gamma_1 d^3\gamma_2$$

$$- \frac{1}{16\pi^2} \int \phi^{(-)*}_{\bar{p}_2}(\bar{\gamma}_2) e^{-i\bar{p}_1.\bar{\gamma}_1} \frac{1}{\gamma_{12}} \gamma_1 e^{i\bar{p}_i.\bar{\gamma}_2} e^{-\lambda_1\gamma_1} d^3\gamma_1 d^3\gamma_2$$

$$+ \frac{1}{16\pi^2} \int \phi^{(-)*}_{\bar{p}_2}(\bar{\gamma}_2) e^{-i\bar{p}_1.\bar{\gamma}_1} \frac{1}{\gamma_2} \gamma_1 e^{i\bar{p}_i.\bar{\gamma}_2} e^{-\lambda_1\gamma_1} d^3\gamma_1 d^3\gamma_2$$

$$= t_{BP1} + t_{BP2} + t_{BP3} + t_{BP4} \tag{4.11}$$

Where

$$t_{BP1} = \frac{1}{8\pi^2} \int \phi^{(-)*}_{\bar{p}_2}(\bar{\gamma}_2) e^{-i\bar{p}_1.\bar{\gamma}_1} \frac{1}{\gamma_{12}} e^{i\bar{p}_i.\bar{\gamma}_2} e^{-\lambda_1\gamma_1} d^3\gamma_1 d^3\gamma_2$$

$$t_{BP2} = - \frac{1}{8\pi^2} \int \phi^{(-)*}_{\bar{p}_2}(\bar{\gamma}_2) e^{-i\bar{p}_1.\bar{\gamma}_1} \frac{1}{\gamma_2} e^{i\bar{p}_i.\bar{\gamma}_2} e^{-\lambda_1\gamma_1} d^3\gamma_1 d^3\gamma_2$$

$$t_{BP3} = - \frac{1}{16\pi^2} \int \phi^{(-)*}_{\bar{p}_2}(\bar{\gamma}_2) e^{-i\bar{p}_1.\bar{\gamma}_1} \frac{1}{\gamma_{12}} \gamma_1 e^{i\bar{p}_i.\bar{\gamma}_2} e^{-\lambda_1\gamma_1} d^3\gamma_1 d^3\gamma_2$$

$$t_{BP4} = \frac{1}{16\pi^2} \int \phi^{(-)*}_{\bar{p}_2}(\bar{\gamma}_2) e^{-i\bar{p}_1.\bar{\gamma}_1} \frac{1}{\gamma_2} \gamma_1 e^{i\bar{p}_i.\bar{\gamma}_2} e^{-\lambda_1\gamma_1} d^3\gamma_1 d^3\gamma_2$$

Here

$$t_{BP3} = \frac{1}{2} \frac{\partial}{\partial \gamma_1} (t_{BP1})$$

$$t_{BP4} = \frac{1}{2} \frac{\partial}{\partial \gamma_1} (t_{BP2})$$

Again

$$T_I = \frac{1}{16\pi^2}\int\left[\phi_{\bar{p}}^{(-)*}(\bar{\gamma})e^{-i\bar{P}.\bar{R}}\left(\frac{1}{\gamma_{12}}-\frac{1}{\gamma_2}\right)e^{i\bar{p}_i.\bar{\gamma}_2}(2-\gamma_1)e^{-\lambda_1\gamma_1}\right]d^3\gamma_1 d^3\gamma_2$$

$$= \frac{1}{8\pi^2}\int\phi_{\bar{p}}^{(-)*}(\bar{\gamma})e^{-i\bar{P}.\bar{R}}\frac{1}{\gamma_{12}}e^{i\bar{p}_i.\bar{\gamma}_2}e^{-\lambda_1\gamma_1}d^3\gamma_1 d^3\gamma_2$$

$$-\frac{1}{8\pi^2}\int\phi_{\bar{p}}^{(-)*}(\bar{\gamma})e^{-i\bar{P}.\bar{R}}\frac{1}{\gamma_2}e^{i\bar{p}_i.\bar{\gamma}_2}e^{-\lambda_1\gamma_1}d^3\gamma_1 d^3\gamma_2$$

$$-\frac{1}{16\pi^2}\int\phi_{\bar{p}}^{(-)*}(\bar{\gamma})e^{-i\bar{P}.\bar{R}}\frac{1}{\gamma_{12}}\gamma_1 e^{i\bar{p}_i.\bar{\gamma}_2}e^{-\lambda_1\gamma_1}d^3\gamma_1 d^3\gamma_2$$

$$+\frac{1}{16\pi^2}\int\phi_{\bar{p}}^{(-)*}(\bar{\gamma})e^{-i\bar{P}.\bar{R}}\frac{1}{\gamma_2}\gamma_1 e^{i\bar{p}_i.\bar{\gamma}_2}e^{-\lambda_1\gamma_1}d^3\gamma_1 d^3\gamma_2$$

$$= t_{I1} + t_{I2} + t_{I3} + t_{I4} \qquad (4.12)$$

Where

$$t_{I1} = \frac{1}{8\pi^2}\int\phi_{\bar{p}}^{(-)*}(\bar{\gamma})e^{-i\bar{P}.\bar{R}}\frac{1}{\gamma_{12}}e^{i\bar{p}_i.\bar{\gamma}_2}e^{-\lambda_1\gamma_1}d^3\gamma_1 d^3\gamma_2$$

$$t_{I2} = -\frac{1}{8\pi^2}\int\phi_{\bar{p}}^{(-)*}(\bar{\gamma})e^{-i\bar{P}.\bar{R}}\frac{1}{\gamma_2}e^{i\bar{p}_i.\bar{\gamma}_2}e^{-\lambda_1\gamma_1}d^3\gamma_1 d^3\gamma_2$$

$$t_{I3} = -\frac{1}{16\pi^2}\int\phi_{\bar{p}}^{(-)*}(\bar{\gamma})e^{-i\bar{P}.\bar{R}}\frac{1}{\gamma_{12}}\gamma_1 e^{i\bar{p}_i.\bar{\gamma}_2}e^{-\lambda_1\gamma_1}d^3\gamma_1 d^3\gamma_2$$

$$t_{I4} = \frac{1}{16\pi^2}\int\phi_{\bar{p}}^{(-)*}(\bar{\gamma})e^{-i\bar{P}.\bar{R}}\frac{1}{\gamma_2}\gamma_1 e^{i\bar{p}_i.\bar{\gamma}_2}e^{-\lambda_1\gamma_1}d^3\gamma_1 d^3\gamma_2$$

Here

$$t_{I3} = \frac{1}{2}\frac{\partial}{\partial\gamma_1}(t_{I1})$$

$$t_{I4} = \frac{1}{2}\frac{\partial}{\partial\gamma_1}(t_{I2})$$

Again

$$T_{PB} = \frac{1}{16\pi^2}\int\left[e^{-i\bar{p}_1.\bar{\gamma}_1}e^{-i\bar{p}_2.\bar{\gamma}_2}\left(\frac{1}{\gamma_{12}}-\frac{1}{\gamma_2}\right)e^{i\bar{p}_i.\bar{\gamma}_2}(2-\gamma_1)e^{-\lambda_1\gamma_1}\right]d^3\gamma_1 d^3\gamma_2$$

$$= \frac{1}{8\pi^2}\int e^{-i\bar{p}_1.\bar{\gamma}_1}e^{-i\bar{p}_2.\bar{\gamma}_2}\frac{1}{\gamma_{12}}e^{i\bar{p}_i.\bar{\gamma}_2}e^{-\lambda_1\gamma_1}d^3\gamma_1 d^3\gamma_2$$

$$-\frac{1}{8\pi^2}\int e^{-i\bar{p}_1.\bar{\gamma}_1}e^{-i\bar{p}_2.\bar{\gamma}_2}\frac{1}{\gamma_2}e^{i\bar{p}_i.\bar{\gamma}_2}e^{-\lambda_1\gamma_1}d^3\gamma_1 d^3\gamma_2$$

$$-\frac{1}{16\pi^2}\int e^{-i\bar{p}_1.\bar{\gamma}_1}e^{-i\bar{p}_2.\bar{\gamma}_2}\frac{1}{\gamma_{12}}\gamma_1 e^{i\bar{p}_i.\bar{\gamma}_2}e^{-\lambda_1\gamma_1}d^3\gamma_1 d^3\gamma_2$$

$$+\frac{1}{16\pi^2}\int e^{-i\bar{p}_1.\bar{\gamma}_1}e^{-i\bar{p}_2.\bar{\gamma}_2}\frac{1}{\gamma_2}\gamma_1 e^{i\bar{p}_i.\bar{\gamma}_2}e^{-\lambda_1\gamma_1}d^3\gamma_1 d^3\gamma_2$$

$$= t_{pb1} + t_{pb2} + t_{pb3} + t_{pb4} \tag{4.13}$$

Where

$$t_{pb1} = \frac{1}{8\pi^2}\int e^{-i\bar{p}_1.\bar{\gamma}_1} e^{-i\bar{p}_2.\bar{\gamma}_2} \frac{1}{\gamma_{12}} e^{i\bar{p}_i.\bar{\gamma}_2} e^{-\lambda_1\gamma_1} d^3\gamma_1 d^3\gamma_2$$

$$t_{pb2} = -\frac{1}{8\pi^2}\int e^{-i\bar{p}_1.\bar{\gamma}_1} e^{-i\bar{p}_2.\bar{\gamma}_2} \frac{1}{\gamma_2} e^{i\bar{p}_i.\bar{\gamma}_2} e^{-\lambda_1\gamma_1} d^3\gamma_1 d^3\gamma_2$$

$$t_{pb3} = -\frac{1}{16\pi^2}\int e^{-i\bar{p}_1.\bar{\gamma}_1} e^{-i\bar{p}_2.\bar{\gamma}_2} \frac{1}{\gamma_{12}} \gamma_1 e^{i\bar{p}_i.\bar{\gamma}_2} e^{-\lambda_1\gamma_1} d^3\gamma_1 d^3\gamma_2$$

$$t_{pb4} = \frac{1}{16\pi^2}\int e^{-i\bar{p}_1.\bar{\gamma}_1} e^{-i\bar{p}_2.\bar{\gamma}_2} \frac{1}{\gamma_2} \gamma_1 e^{i\bar{p}_i.\bar{\gamma}_2} e^{-\lambda_1\gamma_1} d^3\gamma_1 d^3\gamma_2$$

Here

$$t_{pb3} = \frac{1}{2}\frac{\partial}{\partial\gamma_1}(t_{pb1})$$

$$t_{pb4} = \frac{1}{2}\frac{\partial}{\partial\gamma_1}(t_{pb2})$$

T_b, is the first Born term for TDCS and other terms T_b', T_I, T_{PB} have been estimated [41]. The triple differential cross-sections for T-Matrix element has been specified by equation (1.36) in chapter 1 as

$$\frac{d^3\sigma}{d\mu_1 d\mu_2 dE_1} = \frac{p_1 p_2}{p_i}|T_{FI}|^2. \tag{4.14}$$

Integration of TDCS result [41] of equation (4.14), we can acquire the DDCS result using following equation

$$\frac{d^2\sigma}{dE_1 d\mu_1} = \int \frac{d^3\sigma}{dE d\mu_1 d\mu_2} d\mu_2 \tag{4.15}$$

Therefore, double differential cross sections (DDCS) has been determined using computer programming language MATLAB, given by equation (4.15).

Finally, integration of DDCS result of equation (4.15), we can acquire the SDCS result using following equation

$$\frac{d\sigma}{dE_1} = \int \frac{d^2\sigma}{dE d\mu_1} d\mu_1 \tag{4.16}$$

Hence, single differential cross sections (SDCS) has been determined using computer programming language MATLAB, given by equation (4.16).

4.3 RESULTS AND DISCUSSIONS

The objective of this paper is to compare the Single Differential Cross Section (SDCS) results for ionization of hydrogen atoms by electrons of incident energies E_I =100eV, 150eV, 200eV, and 250eV, with respect to the energy E_1 of the ejected electron. The ejected energy E_1 ranges from 0eV to 50eV and is shown on the horizontal axis, while the SDCS is shown on the vertical axis.

In particular, the SDCS results for the hydrogenic ground state and metastable 2S-state compared in this study. The SDCS results for ionization from the ground state obtained by Shyn [6], Das and Seal [3], and Konovalov and Mc Carthy [84] through experimental [6] and computational methods [3], [84] also presented for comparison.

Overall, the agreement between the different results is satisfactory. However, the present study's results show slight deviations in trend compared to the previously mentioned results. In some cases, the present study's results even appear to be slightly better in trend.

In Fig. 4.1(a), when considering an incident energy of E_I =250eV, our results for the SDCS appear to be less steep at lower ejected energies when compared to the results obtained by Das and Seal [3] and Shyn [6]. However, as the ejected energies increase up to 50eV, a similar trend is observed in our results.

On the other hand, our results show good agreement with the results obtained by Konovalov and Mc Carthy [84], both in terms of shape and trend. Thus, the overall comparison shows that our results for the SDCS are in satisfactory agreement with previous experimental [6] and computational studies [3], [84].

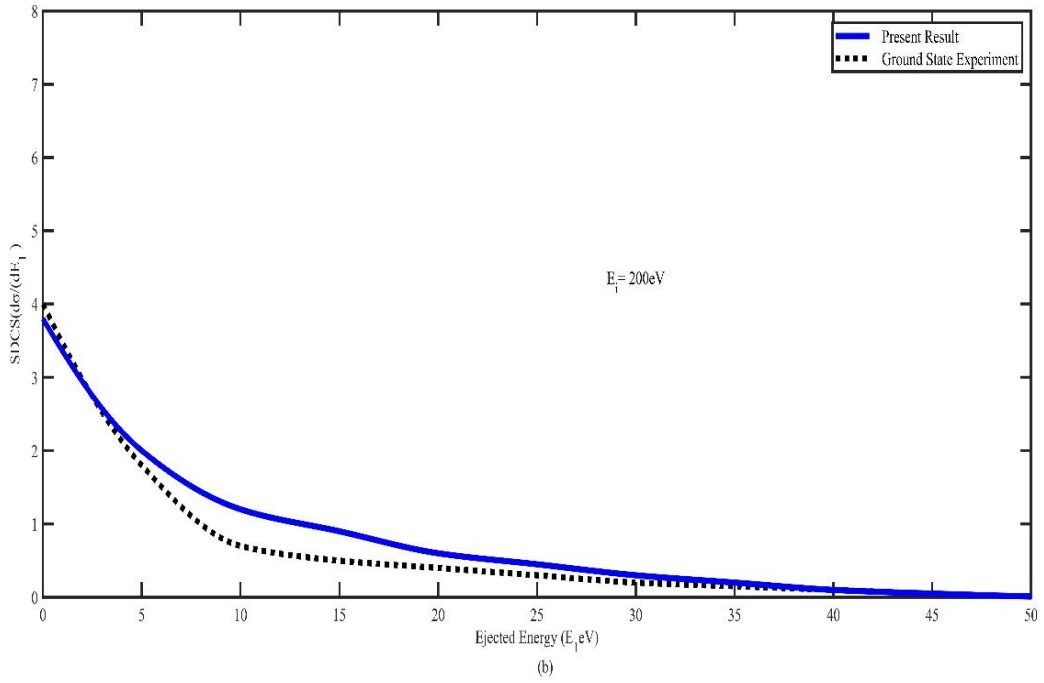

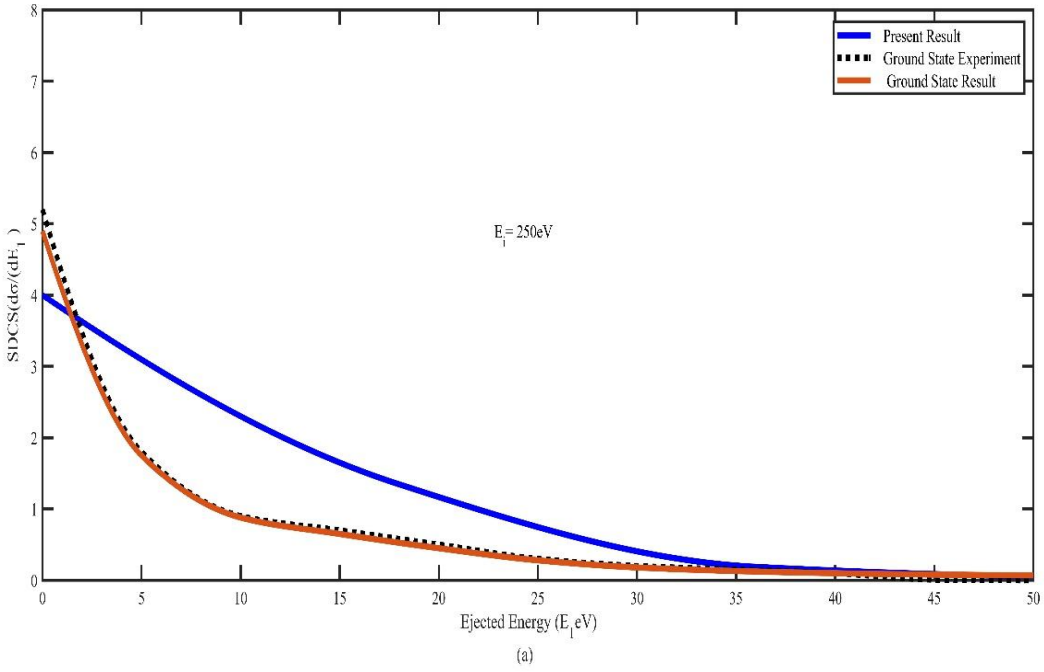

Fig. 4.1 Single Differential Cross Section (SDCS) for ionization of hydrogen atoms by incident electrons with energies of (a) E_I = 250eV and (b) E_I =200eV, plotted against the various values of energy E_1 of the ejected electrons.

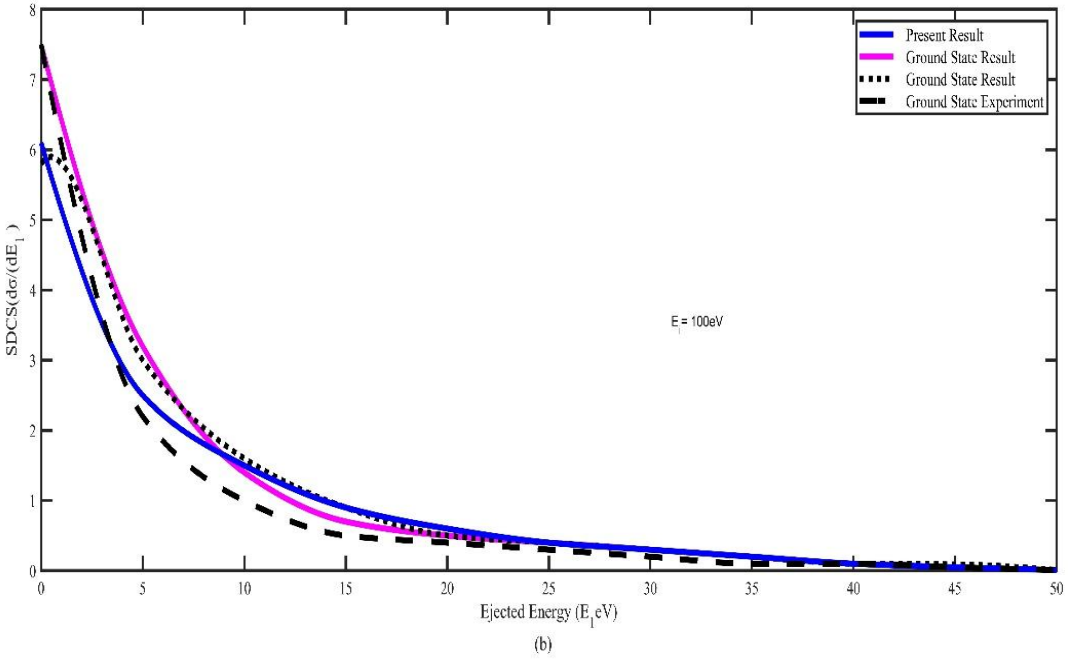

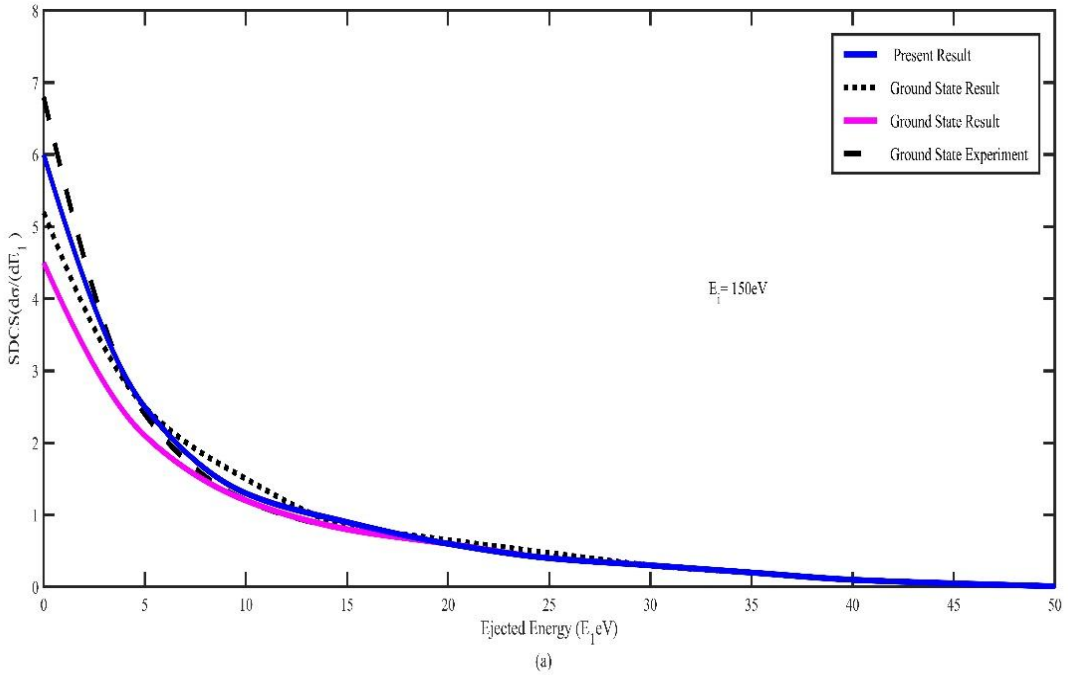

Fig. 4.2 Single Differential Cross Section (SDCS) for ionization of hydrogen atoms by incident electrons with energies of (a) $E_I = 150$eV and (b) $E_I = 100$eV, plotted against the various values of energy E_1 of the ejected electrons.

When analysing Fig. 4.1(b) with an incident energy of E_I =200eV, we observed that the measured results align closely with the calculations by Das and Seal [3] at both lower and higher energies. Additionally, at intermediate energies, the measured data closely follows the trend predicted by Das and Seal [3].

In Fig. 4.2(a), for an incident energy of E_I =150eV, our computed results are in agreement with those obtained by Das and Seal [3] and Shyn [6] and Konovalov and Mc Carthy [84] at very low energies of E_1. At around E_1 =4eV, our results are in agreement with those obtained by Shyn [6] and Konovalov and McCarthy [84]. However, our results show a slightly higher trend upon increasing the ejection energies.

Lastly, our present results are in good agreement with the results obtained by Das and Seal [3], Shyn [6], and the compared results [84] at higher energies. Overall, our results demonstrate satisfactory agreement with previous experimental [6] and computational [3], [84] studies for the SDCS of hydrogen atoms ionized by electrons of various incident energies.

In Figure 4.2(b), when looking at electron energies of E_I =100eV, the current calculation shows less vertical displacement compared to the previous calculation for energies ranging from 0eV to 5eV.

However, as the ejection energies of E_1 increase to 15eV and beyond, the current calculation becomes more consistent with the previous calculation, with only a few percent difference at intermediate energies.

At higher electron energies, the current calculation agrees well with the compared results, demonstrating good qualitative agreement between the two calculations.

4.4 CONCLUSION

We investigated the Single Differential Cross Section (SDCS) for ionization of metastable 2S-state hydrogen atoms by electrons at intermediate and high energies. Overall, we found that our computational results showed a satisfactory qualitative agreement. However, we also observed some notable discrepancies when compared to the calculations performed by Shyn [6], Das and Seal [3], and Konovalov and McCarthy [84]. These inconsistencies might be attributed to variations in the states considered during the calculations.

A significant contribution of our study lies in the use of the multiple scattering theory proposed by Das and Seal [3], which has proven to be valuable in addressing challenges related to metastable 2S-state ionization problems. Despite these developments, we are unable to verify our computational conclusions through experimental comparisons because there is currently no experimental data available for the SDCS results of the hydrogenic metastable 2S-state ionization process.

Therefore, it is imperative that experimental investigations be carried out in the appropriate field in order to establish the reliability and comprehensiveness of our work. Acquiring experimental data on the ionization of metastable 2S-state hydrogen atoms by electrons will not only bring fresh insights to our important work, but will also furnish essential empirical information for future developments in this field.

Chapter 5: DOUBLE AND SINGLE DIFFERENTIAL CROSS-SECTIONS WITH EXCHANGE EFFECT

5.1 INTRODUCTION

It is important to note that theoretical calculations and experimental measurements are both crucial in studying the ionization of hydrogen atoms by electrons. While theoretical calculations [2]-[5], [16], [21], [23], [26], [27], [29]-[31], [35], [37], [41], [42], [46], [47]-[49], [63], [67], [68], [70], [74], [85] provide a framework for understanding the physical processes involved, experimental measurements help validate these theoretical predictions and provide insight into the details of the ionization process.

The double differential cross-sections (DDCS) provide a way to quantify the probability of ionization at various angles and energies. The plane-wave Born approximation, developed by Massey & Mohr [37] and Mc Carrol [51], was one of the earliest theoretical frameworks for calculating DDCS at high energies. However, as the incident energy decreases, other factors such as electron-electron interactions and atomic binding effects become increasingly important, making theoretical calculations more challenging.

Experimental measurements of DDCS have been carried out by various groups, including Shyn [52]-[55] and others [62] at both high and intermediate energies. These measurements provide valuable data for validating theoretical calculations and improving our understanding of the ionization process.

Das [1], Das and Seal [2], [29] developed a multiple scattering theory for calculating DDCS at intermediate energies for hydrogen atoms ionized by electrons. This theory takes into account the effects of electron-electron

interactions and atomic binding, and provides a more accurate description of the ionization process at these energies.

The lifetime of the hydrogen atom in excited state is represented [86], [87] by

$$t_I = \sum(A_{ij})^{-1} \tag{5.1}$$

Here, A_{ij} denote Einstein coefficient. The lifetime of the metastable 2S state of hydrogen atom is approximately 1420 seconds or about 24 minutes. This is a relatively long lifetime compared to other excited states of hydrogen atom, such as the metastable 2P state with a lifetime of 1.6×10^{-9} seconds, and is due to the forbidden nature of the transition from the 2S state to the ground state. The long lifetime of the 2S state makes it useful for certain applications, such as atomic clocks and precision spectroscopy.

However, there has been little theoretical and experimental study on the double differential cross-section (DDCS) for the ionization of metastable 2S-state hydrogen atoms by electrons at intermediate energies with exchange effects. Most of the experimental investigations have focused on ground-state electron hydrogen ionization collisions.

It is worth noting that some theoretical calculations for the triple differential cross-section (TDCS) of hydrogen atoms in various excited states, including 2S, 2P, 3P, 3D [63], [73], [74] with electron exchange effects have been performed. However, there is still a lack of theoretical and experimental studies on the DDCS of hydrogen atoms in metastable 2S state. Therefore, further research in this area would help expand our understanding of the ionization process in excited states of hydrogen atoms.

5.2 THEORY

This study focuses on the direct and exchange amplitude of T-matrix elements for ionization of hydrogen atoms by electrons, which is based on the multiple scattering theory. The theory and equation for the direct T-matrix element with exchange effects are described in detail in Chapter 1.

$$T_{FI} = \left\langle \psi_F^{(-)}(\bar{\gamma}_1, \bar{\gamma}_2) \middle| V_I(\bar{\gamma}_1, \bar{\gamma}_2) \middle| \Phi_i(\bar{\gamma}_1, \bar{\gamma}_2) \right\rangle \tag{5.2}$$

Equation (2.8) in Chapter 5 can be expressed as

$$T_{FI} = T_b + T_b' + T_I - 2T_{PB} \tag{5.3}$$

The terms T_b, T_b', T_I and $2T_{PB}$ are computed using Dhar [41] method, and the direct scattering amplitude is determined using the following equation as

$$f(\overline{p_1}, \overline{p_2}) = -(2\pi)^2 T_{FI} \tag{5.4}$$

The exchange effect amplitude is approximated using the following approximation:

$$g(\overline{p_1}, \overline{p_2}) = f(\overline{p_2}, \overline{p_1}) \tag{5.5}$$

After, obtaining the analytical expressions for T_b, T_b', T_I and T_{PB} numerical calculations were performed using the Lewis integral [88] and Gaussian quadrature formula. The triple differential cross section (TDCS) was obtained from the following numerical results

$$\frac{d^3\sigma}{d\mu_1 d\mu_2 dE_1} = \frac{p_1 p_2}{p_i}\left[\frac{3}{4}|f-g|^2 + \frac{1}{4}|f+g|^2\right] \tag{5.6}$$

Later integration of TDCS result of equation (5.6), we can acquire the DDCS result using following equation

$$\frac{d^2\sigma}{dE_1 d\mu_1} = \int \frac{d^3\sigma}{dE_1 d\mu_1 d\mu_2} d\mu_2 \tag{5.7}$$

Therefore, double differential cross-sections (DDCS) has been determined using computer programming language MATLAB, given by equation (5.7).

Finally, integration of DDCS result of equation (5.7), we can acquire the SDCS result using following equation

$$\frac{d\sigma}{dE_1} = \int \frac{d^2\sigma}{dE_1 d\mu_1} d\mu_1 \tag{5.8}$$

Hence, single differential cross sections (SDCS) has been determined using computer programming language MATLAB, given by equation (5.8).

5.3 RESULTS AND DISCUSSIONS

5.3.1 Double differential cross section

The focus of this research is to determine the DDCS for the hydrogenic metastable 2S state by electron with exchange effect. The incident energy is set at E_i=250eV for five different ejected electron energies, namely E_1=4eV, E_1=10eV, E_1=20eV, E_1=50eV, and E_1=80eV. The intermediate incident energy of E_i=150eV is also studied, with ejected electron energies of E_1=4eV, E_1=10eV, E_1=20eV, E_1=30eV, and E_1=50eV.

The horizontal axis of the figures represents the ejected angle θ_1, ranging from 0^0 to 180^0, while the vertical axis displays the DDCS and the scattered angle θ_2 ranging from 0^0 to 100^0.

In the recoil region, which is represented in the figures as the range of θ_1 from 0^0 to 90^0 and ϕ_1=0^0, the DDCS is displayed. In contrast, the binary region, represented as the range of θ_1 from 90^0 to 180^0 and ϕ_1=180^0, also shows the DDCS. It is worth noting that the figures cover the full range of angles, with θ ranging from 0^0 to 360^0.

In this article, the we compare the experimental results of Shyn [6] and the computational results of Das and Seal [3] for the ionization of hydrogen atoms by electrons from the ground state. We also include the first Born results [5] for comparison. The scattering wave function, $\psi_F^{(-)}(\bar{\gamma}_1, \bar{\gamma}_2)$ used for the final state is the continuum state of atomic hydrogen. Additionally, we consider the contribution of the final continuum state in the ionization of metastable 2S state hydrogen atoms by electrons. The comparison of these results shows a reasonable qualitative agreement between the theoretical and hydrogenic ground state experimental results.

The DDCS exchange results show a much larger amplitude than the present first Born results. However, there are noticeable differences in the forward and backward directions. This suggests that the interactions between the projectile electron and the target atom are particularly important in the vicinity of the peak. Therefore, the current findings are particularly relevant for understanding how atomic hydrogen is ionized at intermediate energies.

The graph in Figure 5.1(a) shows the results for an incident electron energy of 250eV and an ejected electron energy of 4eV. The present exchange result exhibits two peaks at lower and higher ejected angles θ_1 but shows reverse shape at around 100^0 with those of [3], [6]. In summary, the present result is consistent with the compared results.

In Fig. 5.1(b), we consider an incident electron energy, E_I=250eV and an ejected electron energy, E_1=10eV. The present exchange result exhibits a broad peak across the entire range of ejected angles θ_1, from 0^0 to 180^0. This peak closely follows the pattern of the results of Das and Seal [3] but slightly differs from the patterns seen in the first Born result [5] and Shyn [6]. However, at lower angles of 0^0 to 55^0, the present result [5] is consistent with the compared results.

In Fig. 5.2(a), we consider an incident electron energy, E_I=250eV and an ejected electron energy, E_1=20eV. The present DDCS result closely resembles the first Born result [5], indicating their similarity in this energy regime. Additionally, we observe that the present DDCS result for the metastable 2S-state displays a peak pattern similar to that of Das and Seal [3] and Shyn [6], with the peak gradually disappearing as the ejected angle increases beyond 80^0. Moreover, the present DDCS result is higher than both Das and Seal [3] and Shyn [6] at most of the ejected angles, but exhibits a lower shape at lower angles when compared to both the compared results.

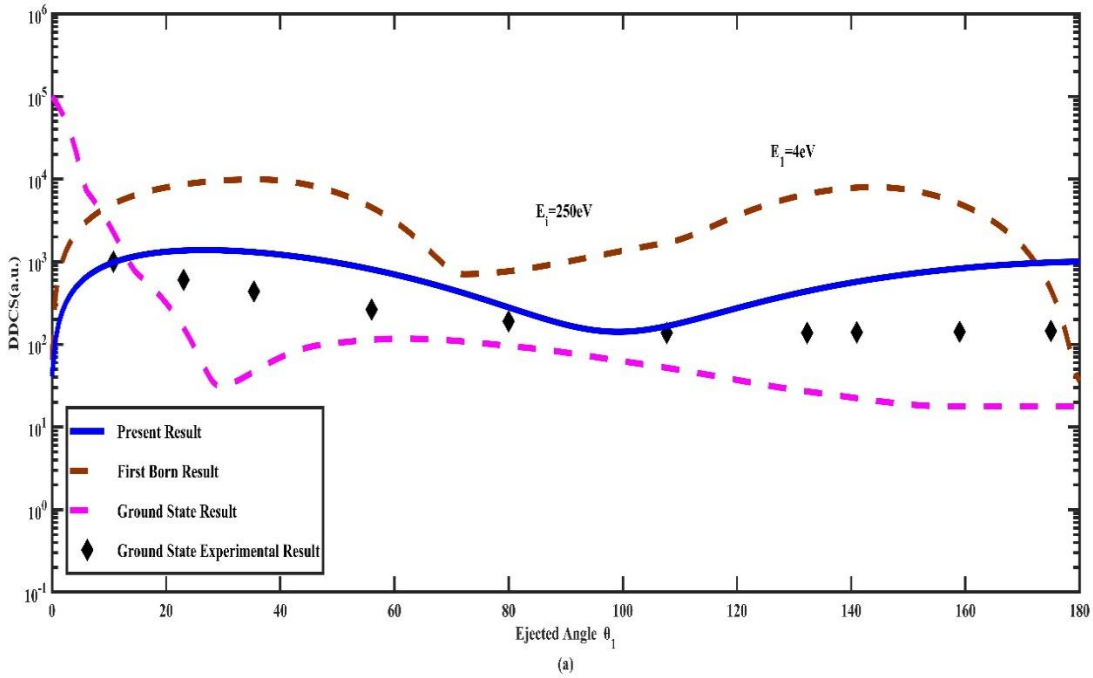

Fig. 5.1 The effect of exchange on the Double Differential Cross Section (DDCS) for electron impact at an energy of 250 eV is shown for two different ejected electron energies: (a) 4 eV and (b) 10 eV.

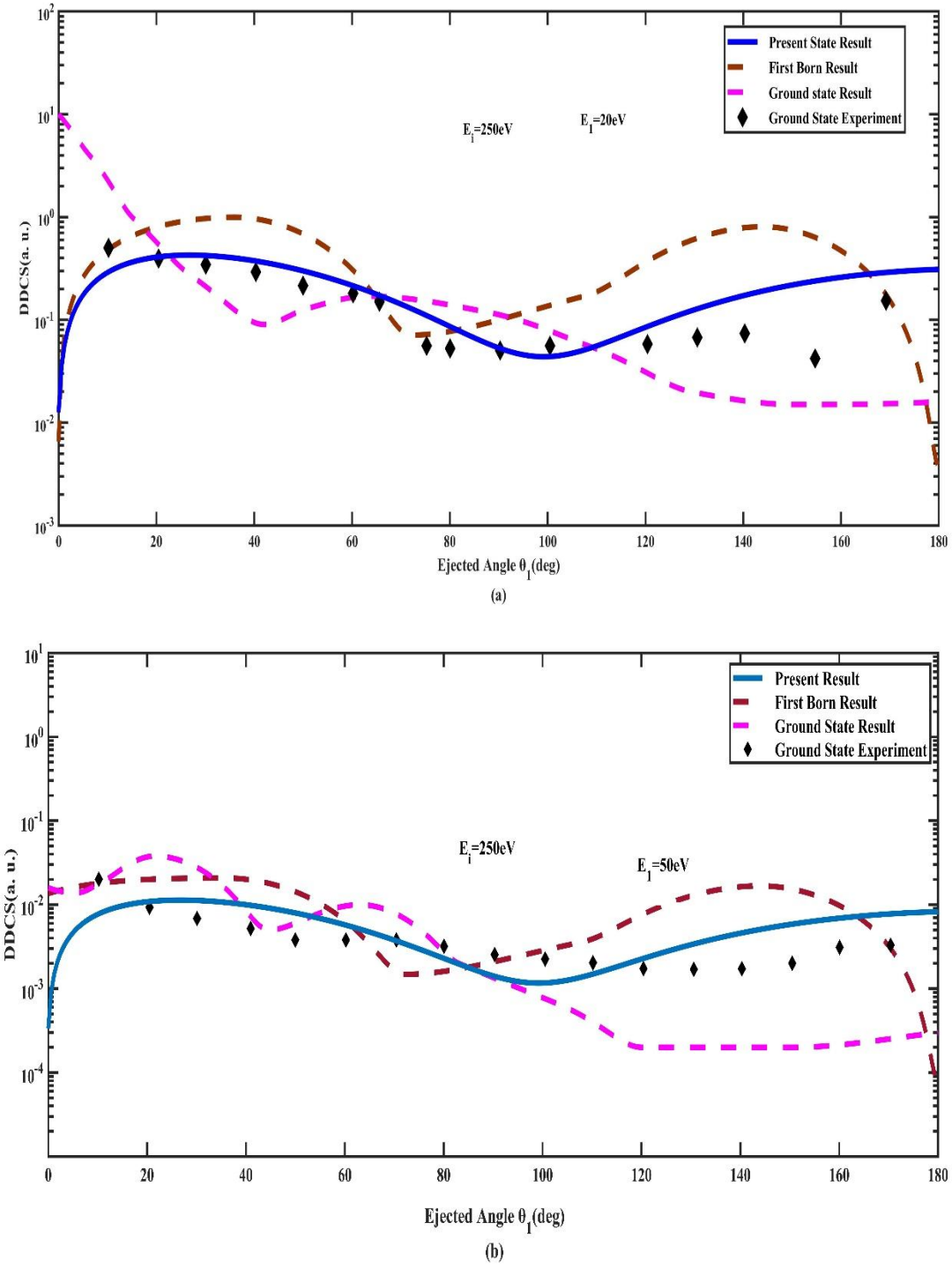

Fig. 5.2 The effect of exchange on the Double Differential Cross Section (DDCS) for electron impact at an energy of 250 eV is shown for two different ejected electron energies: (a) 20 eV and (b) 50 eV.

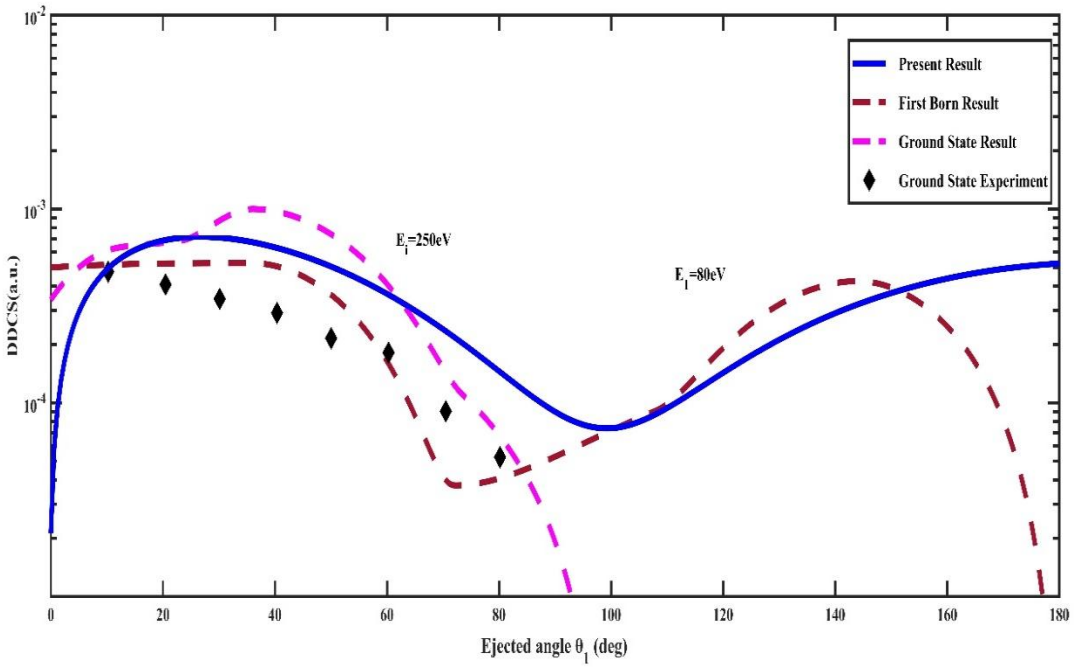

Fig. 5.3 The effect of exchange on the Double Differential Cross Section (DDCS) for electron impact at an energy of 250 eV is shown for ejected electron energy 80 eV

In Fig. 5.2(b), when an incident energy of E_I=250eV and ejected electron energy of E_1=50eV are taken into account, it is observed that the exchange result obtained has a similar shape at different angles, but a reverse shape at lower values of θ_1. The present calculation also shows better agreement with the hydrogenic ground state theoretical result given by Das and Seal [3] as compared to other results.

In the scenario Fig. 5.3, increasing the incident energy E_I=250eV and ejected electron energyE_1=80eV results in different behavior of the DDCS exchange calculation compared to the hydrogenic ground state result. While the present first Born result [5] and hydrogenic ground state result exhibit similar shape, the DDCS exchange calculation shows lower dip pattern at lower ejected angle.

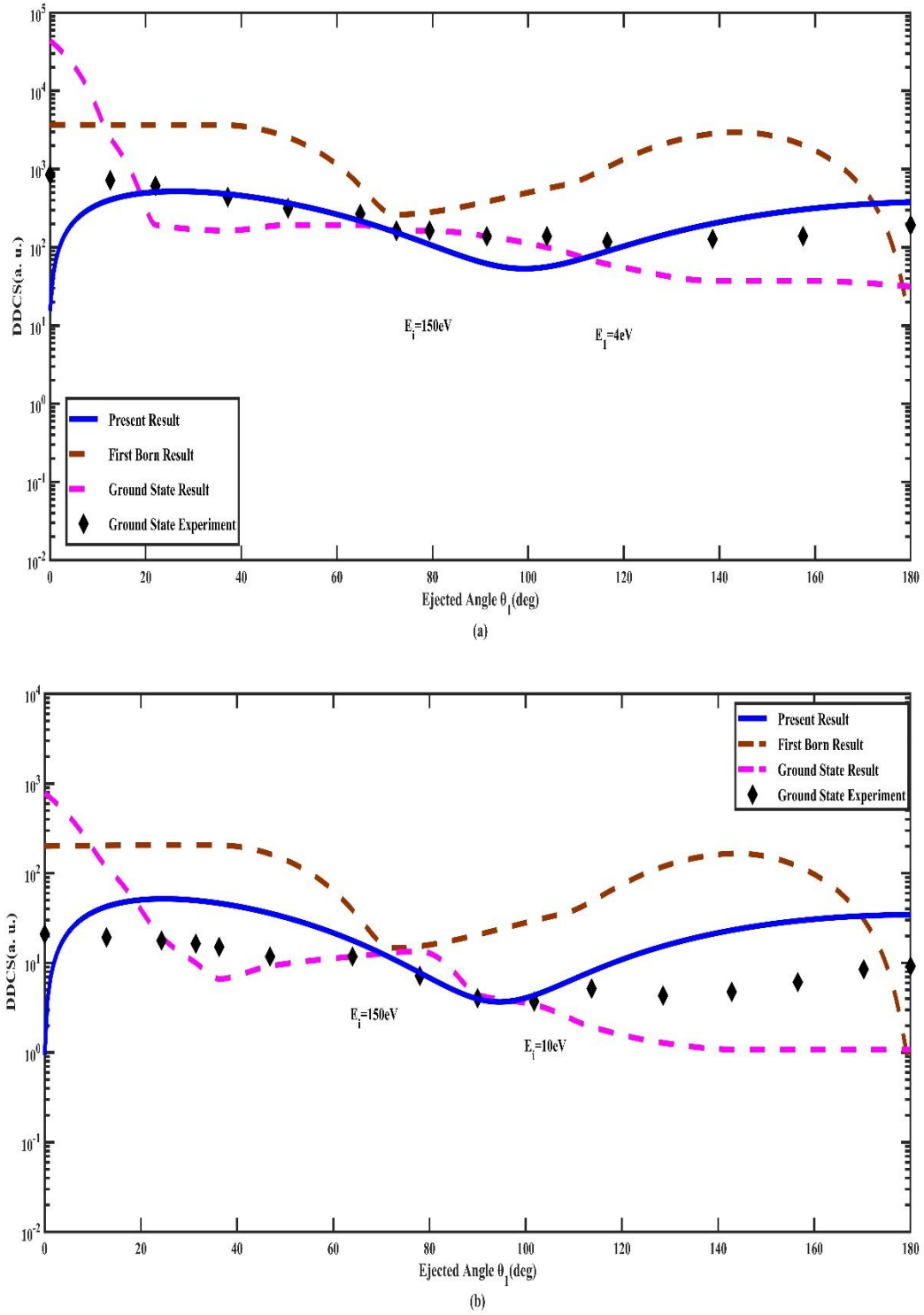

Fig. 5.4 The effect of exchange on the Double Differential Cross Section (DDCS) for electron impact at an energy of 150 eV is shown for two different ejected electron energies: (a) 4 eV and (b) 10 eV.

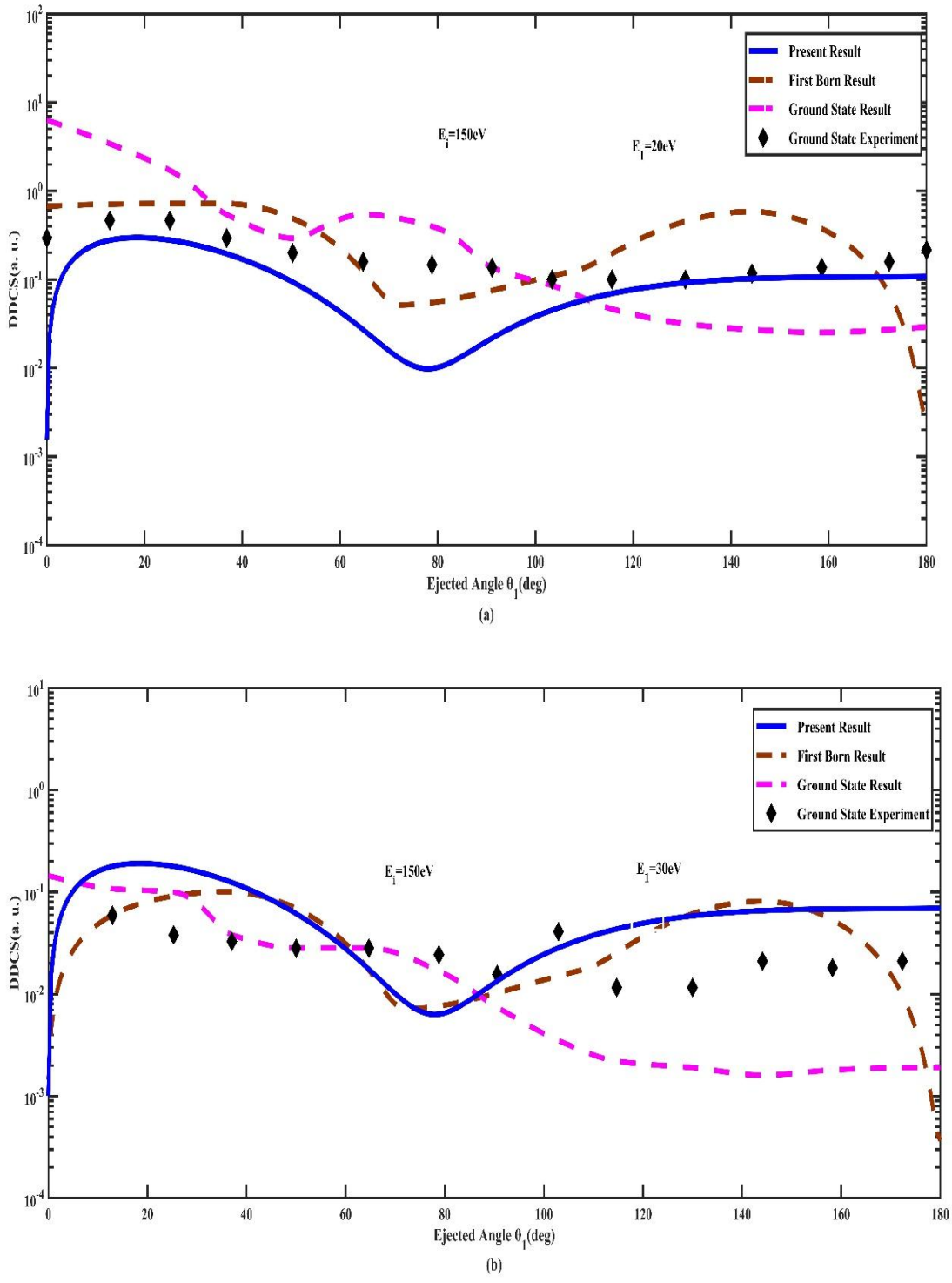

Fig. 5.5 The effect of exchange on the Double Differential Cross Section (DDCS) for electron impact at an energy of 150 eV is shown for two different ejected electron energies: (a) 20 eV and (b) 30 eV.

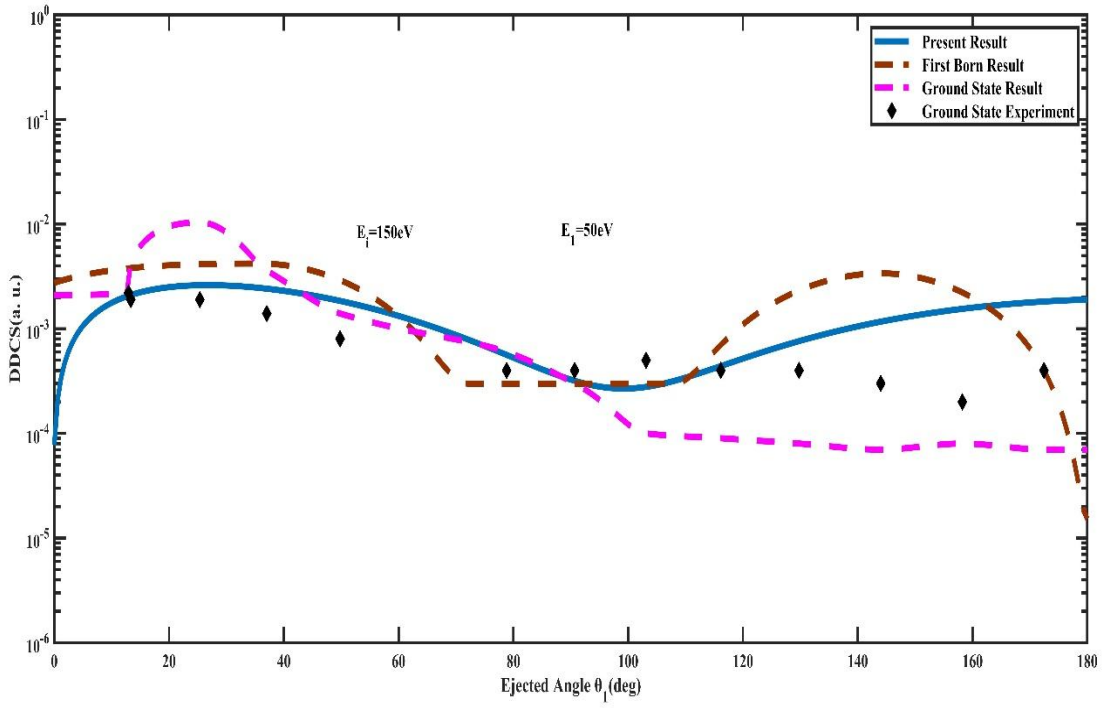

Fig. 5.6 The effect of exchange on the Double Differential Cross Section (DDCS) for electron impact at an energy of 150 eV is shown for ejected electron energy 50 eV

When considering the incident energy E_I=150eV and E_1=4eV, we can see from Fig. 5.4(a) that our present result and the first Born result [5] are very similar, with the exception of a lower peak at θ_1 =100° in the present result. Interestingly, the position of this lower peak in the present first Born result [5] is closer to the results obtained for the ionization of ground state hydrogen atoms by electrons than to the present DDCS exchange calculation.

In the Fig. 5.4(b) when the energy of the ejected electron is increased to E_1=10 electron volts (eV) and the incident energy is E_I=150eV, the results obtained using the first Born model [5] and the present model shows similar behaviour. However, these results are found to be overestimated compared to the results obtained by Das and Seal [3] over a certain range of ejected angles. On the other hand, the present model is found to be in better agreement with the theoretical ground state result.

In a certain scientific context, the present model and the hydrogenic ground state theoretical model exhibit similar shapes for ejected angles from

120° to 180°. In comparison, experimental data [62] is found to be closer to the present model for an incident energy, E_I=150eV and an ejected electron energy, E_1=20 eV as shown in Fig. 5.5 (a). However, the present model shows a peak and the results obtained are closer to the present first Born model.

In Fig. 5.5(b), when the incident energy is taken as E_I =150eV and the final energy is E_1=30eV, the first Born and present results exhibit a similar shape, which indicates good agreement between the two. Specifically, at lower angular values, the results are close to the findings of Das and Seal [3], while at higher angular values, they are consistent with experimental data [62]. This suggests that the results for the metastable 2S state are qualitatively similar to those of the ground state.

In Fig. 5.6, we increased the ejected electron energy to E_1=50eV while keeping the incident energy constant at E_I =150eV. The present calculation and the hydrogenic ground state theoretical result [3] show a similar peak pattern with a shifted position, whereas the present first Born result exhibits a lobe-peak structure. Additionally, we observed that the present DDCS exchange result is relatively closer to the experimental result of Shyn [6] than the present first Born result.

The DDCS results for the hydrogenic metastable 2S state with exchange effects, in the current study, indicate good qualitative accord with hydrogenic ground state results from theory and experiment [3], [6] except for E_1=4eV in both cases, which show a similar pattern. On the other hand, both the present calculation and the present first Born result reveal a similar attitude but opposite behavior with the ground state data. However, our present results show some overall disagreement, and it would be beneficial to perform advanced calculations in future experimental work.

In this study, we analysed the ionization techniques which is used to obtain a qualitative understanding of the results. We looked at four distinct scattering amplitudes that matched the variables in equation (5.3) on the right

side. The third term describes a process where the projectile first scatters off the bound electron and then scatters multiple times off the massive nucleus through large angles, leading to a significant enhancement of the DDCS for large scattering angles. The first two terms express T-matrix elements corresponding to the amplitude in the first Born approximation. A higher-order process that makes up the fourth term makes a minimal contribution.

We found that the amplitude associated with the interactions between projectiles and electrons is substantially greater than other amplitudes, like the first Born. This implies that the most significant interaction in the final channel is the projectile-electron binary collision. Double binary collisions, in which the projectile-electron binary collision is characterized by the first term of equation (5.3) and exists even in a basic plane-wave approximation, may be the cause of the ionization process. When the projectile is initially scattered from the nucleus and can be deflected in any direction, corresponding to the amplitude in the second term of equation (5.3), another double binary collision may happen.

The coherent superposition of the two transition matrices of the second and third terms, which correspond to equation (5.3) and are defined by equation (5.5), determines the final shape and magnitude of the DDCS.

To gain a better understanding of the structures observed in the DDCS exchange effects results, we can refer to Table 5.1 and Table 5.2. These tables present the values of the ejection angle, θ_1 for different scattering angles θ_2 at four different values of ejected electron energy E_I for the cases E_I =250eV and E_I =150eV. By examining these tables, we can gain insight into how the ejection angle varies with respect to the scattering angle and ejected electron energy, which can help explain the observed structures in the DDCS exchange effects results.

Table 5.1. DDCS results with exchange effect for emitted angles θ_1 corresponding to various scattering angles θ_2 for four different values of emitted electron energies are E_1=4eV, E_1=20eV, E_1= 50eV and E_1= 80eV in ionization of hydrogen atoms for 250eV electron.

θ_2(deg)	θ_1(deg)	$E_1 = 4eV$	$E_1 = 20eV$	$E_1 = 50eV$	$\mathbf{E_1 = 80eV}$
		DDCS	DDCS	DDCS	DDCS
0	0	1.52871238	0.00296045	0.00007876	0.00000499
1	36	233.45081594	0.45206484	0.01202724	0.00076234
2	72	16.63991223	0.03222280	0.00085725	0.00005434
4	108	40.43308509	0.07829844	0.00208304	0.00013202
10	144	188.60279108	0.36522577	0.00971667	0.00061586
20	180	0.84970343	0.00164551	0.00004377	0.00000277
30	216	265.55552973	0.51429411	0.01368336	0.00086728
40	252	4.22914604	0.00818927	0.00021788	0.00001381
60	288	76.30460798	0.14776095	0.00393116	0.00024917
90	324	138.48086190	0.26816678	0.00713450	0.00045219
100	360	0	0	0	0

Table 5.2. DDCS results with exchange effect for emitted angles θ_1 corresponding to various scattering angles θ_2 for four different values of emitted electron energies are E_1=4eV, E_1=20eV, E_1= 30eV and E_1= 50eV in ionization of hydrogen atoms for 150eV electron.

θ_2(deg)	θ_1(deg)	$E_1 = 4eV$	$E_1 = 20eV$	$E_1 = 30eV$	$\mathbf{E_1 = 50eV}$
		DDCS	DDCS	DDCS	DDCS
0	0	3.61129504	0.00132675	0.00085357	0.00001814
1	36	551.47026237	0.20260666	0.13034555	0.00277042
2	72	39.30780506	0.01444143	0.00929091	0.00019748
4	108	95.51025398	0.03509082	0.02257579	0.00047988
10	144	445.52580817	0.16368404	0.10530624	0.00223825
20	180	2.00727759	0.00073745	0.00047444	0.00001008
30	216	627.382757	0.23049988	0.14828528	0.00315197
40	252	9.99011503	0.00367035	0.00236136	0.00005019
60	288	180.24575364	0.06622294	0.04259879	0.00090561
90	324	327.12478083	0.12018448	0.07731801	0.00164354
100	360	0	0	0	0

5.3.2 Single differential cross section

The single differential cross section (SDCS) with exchange effect is investigated to study the ionization of hydrogen atoms by electrons with incident energies of E_I =100 eV, 150 eV, 200 eV, and 250 eV. The emitted energy, E_1 is varied from 0 eV to 50 eV. The SDCS values is plotted on the

horizontal axis, while the vertical axis has been represented the emitted energy, E_1 in all figures.

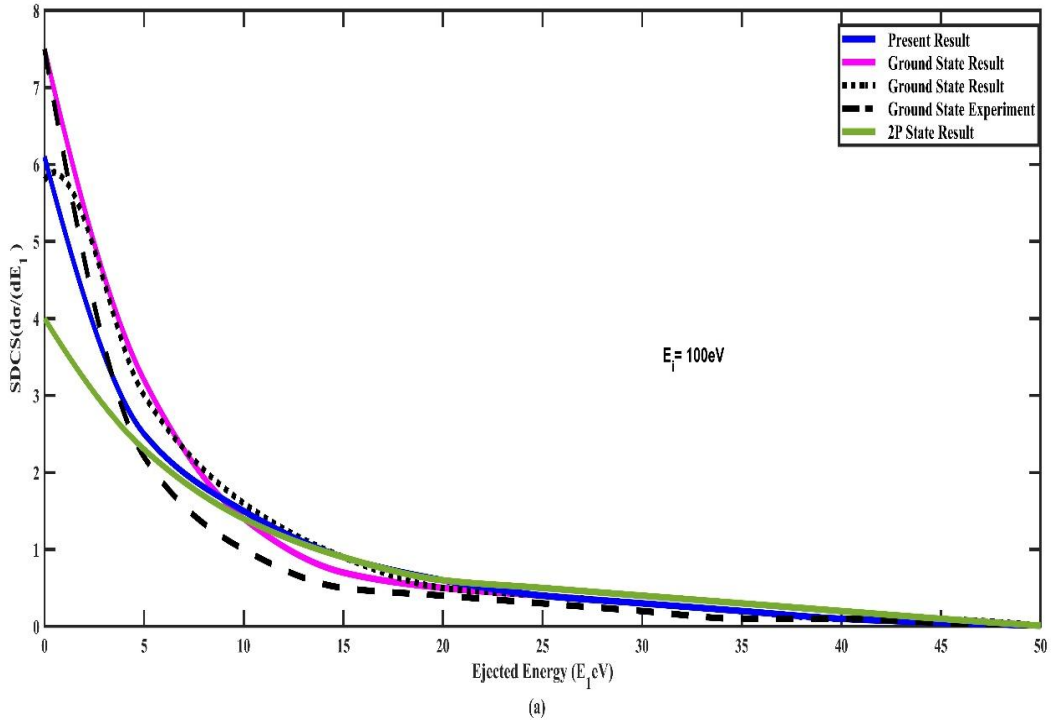

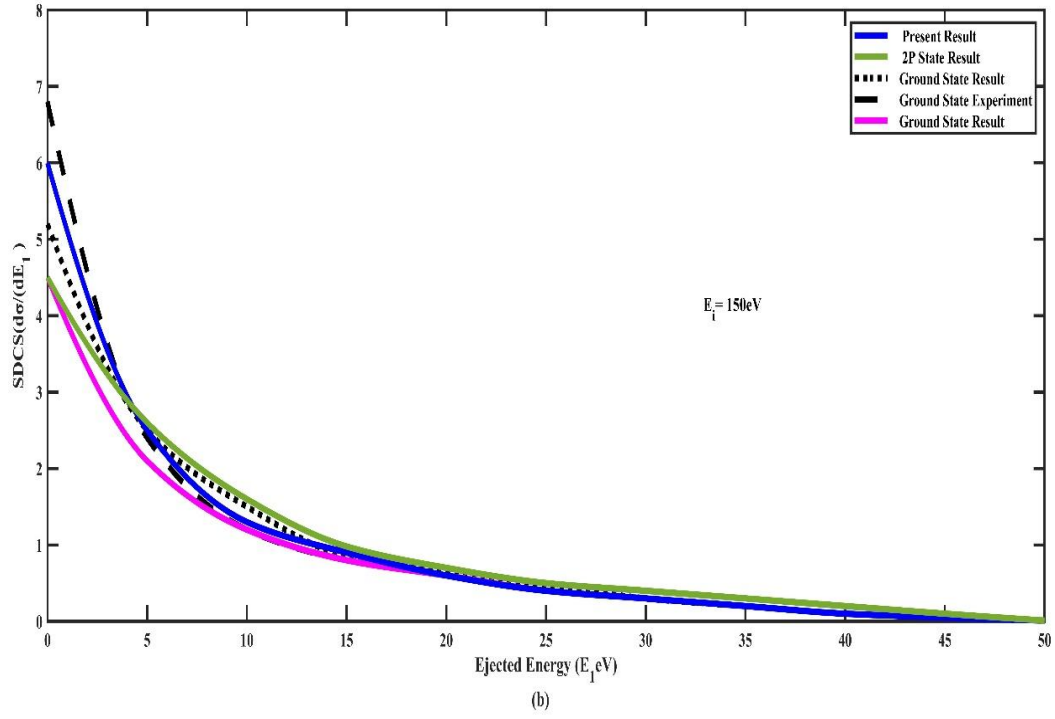

Fig. 5.7 Exchange effect in Single Differential Cross Section (SDCS) for incident

energies (a) E_I =100eV and (b) E_I =150eV respectively.

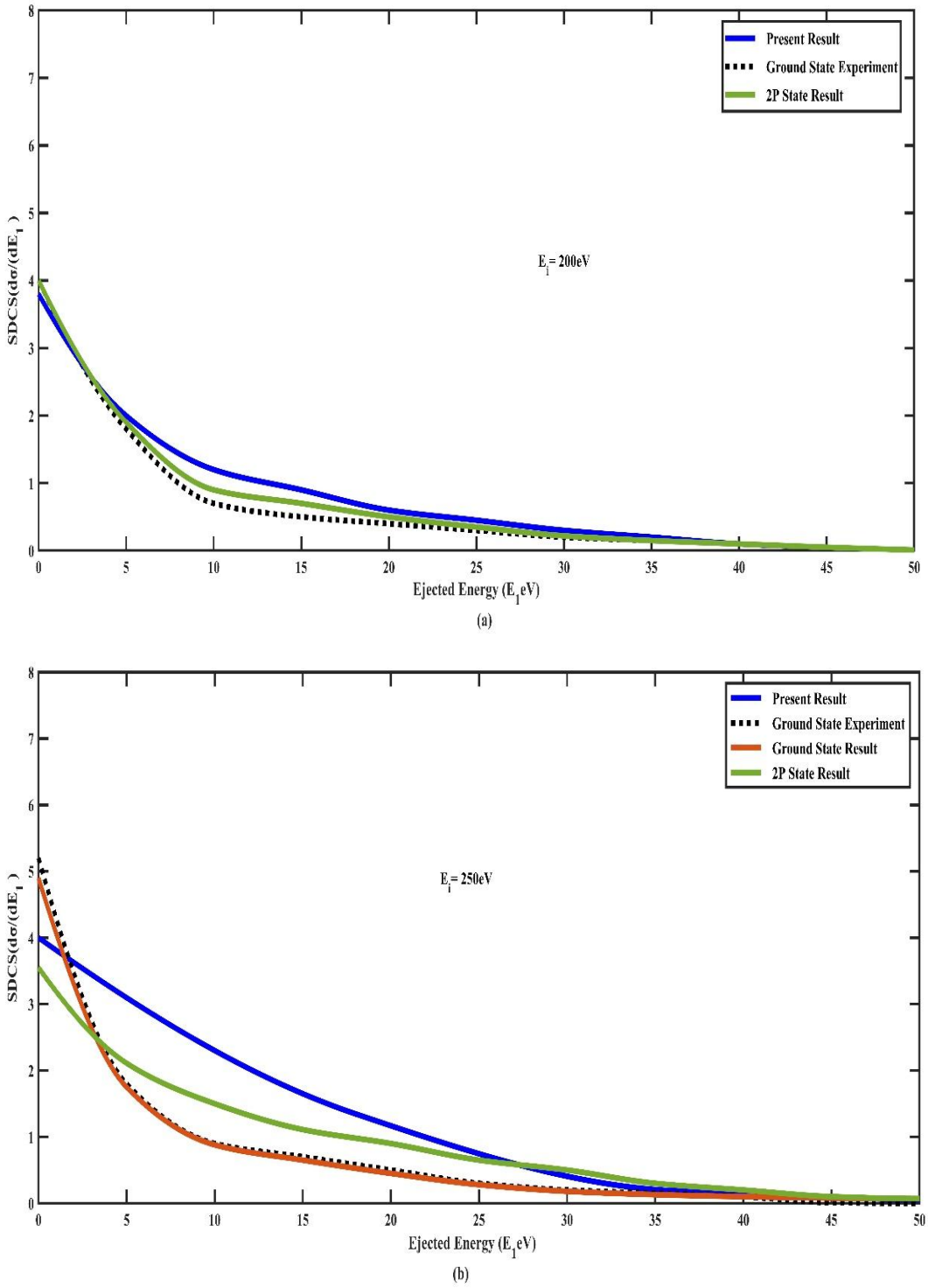

Fig. 5.8 Exchange effect in Single Differential Cross Section (SDCS) for incident energies (a) E_I =200eV and (b) E_I =250eV respectively.

The main objective of this study is to compare the SDCS results obtained in this work with those reported in previous studies, namely the hydrogenic ground state experimental results of Shyn [6], computational results of Das and Seal [3], and 2P state results of Hoque [67], Konovalov and McCarthy [84], for the ionization of hydrogen atoms by electrons.

The results from the present estimations show slight discrepancies at lower emitted energies compared to the results obtained in [3], [6], [67], [84]. However, as the emitted energies increased up to 50 eV, the present estimations and the previous calculations exhibited a similar nature, indicating a good agreement. Specifically, when considering incident energies of 100 eV, 150 eV, 200 eV, and 250 eV in Figures 5.7(a), 5.7(b), 5.8(a) and 5.8(b) respectively, the present estimations and the previous calculations demonstrate good accord at higher emitted energies.

In summary, the SDCS estimations has been conducted in this study exhibited good agreement with the previous calculations for the ionization of hydrogen atoms by electrons, particularly at higher emitted energies.

5.4 CONCLUSION

This study focused on estimating the Double Differential Cross Section (DDCS) and Single Differential Cross Section (SDCS) with exchange effect for the ionization of hydrogenic metastable 2S-state by electrons under various kinematic conditions. To obtain accurate estimations, the multiple scattering theory [3] was employed, which plays a crucial role in addressing ionization problems related to the metastable 2S-state.

Due to the absence of previous experimental data specifically for the ionization of metastable 2S-state hydrogen atoms, it was not possible to directly compare the present computational results with experimental findings. However, by comparing the results with experimental data available for

ionization of hydrogen atoms in the ground state, valuable insights can be gained. These ground state experimental results serve as an important reference point for comparing the computational results obtained for electron impact ionization of the hydrogenic metastable 2S-state.

Our present study provides significant contributions to the field of ionization problems, particularly for the understanding of ionization processes involving the hydrogenic metastable 2S-state. The estimated DDCS and SDCS values offer valuable insights that can guide future research in this area. By building upon these findings, researchers can further investigate and explore the ionization dynamics of metastable hydrogen atoms, leading to advancements in the field of ionization studies.

Chapter 6: SUMMARY AND FUTURE DIRECTIONS

The significant insights from the earlier chapters are summed up as follows.

In chapter 1, an overview of the theoretical background, presents a comprehensive summary of the relevant literature review and methodology relevant to our work have been provided.

In chapter 2, the First Born Double Differential Cross Sections (DDCS) for the ionization of metastable 2S state hydrogen atoms by electrons at 150eV and 250eV energy levels are shown. Distinct features are showed by these DDCS plots, and noteworthy comparisons with existing experimental and theoretical findings related to hydrogenic ground states are made. The corresponding outcomes observed in hydrogenic ground state experiments and theoretical predictions are significantly surpassed by our metastable 2S state DDCS results, emphasizing the unique and intricate nature of ionization in these metastable states. A significant contribution to the understanding of ionization in the context of metastable 2S states is represented by our findings, shedding light on this intriguing area of research.

In chapter 3, the second Born double differential cross section for ionization of metastable 2S state hydrogen atoms by electrons impact, both in theoretical analysis and numerical computations has been estimated. Qualitative alignment of our current findings with established, hydrogenic ground states experimental data and theoretical studies such as ground state

data, 2P state results, are exhibited. For better understanding, our first Born results are also included here.

In chapter 4, the Single Differential Cross Sections (SDCS) for ionization of metastable 2S state hydrogen atoms by electrons at intermediate and high energies are estimated which show better configurations than considered results which demand experimental set up for better comparison.

In chapter 5, the present calculation on the double and single differential cross sections for ionization of metastable 2S state hydrogen atoms by 100Ev, 150eV, 200eV and 250eV electron impact with exchange effects are presented which show very interesting configuration. It will be more interesting to judge the present exchange effects with the experimental results in this regards.

We have interestingly noticed that the implementation of the final state wave function of the multiple scattering yields good qualitative agreement with hydrogenic ground state as well as metastable 2s state for qualitative enhancement.

6.1 LIMITATION OF THE STUDY

Our calculations demonstrate a gradual flattening trend for higher ejection energies, a pattern that resembles Shyn's findings but contrasts with the observations made by Das & Seal. This discrepancy suggests the need for further experimental investigations to enhance our understanding of DDCS behaviour in this context.

In essence, while our work aligns with existing theoretical and experimental knowledge concerning hydrogenic ground states, the variations observed in the DDCS patterns emphasize the importance of additional experimental studies to refine our comprehension of these ionization processes.

6.2 RECOMMENDATION FOR FURTHER WORK

Our present computational findings results are encouraging for the future experiments, which may play a vital role to provide more interesting and significant results in this field of research.

Further works on energy spectrum, total as well as single, double and triple differential cross sections applying this multiple scattering theory at various kinematic condition in different hydrogenic metastable state and helium atom by electron and positron impact will be interesting.

Exploring total differential cross sections using the same theoretical framework in various metastable states of hydrogen atoms and helium atoms, both with electrons and positrons, holds promise as an intriguing avenue for future research. This area presents an array of compelling challenges and opportunities that warrant further investigation in the coming years.

In conclusion, it is worth noting that the multiple scattering theory has proven to be highly effective when addressing atomic ionization issues. There are many opportunities for extending the application of this theory to a wide range of ionization problems, opening up new avenues for exploration and research.

Appendix

Programming Code of the mathematical calculation using MATLAB:

```
lamda1=1/2;
E1=4;
E3=250;
E2=E3-E1-13.6058/4;
p1=(sqrt(2*E1));
p2=(sqrt(2*E2));
p3=(sqrt(2*E3));
phi=(0:180:180);
phi1=[phi 0 0 0 0 0 0 0 0];
theta1=(0:36:360);
theta2=[0 1 2 4 10 20 30 40 60 90 100];
theta12=cos(theta1)*(cos(theta2))'+sin(theta1)*(cos(phi1))'*(sin(theta2));
p=sqrt(p1.^2+p2.^2-2*p1*p2*cos(theta12));
alpha=-1*(p.^(-1));
alpha1=1/p1;
alpha2=1/p2;
tsq=p2.^2+p3.^2-2*p2*p3*cos(theta2);
pt1=lamda1^2+p1^2+tsq-2*p3*p1*cos(theta1)+2*p1*p2*cos(theta12);
pt2=lamda1^2-p1^2+tsq;
pt3=(2*lamda1*p1)*(pt2).^(-1);
pt4=pt2.^2+4*lamda1^2*p1^2;
pte1=(lamda1*sqrt(1+alpha1.^2))*(exp(-alpha1*atand(pt3))).*(pt1.^-2);
pt21=alpha1*log(pt1)-alpha1*(1/2)*log(pt4)-atand(alpha1);
almp=lamda1^2+p1^2;
ptc=cos(pt21);
pts=sin(pt21);
TPB1dr=pte1*ptc';
TPB1di=pte1*pts';
pmtl1=(sqrt(almp)*(exp(-alpha1*atand((2*lamda1*p1)*pt2.^(-
1))))).*(pt1*(sqrt(pt4).^(-1))');
ptlm1=alpha1*log(pt1)-atand(p1/lamda1)-
alpha1*(1/2)*log(pt4)+atand((2*lamda1*p1)*(pt2).^(-1));
b=pi*alpha1;
ep2=(2*b)/(exp(b)-exp(-b));
ep=sqrt(ep2);
delta=2*alpha2*log(p1);
hpr=ep*cos(delta);
hpi=ep*sin(delta);
```

```
TPB2dr=pmtl1*cos(ptlm1)';
TPB2di=pmtl1*sin(ptlm1)';
TPBldr=TPB1dr-alpha1*TPB2di;
TPBldi=TPB1di+alpha1*TPB2dr;
B11tpr=hpr*TPBldr+hpi*TPBldi;
B11tpi=hpr*TPBldi-hpi*TPBldr;
B11r=8*pi*exp((pi*alpha1)/2)*B11tpr;
B11i=8*pi*exp((pi*alpha1)/2)*B11tpi;
M=1*((pi*(tsq)).^(-1));
tb1r=M*B11r;
tb1i=M*B11i;
pt5=lamda1^2+p1^2-tsq;
pt6=lamda1^2+p1^2+tsq;
Q=(2*alpha1*lamda1)*(pt1).^(-1)-(2*alpha1*lamda1*pt6).*(pt4.^(-1));
P=1/lamda1-(4*lamda1)*(pt1.^(-1))+(2*alpha1*p1*pt5).*((pt4).^(-1));
tb31r=pte1*cos(pt21)';
tb31i=pte1*sin(pt21)';
tb31dr=tb31r.*P-tb31i.*Q;
tb31di=tb31r.*Q+tb31i.*P;
X=lamda1/almp-(2*lamda1)*(pt1).^(-1)-(2*lamda1*(pt6)-
2*alpha1*p1*pt5).*(pt4).^(-1);
Y=p1/almp+(2*alpha1*lamda1)*pt1.^(-1)-
(2*p1*pt5+2*alpha1*lamda1*pt6).*pt4.^(-1);
tb32i=pmtl1*sin(ptlm1)';
tb32r=pmtl1*cos(ptlm1)';
tb32dr=tb32r*X-tb32i*Y;
tb32di=tb32r*Y+tb32i*X;
tpb3r=hpr*(tb31dr-alpha1*tb32di)+ hpi*(tb31di+alpha1*tb32dr);
tpb3i=-hpi*(tb31dr-alpha1*tb32di)+ hpr*(tb31di+alpha1*tb32dr);
B33r=(-8)*pi*(exp(pi*alpha1/2))*tpb3r;
B33i=(-8)*pi*(exp(pi*alpha1/2))*tpb3i;
tb3r=(-1/4)*M.*B33r;
tb3i=(-1/4)*M.*B33i;
tbr=tb1r+tb3r;
tbi=tb1i+tb3i;
tcp3=-(exp((pi*alpha2)/2)/pi^3)*(( exp(pi*alpha2)- exp(-(pi*alpha2)))/2);
tc1p3=-(2*exp((pi*alpha2)/2))/(pi^3);
x=(0:10);
Q2=p2^2+p3^2+x.^2*p2^2-2*p2*p3*cos(theta2)+2*p2*p3*x.*cos(theta2);
Z1=1+(p1^2/lamda1^2);
lamda3=x*p2;
A1=(2*pi^2)*(lamda1^4*(Q2-lamda3.^2).^-1);
A11=(-8*pi^2)*(lamda1^5*(Q2-lamda3.^2).^-1);
```

```
A21=(1+lamda1*lamda3*Z1).*(Q2.^2-lamda3).^-1;
A2=1./(((1-3*A21.^2).^2)+((A21.^3-3*A21).^2));
A211=(1+lamda3./(Q2-lamda3.^2).*(1-p1.^2/lamda1^2));
A22=((1-6*A21.^5.*A211+60*A21.^3.*A211-30*A21.*A211).*A2.^2);
A31=4*lamda3.*Q2-4*lamda3.^3+4*lamda3*p1.^2;
A3=(1-3*A21.^2).*(lamda1*A31);
A33=(1-3*A21.^2).*A31+((lamda1*A31).*(-6*A21.*A211));
A41=6*lamda1^2*lamda3+6*p1.^2.*Q2;
A4=((A21.^3)-3*A21).*A41;
A44=((3*A21).^2.*A211-3*A211).*A41+((A21.^3)-3*A21).*(12*lamda1*lamda3);
A5=(6*pi^3*lamda3).*((lamda1^5*(Q2-lamda3.^2).^4).^(-1));
A6=1./(((1-6*A21.^2+A21.^4).^2)+((4*A21.^3-4*A21).^2));
A71=6*lamda1^4*lamda3.^2-2*p1.^2.*Q2*lamda1^2-
6*lamda1^2*lamda3.^2*p1.^2+2*p1.^4.*Q2;
A7=(1-6*(A21).^2+(A21).^4).*A71;
A81=2*lamda3.*Q2*lamda1-2*lamda1^3*lamda3.^3+2*lamda3*lamda1^5-
2*p1.^2*lamda1 *lamda3.*Q2+2*p1.^2*lamda1*lamda3.^3-
2*p1.^4*lamda1*lamda3;
A8=(4*(A21).^3-4*A21).*A81;
B1=A1;
B2=A2;
B3=(1-(3*A21.^2)).* A41;
B4=((A21.^3)-3*A21).*(lamda1*A31);
B5=A5;
B6=A6;
B7=(4*A21.^3-4*A21).*A71;
B8=(1-6*A21.^2+A21.^4).*A81;
B22=A22;
I3R=(A3-A4)*(A1.*A2)'-(A7+A8)*(A5.*A6)';
I3I=(B1.*B2)*(B3+B4)'-(B5.*B6)*(B7+B8)';
Q20=p2.^2+p3.^2-2*p2*p3*cos(theta2);
A10=(2*pi.^2)*(lamda1.^4*(Q20-lamda3.^2).^3).^(-1);
A10=(2*pi.^2)*(lamda1.^4*(Q20-lamda3.^2).^3).^(-1);
A210=(lamda1*lamda3.*Z1).*((Q20-lamda3.^2).^(-1))';
A20=((1-3*A210.^2).^2.*(1+A210.^3-3*A210).^2).^(-1);
A310=4*lamda3*Q20'-4*lamda3.^3+4*lamda3*p1.^2;
A30=(1-3*(A210.^2)).*lamda1.*A310;
A410=6*lamda1.^2.*lamda3+6*p1.^2.*Q20;
A40=((A210).^3-3*A210).*A410;
A50=(6*pi.^3*lamda3)*((lamda1.^5*(Q20-lamda3.^2).^4).^(-1))';
A60=(((1-6*(A210).^2+(A210).^4).^2)+((4*(A210).^3-4*A210).^2)).^(-1);
A710=6*lamda1.^4.*lamda3.^2-2*p1.^2.*Q20.*lamda1.^2-
6*lamda1.^2.*lamda3.^2.*p1.^2+2*p1.^4.*Q20;
```

```
A70=(1-6*(A210).^2+(A210).^4).*A710;
A810=2*lamda3*Q20'*lamda1-2*lamda1.^3*lamda3.^3+2*lamda3*lamda1.^5-
2*p1.^2*lamda1*lamda3*Q20'+2*p1.^2*lamda1*lamda3.^3-
2*p1.^4*lamda1*lamda3;
A80=(4*(A210).^3-4*A210).*A810;
B10=A10;
B20=A20;
B30=(1-3*(A210.^2)).*A410;
B40=((A210.^3)-3*A210).*(lamda1.*A310);
B50=A50;
B60=A60;
B70=(4*(A210).^3-4*A210).*A710;
B80=(1-6*(A210).^2+(A210).^4).*A810;
A11=-8*pi.^2*((lamda1.^5.*(Q2-lamda3.^2).^3)).^(-1);
A211=(lamda3./(Q2-lamda3.^2)).*(1-p1.^2./lamda1.^2);
A22=(-6*(A211).^2).*A31+(lamda1.*A31.*(-6*A21.*A211));
A33=(1-3*A21.^2).*A31+lamda1.*A31.*(-6*A21.*A211);
A44=(3*(A21).^2.*A211-3*A211).*A41+((A21).^3.*A21).*12*lamda1.*lamda3;
A55=(-30*pi.^3*lamda3)./(lamda1.^6.*(Q2-lamda3.^2).^4);
A66=(-8*A211.*(A21+3*(A21).^3+3*(A21).^5+(A21).^7)).*(((1-
6*(A21).^2+(A21).^4).^2+(4*(A21).^3-4*A21).^2).^2).^(-1);
A711=24*lamda1.^3*lamda3.^2-4*p1.^2.*Q2*lamda1-12*lamda1-
12*lamda1*lamda3.^2.*p1.^1;
A77=((1-6*(A21).^2+(A21).^4).*A711)+(A71.*(-12*A21.*A211+4*(A21).^3.*A211));
A811=2*lamda3*Q2'-6*lamda1.^2*lamda3.^3+10*lamda3*lamda1.^4-
2*p1.^2*lamda3*Q2'+2*p1.^2*lamda3.^3-2*p1.^4*lamda3;
A88=((4*A21).^3-4*(A21).*A811)+((12*(A21).^2.*A211-4*A211).*A81);
B311=12*lamda1*lamda3.^2;
B33=(1-3*A21.^2).*B311-6*A211.*A21.*A41;
B44=(A21.^3-3*A21).*A31+(3*A21.^2.*A211-3*A211).*(lamda1*A31);
B55=A55;
B66=A66;
B711=A711;
B71=A71;
B77=(4*A21.^3-4*A21).*B711+(12*A21.^2.*A211-4*A211).*B71;
B81=A81;
B811=A811;
B88=(1-6*A21.^2+A21.^4).*B811+(-12*A21.*A211+4*A21.^3.*A211).*B81;
sphi1xr=(A11*A2')*(A3-A4)'+(A1*A22')*(A3-A4)'+(A1*A2')*(A33-A44)'-
(A55*A6')*(A7+A8)'-(A5*A66')*(A7+A8)'-(A5*A6')*(A77+A88)';
sphi1xi=(A11*B2')*(B3+B4)'+(B1*A22')*(B3+B4)'+(B1*B2')*(B33+B44)'-
(B55*B6')*(B7+B8)'-(B5*B66')*(B7+B8)'-(B5*A6')*(B77+B88)';
A110=-8*pi.^2*((lamda1.^5*(Q20-lamda3.^2).^3)).^(-1);
```

```
A2110=(lamda3./(Q20-lamda3.^2)).*(1-p1.^2/lamda1.^2);
A220=(-6*(A2110).^2).*A310+(lamda1*A310.*(-6*A210.*A2110));
A330=(1-3*A210.^2).*A310+lamda1*A310.*(-6*A210.*A2110);
A440=(3*(A210).^2.*A2110-
3*A2110).*A410+((A210).^3*A210).*(12*lamda1*lamda3);
A550=(-30*pi.^3*lamda3).*(((lamda1.^6*(Q20-lamda3.^2).^4)).^(-1))';
A660=(-8*A2110.*(A210+3*(A210).^3+3*(A210).^5+(A210).^7)).*(((1-
6*(A210).^2+(A210).^4).^2+(4*(A210).^3-4*A210).^2).^2).^(-1);
A7110=24*lamda1.^3*lamda3.^2-4*p1.^2.*(Q20*lamda1)-
12*lamda1*lamda3.^2*p1.^1;
A770=((1-6*(A210).^2+(A210).^4).*A7110)+(A710.*(-
12*A210.*A2110+4*(A210).^3.*A2110));
A8110=2*lamda3*Q20'-6*lamda1.^2*lamda3.^3+10*(lamda3*lamda1.^4)-
2*p1.^2.*lamda3*Q20'+2*p1.^2*lamda3.^3-2*p1.^4.*lamda3;
A880=((4*(A210).^3-4*A210).*A8110)+((12*(A210).^2.*A2110-4*A2110).*A810);
B3110=12*lamda1*lamda3.^2;
B330=(1-3*A210.^2).*B3110-6*A2110.*A210.*A410;
B440=(A210.^3-3*A210).*A310+(3*A210.^2.*A2110-3*A2110).*(lamda1*A310);
B550=A550;
B660=A660;
B7110=A7110;
B710=A710;
B770=(4*A210.^3-4*A210).*B7110+(12*A210.^2.*A2110-4*A2110).*B710;
B810=A810;
B8110=A8110;
B880=(1-6*A210.^2+A210.^4).*B8110+(-
12*A210.*A2110+4*A210.^3.*A2110).*B810;
sphi1or=(A110.*A20).*(A30-A40)+(A10.*A220).*(A30-A40)+(A10.*A20).*(A330-
A440)-(A550.*A60).*(A70+A80)-(A50.*A66).*(A70+A80)-
(A50.*A60).*(A770+A880);
sphi1oi=(A110.*B20).*(B30+B40)+(B10.*A220).*(B30+B40)+(B10.*B20).*(B330+B440
)-(B550.*B60).*(B70+B80)-(B50.*B660).*(B70+B80)-(B50.*B60).*(B770+B880);
pitc1r=cos(alpha2*log(x/(1-x)));
pits1i=sin(alpha2*log(x/(1-x)));
xp1r=(sphi1xr-sphi1or)/x;
xp1i=(sphi1xi-sphi1oi)/x;
pit1sr=(pitc1r*xp1r-pits1i*xp1i)';
pit1si= (pits1i*xp1r+pitc1r*xp1i)';
MN=@(x)(x./(1-x)).^(1i*alpha2);
MN1=integral(MN,0,1);
pit1r=pit1sr.* MN1;
pit1i=pit1si.* MN1;
b=pi*alpha1;
```

```
ep2=(2*b)/(exp(b)-exp(-b));
ep=sqrt(ep2);
delta=2*alpha2*log(p1);
hpr=ep*cos(delta);
hpi=ep*sin(delta);
sphior=[-3.1520 -2.5612 0 0 0 0 0 0 0 0 0];
sphioi=[-2.1419 -2.2857 0 0 0 0 0 0 0 0 0];
tbp1r=tcp3*(hpr*pit1r+hpi*pit1i)+tc1p3*(hpi*sphior-hpr*sphioi);
tbp1i= -(tcp3*(hpi*pit1r-hpr*pit1i)-tc1p3*(hpi*sphioi+hpr*sphior));
pitir=2*pit1r;
pitii=2*pit1i;
tbp2r= tcp3*(hpr*pitir+hpi*pitii)+tc1p3*(hpi*sphior-hpr*sphioi);
tbp2i= -(tcp3*(hpi*pitir-hpr*pitii)-tc1p3*(hpi*sphioi+hpr*sphior));
tc3p3= (-(exp((pi*alpha2)/2))/exp(2*(log(p1))));
bte1=(lamda1/(lamda1^2+p1^2)^2);
bt4=alpha2*log(lamda1^2+p1^2);
btc=cos(bt4);
bts=sin(bt4);
tbp3dr=bte1*btc;
tbp3di=bte1*bts;
tbc4r=hpr*tbp3dr+hpi*tbp3di;
tbc4i=hpr*tbp3di-hpi*tbp3dr;
tbp3r=tc3p3*(cos(delta)*tbc4r+sin(delta)*tbc4i);
tbp3i=tc3p3*(cos(delta)*tbc4i-sin(delta)*tbc4r);
tb4d11pr=1/lamda1-(4*lamda1)/(lamda1^2+p1^2);
tb4d11pi=(2*lamda1*alpha2)/(lamda1^2+p1^2);
tbp4dpr=tbp3dr*tb4d11pr-tbp3di*tb4d11pi;
tbp4dpi=tbp3dr*tb4d11pi+tbp3di*tb4d11pr;
tp4pr=hpr*tbp4dpr+hpi*tbp4dpi;
tp4pi=hpr*tbp4dpi-hpi*tbp4dpr;
tbp4r=tc3p3*(cos(delta)*tp4pr+sin(delta)*tp4pi);
tbp4i=tc3p3*(cos(delta)*tp4pi-sin(delta)*tp4pr);
tbpr=tbp1r+tbp2r+tbp3r+tbp4r;
tbpi=tbp1i+tbp2i+tbp3i+tbp4i;
tsq=p2.^2+p3.^2-2*p2*p3*cos(theta2);
nue=tsq/(p1^2+2*p1*p2*cos(theta12));
ti11r=hpr*cos(alpha*log(nue))+ hpi*sin(alpha*log(nue));
ti11i=hpr*sin(alpha*log(nue))- hpi*cos(alpha*log(nue));
tic1=(4*exp((pi*alpha)/2)*lamda1)/((pt1).^2);
ti1r=tic1*ti11r;
ti1i=tic1*ti11i;
tip2=(-1/(16*pi^3))*(exp((pi*alpha)/2)).*(exp(pi*alpha)-exp(-pi*alpha));
tcip2=(1/(16*pi^3))*exp((pi*alpha)/2);
```

```
ti2r=tip2.*(hpr*pit1r+hpi*pit1i)-tcip2.*(hpr*sphi1oi-hpi*sphi1or);
ti2i=tip2.*(hpr*pit1i-hpi*pit1r)+tcip2.*(hpr*sphi1or+hpi*sphi1oi);
ti3c1=((2*exp((pi*alpha)/2)/tsq).*((4*lamda1^2-pt1.^2)/pt1.^3));
ti31r=hpr*cos(alpha*log(nue))+hpi*sin(alpha*log(nue));
ti31i= hpr*sin(alpha*log(nue))-hpi*cos(alpha*log(nue));
ti3r=ti3c1* ti31r;
ti3i=ti3c1* ti31i;
ti4q=((1/(32*pi^3))* exp((pi*alpha)/2)).*( exp(pi*alpha)-exp(-pi*alpha));
xpr= xp1r;
xpi= xp1i;
ptispr=pitc1r*xpr-pits1i*xpi;
ptispi=pits1i*xpr+pitc1r*xpi;
p1t4ir=ptispr*x;
p1t4ii=ptispi*x;
tip4=(1/(32*pi^3))* exp((pi*alpha)/2).* ( exp(pi*alpha)-exp(-pi*alpha));
ti4pr=tip4.*p1t4ir;
ti4pi=tip4.*p1t4ii;
ti4r=ti4pr*hpr+ti4pi*hpi;
ti4i=ti4pi*hpr-ti4pr*hpi;
tir=ti1r+ ti2r+ ti3r+ti4r;
tii=ti1i+ ti2i+ ti3i+ti4i;
tpb1=((4*tsq).*(lamda1*(pt1.^2)));
tpb2=((-4*tsq)*(lamda1/almp^2));
tpb3=((2*tsq).*((-4*lamda1.^2+pt1).*(pt1.^3)));
tpb4=((2*tsq).*((p1.^2-3*lamda1.^2).*(almp).^3));
tpbr=tpb1+tpb2+ tpb3+tpb4;
tpbi=[0 0 0 0 0 0 0 0 0 0 0];
tfir=tbr+tbpr+tir-2*tpbr;
tfii=tbi+tbpi+tii-2*tpbi;
TDCS1=(p1*p2/p3)*(tfir.^2+tfii.^2);
TDCS=abs(TDCS1);
y=(0:10:100);
fun=@(y) 913.3026*sin(y);
q1=integral(fun,0,100);
q2=integral(fun,10,100);
q3=integral(fun,20,100);
q4=integral(fun,30,100);
q5=integral(fun,40,100);
q6=integral(fun,50,100);
q7=integral(fun,60,100);
q8=integral(fun,70,100);
q9=integral(fun,80,100);
q10=integral(fun,90,100);
```

```
q11=integral(fun,100,100);
Q11f=[1.3070e+02 -1.62e+03  -4.31e+02   -6.7217e+02   -1.4517e+03  97.4432   -
1.7227e+03   -2.1739e+02   -9.2341e+02   -1.2439e+03   0].^2;
DDCS=(1/(2*pi).^4)*Q11f;
plot(theta1,DDCS);
```